DEVELOPMENT OF A HIGH-RESOLUTION MS-BASED METHOD FOR THE STRUCTURAL ELUCIDATION OF POLYAMINE SPIDER TOXINS

Dissertation

zur

Erlangung der naturwissenschaftlichen Doktorwürde
(Dr. sc. nat.)

vorgelegt der

Mathematisch-naturwissenschaftlichen Fakultät

der

Universität Zürich

von

Silvan Eichenberger

von

Gränichen AG

Promotionskomitee

Prof. Dr. Stefan Bienz (Vorsitz)

Prof. Dr. Jay Siegel

Dr. Laurent Bigler

Zürich, 2009

Die vorliegende Arbeit wurde von der Mathematisch-naturwissenschaftlichen Fakultät der Universität Zürich im Frühjahrssemester 2009 als Dissertation angenommen.

Promotionskomitee: Prof. Dr. Stefan Bienz (Vorsitz), Prof. Dr. Jay Siegel, Dr. Laurent Bigler

The author would like to thank **Thermo Scientific** for providing the funds necessary to print this dissertation.

TABLE OF CONTENTS

INTRODUCTION

1. Polyamine Spider Toxins

Aliphatic di- and polyamines, also called biogenic amines, as well as their conjugatives are widely found throughout the animal and plant kingdom. They are known as early as 1678 when Antoine van Leeuwenhoek obtained crystals during microscopic examinations of animal sperm, that were later interpreted as spermine phosphate [1,2]. In addition to the almost ubiquitous spermine PA343[1], a great number of other biogenic amines are known ranging from diamines, like the widespread putrescine (PA4), to hexamines, like homocaldohexamine (PA33334), which were extracted from the thermophilic eubacteria *Bacillus schlegelii* [4] (*Figure 1*). Apart from the unsubstituted bases, also many *N*-alkylated and *N*-acylated polyamine alkaloids have been isolated from natural sources [3,5].

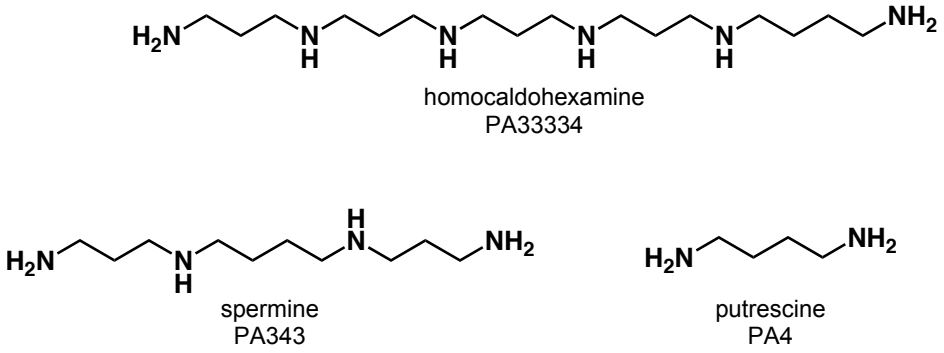

***Figure 1**. Representatives for biogenic amines.*

[1] According to the "PA-nomenclature" introduced by Bienz *et al.* [3], the linear polyamines are abbreviated by the prefix "PA" followed by the number of methylene units in-between the several N-atoms.

In the past decades numerous structurally different polyamine derivatives were found, particularly in spider venoms [6,7]. With few exceptions,[1] all polyamine toxins of spiders share the same general structure (*Figure 2)*: The toxins all consist of a linear α,ω-diamino polyazaalkane backbone (C) modified at one end with a lipophilic type unit, in most cases an aromatic acyl group (A). For some classes of toxins, the head portion A is separated from the polyamine backbone by one or more α-amino acid moieties (B), and other compounds are further modified at the tail of the polyamine backbone with an additional basic amino acid portion (D).

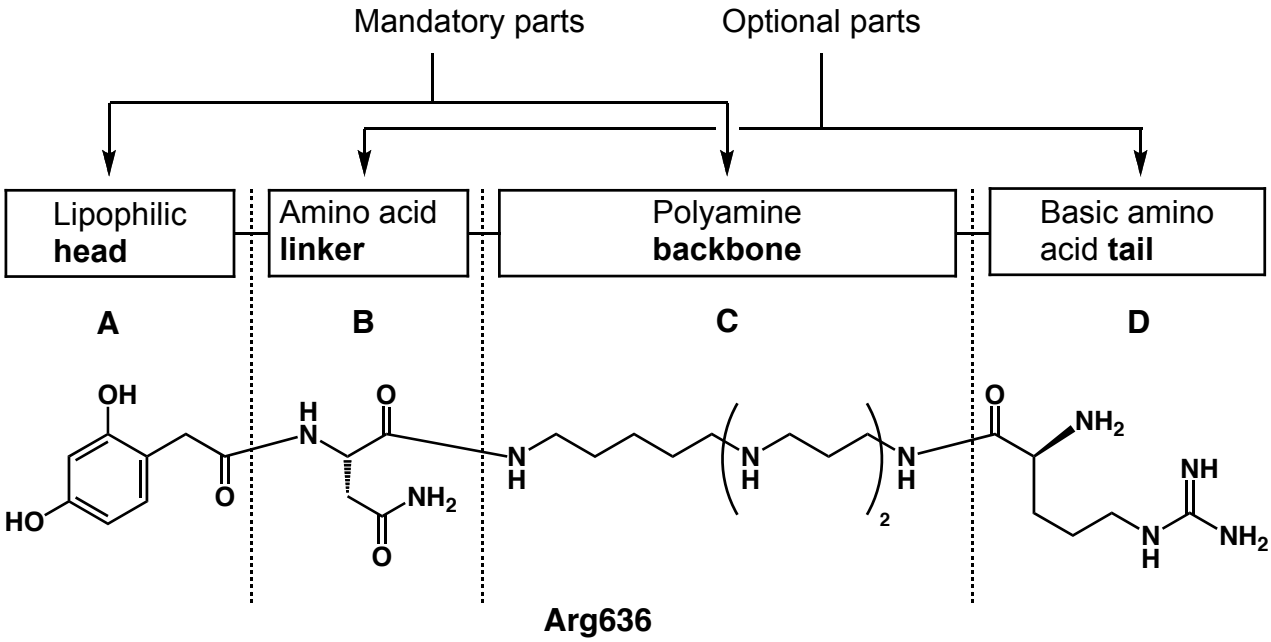

Figure 2*. Structures of polyamine spider toxins exemplified by* ***Arg636****.*

Polyamines and their derivatives exhibit a variety of interesting and important biological activities. They were found to play important roles in DNA stabilization [8,9] and modification [10-12], to affect protein biosynthesis [13-18], to be involved in modifications of neuroreceptors and their associated ion channels in mammalian central nervous system [19-22], and to interact with phospholipids in biological membranes [23,24]. Because of these significant biological functions and the fact that polyamine derivatives are considered as therapeutic leads for the treatment of a variety of diseases like brain disorders

[1] Bis-acylated compounds were found in *Drassodes sp.* venom (*Chapter 3*).

such as *Parkinson's* and *Alzheimers's* diseases [25-28], new and efficient methods for their synthesis as well as more sensitive and selective methods for the identification and structural elucidation of new compounds from natural sources are being sought.

2. MS-Based Characterization of Acylpolyamines Contained in Spider Venom

The first report on the evidence of polyamine derivatives in spider venom is dated in 1964 [29]. In the following 30 years, mainly classical analytic procedures of isolation and purification were used. These were then followed by the investigation of the purified compounds by IR-, UV-, and NMR-spectroscopy as well as mass spectrometry for their structural elucidation. These classical procedures are time consuming, as several separation steps were needed to isolate and purify the acylpolyamines in large enough amounts for the various spectroscopic methods. Due to the low overall sensitivity of the method, only the major constituents of the venoms could be structurally elucidated. A detailed description of the structural elucidation of acylpolyamines by the classical method is reviewed by Schäfer *et al.* [7].

During the early period of venom analyses, mass spectrometry was only used to determine the molecular masses of the isolated compounds. The two ionization techniques widely used at that time, electron impact (EI) and chemical ionization (CI), could not be applied because acylpolyamines were either not volatile enough or decomposed completely during the ionization process. Fast atom bombardment (FAB) was the sole ionization technique available bringing non-volatile compounds in the gas phase and providing their molecular masses. FAB-MS was, therefore, the method of choice to obtain the molecular masses of the labile and non-volatile polyamine spider toxins.

Interpretation of MS fragmentation was used 1990 for the first time as a tool for the structural elucidation of polyamine spider toxins [30]. Acylpolyamines of *Agelenopsis aperta* venom were purified by preparative HPLC and subsequently analyzed by ^{1}H-NMR, ^{13}C-NMR, and FAB-MS. Whereas ^{1}H-

NMR, ^{13}C-NMR, and UV spectroscopy provided important structural data for the determination of the aromatic acyl portions, FAB-MS allowed for the characterization of the polyamine backbones. The fragment ions formed were indicative for the determination of the positions of the N-atoms in the polyamine backbones. With this method, five new acylpolyamines were isolated and characterized from the venom of *A. aperta*, and their structures were confirmed by total synthesis [30].

In the same year, also tandem mass spectrometry (MS/MS) was first employed as a tool for the structural elucidation of acylpolyamines. Analogously to the FAB-MS experiments, the positions of N-atoms and N–OH-groups in polyamine backbones were determined by interpretation of the specific fragmentations [31]. In contrast to the previous methods, the fragment ions were generated by MS/MS experiments obtained with a triple quadrupole mass analyzer using collision-induced dissociation (CID) in a collision cell, and not during FAB ionization. Because of mass selective isolation of the precursor species prior fragmentation, mass spectra no longer contained interfering FAB matrix signals from the ionization. With this method, five additional toxins from *A. aperta* [31], and ten acylpolyamines from *Hololena curta* were identified [32].

It is important at this point to mention that all these experiments were restricted to the most abundant components present in the venom and were performed in two steps, *i.e.* by initial purification of venom fractions and subsequent analysis. Only with the advent of more sensitive and selective analytical methods — in particular of MS-based approaches — also minor constituents of the complex venoms could be detected and characterized. In particular by the development of HPLC on-line coupled to MS and MS/MS, separation, detection, and structural elucidation of minor constituents within complex mixtures became possible.

In 1994, Itagaki *et al.* were the first to use HPLC-MS for the analysis of spider venom [33]. A reversed phase HPLC column was linked to a continuous flow (CF) frit FAB inlet probe, which allowed the detection of 40 acylpolyamines

from *Nephilengys borbonicaI* venom without prior purification [33,34]. Interestingly, only CID of the sodiated adducts $[M+Na]^+$ and not of the protonated molecules $[M+H]^+$ provided intense structure-related fragment ions. In a similar manner, new compounds were also characterized from the venom of *Nephila clavata* [35], *Nephila madagascariencis* [36], and *Nephilengys cruentata* [37]. Overall, 91 different acylpolyamines were found by this method and were recently classified into seven subtypes according to their types of polyamine backbones [6].

HPLC equipped with a UV diode array detector (DAD) and on-line coupled to atmospheric pressure chemical ionization (APCI) MS and MS/MS was introduced 2000 by Chesnov *et al.* for the analysis of spider venom [38-41]. APCI provided protonated molecules of the acylpolyamines that were isolated and subsequently submitted to CID in a triple quadrupole mass spectrometer. Analogously to the HPLC-FAB-MS/MS method, the structures of the polyamine backbones were determined by MS/MS. With HPLC-UV(DAD)-APCI-MS and MS/MS, three acylpolyamines, containing a characteristic guanidyl group at the end of the polyamine backbone, were found in *Paracoelotes birulai* [38], and the re-investigation of *A. aperta* venom allowed for the identification of not less than 33 acylpolyamines, significantly (25) more than with the classical procedure [39]. It was shown that independent MS/MS data of isomeric acylpolyamines could be acquired in one chromatographic separation as long as the compounds exhibit a different chromatographic behavior.

Investigations of such complex samples, however, also demonstrated that not all isomeric acylpolyamines of *A. aperta* could be chromatographically resolved. Therefore, mixed fragmentation data of co-eluting isomers were obtained, making structural elucidation more complicated if not impossible. Unambiguous interpretation of the obtained fragmentation data were only possible by the synthesis of combinatory libraries of isomeric polyamine spider toxins and comparing their analytical data with the data acquired of the natural products [41]. These comparative investigations confirmed the structures and assignments of seven previously found toxins and allowed the

identification of five additional polyamine derivatives in the venom of *A. aperta*.

The MS/MS data obtained for the isomerically pure synthetic polyamine derivatives further showed that CID also provides unexpected fragment ions that can lead to misinterpretation in the course of the structural characterization of unknown acylpolyamines. Analyses of ^{15}N-labelled derivatives disclosed that these unexpected fragment ions correspond to internal positions of the polyamine backbones and arise from sequential fragmentations [42].

Recently, it was shown that the HPLC-APCI-MS method is inappropriate for the analysis of unknown polyamine derivatives due to potential artifact formation. Analyses of synthetic polyamine-containing compounds using APCI revealed that *N*-hydroxylated compounds were partially decomposed during the APCI-process resulting in artificial MS signals. By the re-investigation of *A. aperta* venom, it was clearly shown that signals previously thought to be real sample constituents could in fact be attributed to reduction products generated during the APCI process. The partial reduction could be circumvented either by post-column addition of ammonia for HPLC-APCI-MS or by using an alternative ionization like ESI, instead (*Chapter* 1).

This method also proved insufficient for the structural elucidation of structurally more complex toxins as were found in *Larinioides folium* venom. Therefore, the method was supplemented with on-column H/D-exchange HPLC-MS, nanoLC coupled to high accuracy and high-resolution *Fourier* transform MS, and amino acid analysis of venom fractions. This extended analytical procedure allowed for the detection and structural characterization of 60 acylpolyamine derivatives in the venom of the spiders *L. folium*, *Ozyptila lugubris*, *Lachesana sp.*, and *Drassodes sp.* (*Chapters 2* and *3*).

3. References

[1] D. A. Lewenhoeck, *The Royal Society of London, Philosophical Transactions* **1678**, *12*, 1040.

[2] O. Rosenheim, *Biochem. J.* **1924**, *18*, 1253.

[3] S. Bienz, R. Detterbeck, C. Ensch, A. Guggisberg, U. Häusermann, C. Meisterhans, B. Wendt, C. Werner, M. Hesse, in *The Alkaloids, Vol. 58* (Ed.: G. A. Cordell), Academic Press, New York, **2002**, pp. 83.

[4] K. Hamana, M. Niitsu, S. Matsuzaki, K. Samejima, Y. Igarashi, T. Kodama, *Biochem. J.* **1992**, *284*, 741.

[5] S. Bienz, P. Bisegger, A. Guggisberg, M. Hesse, *Nat. Prod. Rep.* **2005**, *22*, 647.

[6] M. S. Palma, T. Nakajima, *Toxin Rev.* **2005**, *24*, 209.

[7] A. Schäfer, H. Benz, W. Fiedler, A. Guggisberg, S. Bienz, M. Hesse, in *The Alkaloids, Vol. 45* (Ed.: G. A. Cordell), Academic Press, New York, **1994**, pp. 1.

[8] H. Ohishi, M. Odoko, K. Grzeskowiak, Y. Hiyama, K. Tsukamoto, N. Maezaki, T. Ishida, T. Tanaka, N. Okabe, K. Fukuyama, D.-Y. Zhou, K. Nakatani, *Biochem. Biophys. Res. Commun.* **2008**, *366*, 275.

[9] Y. Terui, M. Ohnuma, K. Hiraga, E. Kawashima, T. Oshima, *Biochem. J.* **2005**, *388*, 427.

[10] H. Robinson, A. H.-J. Wang, *Nucleic Acids Res.* **1996**, *24*, 676.

[11] P. Terrier, J. Tortajada, G. Zin, W. Buchmann, *J. Am. Soc. Mass Spectrom.* **2007**, *18*, 1977.

[12] T. J. Thomas, U. B. Gunnia, T. Thomas, *J. Biol. Chem.* **1991**, *266*, 6137.

[13] M. H. Park, Y. A. Joe, K. R. Kang, Y. B. Lee, E. C. Wolff, *Amino Acids* **1996**, *10*, 109.

[14] S. Miyamoto, K. Kashiwagi, K. Ito, S. Watanabe, K. Igarishi, *Arch. Biochem. Biophys.* **1993**, *300*, 63.

[15] K. Mikulik, M. Anderova, *Arch. Microbiol.* **1994**, *161*, 508.

[16] K. Igarishi, T. Saisho, M. Yuguchi, K. Kashiwagi, *J. Biol. Chem.* **1997**, *272*, 4058.

[17] Y. He, T. Suzuki, K. Kashiwagi, K. Kusama-Eguchi, A. Shirahata, K. Igarishi, *Eur. J. Biochem.* **1994**, *221*, 391.

[18] B. Frydman, W. M. Westler, K. Samejima, *J. Org. Chem.* **1996**, *61*, 2588.

[19] K. Williams, *Biochem. J.* **1997**, *325*, 289.

[20] K. Strømgaard, I. Mellor, *Med. Res. Rev.* **2004**, *24*, 589.

[21] K. Kashiwagi, A. J. Pahk, T. Masuko, K. Igarashi, K. Williams, *Mol. Pharmacol.* **1997**, *52*, 701.

[22] R. J. Bergeron, W. R. Weimar, Q. Wu, Y. Feng, J. S. Mc Manis, *J. Med. Chem.* **1996**, *39*, 5257.

[23] B. Matkovics, V. Kecskemeti, S. Z. I. Varga, Z. Novak, Z. S. Kertesz, *Comp. Biochem. Physiol.* **1993**, *104B*, 475.

[24] G. M. Gilad, V. H. Gilad, *Biochem. Pharmacol.* **1992**, *44*, 401.

[25] A. Antonello, R. Banzi, M. L. Bolognesi, A. Minarini, M. Rosini, V. Tumiatti, C. Melchiorre, *Med. Res. Rev.* **2003**, *23*, 200.

[26] M. L. Bolognesi, V. Andrisano, M. Bartolini, R. Banzi, C. Melchiorre, *J. Med. Chem.* **2005**, *48*, 24.

[27] C. Gomes-Trolin, I. Nygren, S.-M. Aquilonius, H. Askmark, *Exp. Neurol.* **2002**, *177*, 515.

[28] V. Tumiatti, V. Andrisano, R. Banzi, M. Bartolini, A. Minarini, M. Rosini, C. Melchiorre, *J. Med. Chem.* **2004**, *47*, 6490.

[29] C. M. Gilbo, N. W. Coles, *Aust. J. Biol. Sci.* **1964**, *17*, 758.

[30] V. J. Jasys, P. R. Kelbaugh, D. M. Nason, D. Phillips, K. J. Rosnack, N. A. Saccomano, J. G. Stroh, R. A. Volkmann, *J. Am. Chem. Soc.* **1990**, *112*, 6696.

[31] G. B. Quistad, S. Suwanrumpha, M. A. Jarema, M. J. Shapiro, W. S. Skinner, G. C. Jamieson, A. Lui, E. W. Fu, *Biochem. Biophys. Res. Commun.* **1990**, *169*, 51.

[32] G. B. Quistad, C. C. Reuter, W. S. Skinner, P. A. Dennis, S. Suwanrumpha, E. W. Fu, *Toxicon* **1991**, *29*, 329.

[33] Y. Itagaki, T. Fujita, H. Naoki, T. Yasuhara, M. Andriantsiferana, T. Nakajima, *Nat. Toxins* **1997**, *5*, 1.

[34] T. Fujita, Y. Itagaki, H. Naoki, T. Nakajima, K. Hagiwara, *Rapid Commun. Mass Spectrom.* **1995**, *9*, 365.

[35] M. Hisada, T. Fujita, H. Naoki, Y. Itagaki, H. Irie, M. Miyashita, T. Nakajima, *Toxicon* **1998**, *36*, 1115.

[36] T. Fujita, Y. Itagaki, M. Hisaka, H. Naoki, T. Nakajima, M. Andriantsiferana, *Rapid Commun. Mass Spectrom.* **1997**, *11*, 1115.

[37] M. S. Palma, Y. Itagaki, T. Fujita, M. Hisada, H. Naoki, T. Nakajima, *Nat. Toxins* **1997**, *5*, 47.

[38] S. Chesnov, L. Bigler, M. Hesse, *Helv. Chim. Acta* **2000**, *83*, 3295.

[39] S. Chesnov, L. Bigler, M. Hesse, *Helv. Chim. Acta* **2001**, *84*, 2178.

[40] S. Chesnov, L. Bigler, M. Hesse, *Eur. J. Mass Spectrom.* **2002**, *8*, 1.

[41] N. Manov, M. Tzouros, S. Chesnov, L. Bigler, S. Bienz, *Helv. Chim. Acta* **2002**, *85*, 2827.

[42] M. Tzouros, N. Manov, S. Bienz, L. Bigler, *J. Am. Soc. Mass Spectrom.* **2004**, *15*, 1636.

ORGANIZATION OF THE TREATISE, GOALS AND OBJECTIVES

The research presented in this treatise deals primarily with the mass spectrometric investigation of polyamine derivatives, particularly of compounds contained in spider venom. It consists of four separate chapters describing our detailed analytical investigations. Each chapter is independent from the others and has its own numbering of the schemes, figures, substances, and references.

Chapter 1 presents the results of our first objective, which was the study of some acylpolyamines of *Agelenopsis aperta* that evaded full structural elucidation in earlier investigations.

> While most of the toxins of *A. aperta* have been fully characterized, some of them remained structurally undisclosed. It was claimed, for instance, that a number of isomeric compounds must exist that differ in the positions of a hydroxy group in the chromophoric part of the molecules. A preliminary re-investigation of the venom suggested, however, that these "isomeric compounds" were rather artifacts, formed during APCI (atmospheric pressure chemical ionization), than real natural products.
>
> It was thus the goal to verify the nature of the previously undisclosed polyamine toxins of *A. aperta* and, if it in fact turns out that artifact formation occurs during ionization, to study the reactions leading to these artifacts. Furthermore, we were encouraged develop a method to recognize such reactions in order to avoid misinterpretation of analytical data.

Chapter 2 describes the development and first application of a new extended analytical procedure allowing the unambiguous characterization of polyamine derivatives of higher structural complexity.

Screening of the venoms of twenty different spider species revealed that the venom of *Larinioides folium* contains numerous toxins that could not be structurally elucidated with the method that has been used in our laboratories so far.

The goal of the second part of the PhD research was to extend or modify the hitherto applied analytical procedure in a way that it reveals also the structures of toxins of more complex composition.

Chapter 3 can be regarded as a sequel to *Chapter 2* in the sense that the analytical procedure developed in the previous investigation is applied to the study of new venoms.

The goal of this part was to show with the analysis of the venoms of *Ozyptila lugubris*, *Lachesana sp.*, and *Drassodes sp.*, that the new procedure allows for the structural elucidation of hitherto unknown acylpolyamines of new spider sources.

Chapter 4 is meant to serve as a reference for chemists that are no MS specialists but are more deeply interested in the mass spectrometric aspects of the investigations presented in *Chapter 2* and *3*.

Since *Chapter 2* and *3* are conceptually designed as full papers to be published in specialized journals on mass spectrometry, some aspects of mass spectrometry might not have obtained enough weight for non-specialists.

It was the goal of this part of the treatise to present the methods used to attain the results presented in the *Chapters 2* and *3* in more detail to the scientifically educated, but not analytically specialized audience. We also discuss the potential impact of the newly developed analytical procedure for mass spectrometric investigations in a more general context.

CHAPTER 1

Decomposition of *N*-Hydroxylated Compounds During APCI

Abstract

N-Hydroxylated polyamine derivatives were found to decompose during the ionization process of HPLC-APCI-MS experiments. The phenomenon was studied with a model compound, a synthetic *N*-hydroxylated tetraamine derivative. It was found that reduction, oxidation, and elimination of H_2O occurred with the N-OH-functionalized compound upon APCI, leading to the corresponding amine, *N*-oxide, and imine. The investigation further revealed that the APCI decomposition of hydroxylamines is dependent on the concentration of the analyte and on the acidity of the solution introduced into the ionization source. The pH-dependence of the decomposition reactions — artifact formation can likewise be enforced or inhibited by the addition of acid or base, respectively — was utilized for the development of an MS method that allows the identification of N-OH functionalities within sample compounds. The method was applied for the study of some natural products: polyamine toxins from the venom of the spider *Agelenopsis aperta* and mayfoline, a cyclic polyamine derivative of the shrub *Maytenus buxifolia*.

1.1 Introduction

Over the last two decades, electrospray ionization (ESI) and atmospheric pressure chemical ionization (APCI) have been established as two of the most important ionization techniques for mass spectrometry. The methods have been proven to be of particular value for analytical setups in which mass spectrometry is on-line coupled to liquid chromatography (LC/MS). Since ESI and APCI represent very mild ionization methods, they typically produce solely quasi-molecular ions of the analytes; fragmentations of the sample molecules are observed only occasionally. Hence, the ions generated by ESI and APCI usually provide direct and unequivocal information about the sample molecules. Such unambiguous information, however, is not obtained when the analytes undergo fragmentations or decompositions prior to the MS analysis, *e.g.*, before or during the ionization process. Chemical transformations of this kind lead to artifacts, and misinterpretation of MS data might occur.

The formation of artifacts is actually not problematic, as long as knowingly pure sample compounds are investigated and the decomposition reactions are not proceeding to completion. If mixtures of compounds are studied, however, or if the rate of decomposition is high enough to run to completion, artifacts might be erroneously interpreted as real sample compounds. For more complex investigations, particularly for the investigation of natural products arising as mixtures, it is, thus, of relevance to be aware of potential decomposition reactions.

In particular with APCI, for which the analyte solutions are typically heated to 300 – 400 °C prior to ionization, the risk of formation of artifacts can be expected to be relatively high. This could allow for thermally induced decomposition. In fact, decomposition reactions during APCI were found, *e.g.*, in MS investigations of aromatic nitro compounds [1,2], *N*-oxides [3-7], and imines [8]. Upon APCI, all three types of oxidized N-containing compounds were partially reduced to the corresponding amines. Recently, analogous

reactions were also observed in the course of our investigations of spider venoms [9-12]. *N*-hydroxylated polyamine derivatives were found to be partially reduced to the respective amines upon APCI. These reduction products, however, were not detected when an ESI source was used. To the best of our knowledge, the formation of artifacts from *N*-hydroxylated compounds during APCI has not been reported in literature so far. Considering the fact that (1) *N*-hydroxylamines are frequent constituents of natural samples and also potential metabolites of drugs and (2) LC-APCI-MS is widely used for the study of natural products and drug metabolism, the lack of awareness of this APCI-reduction could broadly lead to wrong conclusions. Since APCI cannot be replaced in all cases by ESI, particularly due to the higher sensitivities that can be attained for some compound classes with this method [11], we were interested to learn more about in-source reactions occurring during APCI. Such an investigation would possibly allow us to gain a better knowledge of their prerequisites, and, thus, to obtain a means to recognize and control them.

The following study presents the APCI investigation of a synthetic *N*-hydroxylated polyamine derivative and the application of the obtained cognitions for the development of a method that allows the identification of the hydroxylamine functionality within a sample molecule.

1.2 Results and Discussion

1.2.1 Investigations with Synthetic *N*-Hydroxylated Compounds

Tetraamine derivative **1** (*Figure 1*) was chosen as the sample compound for our study of the APCI behavior of *N*-hydroxylated secondary amines from a number of *N*-hydroxylated polyamine derivatives that were prepared in connection with our synthetic approaches towards polyamine spider toxins [13]. This for four major reasons: (1) The core structure of **1** is closely related to the *N*-hydroxylated acylpolyamines found in spider venoms, which are the compounds of central interest to our ongoing research program. They are all composed of a polyamine that is hydroxylated at an internal N-atom. (2) The compound possesses a nitroaryl group. Aromatic nitro groups are known from literature to undergo reductive decomposition upon APCI [1], which allows, thus, the concurrent study of the decomposition rates of *N*-hydroxy and aromatic nitro functionalities. (3) The three amine functionalities of the tetraamine derivative **1** are all protected, internally with the 2-nitrobenzenesulfonyl (Ns) and terminally with two phthaloyl groups (Phth). The fully protected compounds allowed an efficient purification of the synthetic product by HPLC. (4) Preliminary APCI-measurements revealed that compound **1** underwent rather readily the decomposition reactions to be investigated, significantly more readily than other *N*-hydroxylated polyamine compounds that were available in our laboratories.

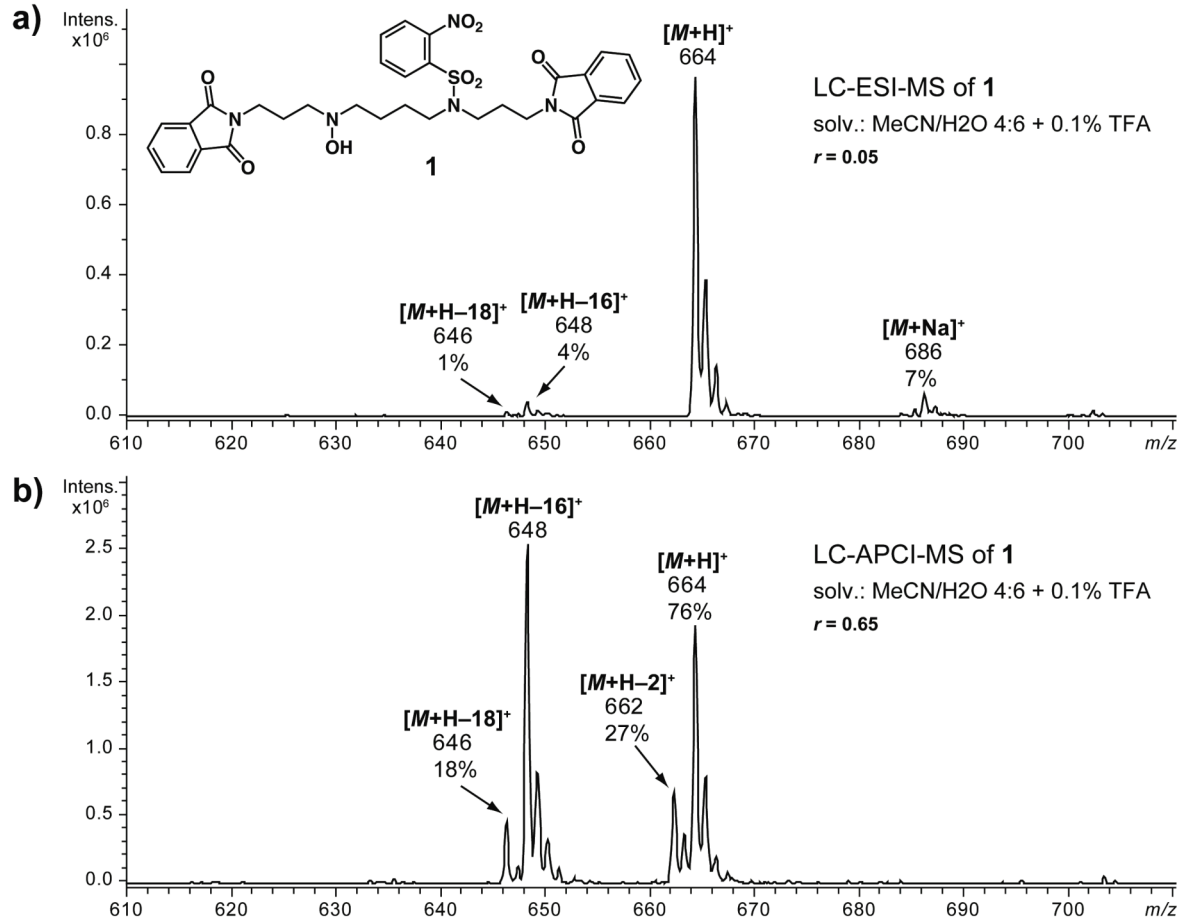

***Figure 1**. (**a**) HPLC-ESI-MS and (**b**) HPLC-APCI-MS of* N*-hydroxylated tetraamine derivative **1** in MeCN/H_2O (4:6) + 0.1% TFA.*

The investigation of the MS behavior of compound **1** started with two HPLC-API-MS runs performed with an ESI and an APCI source under conditions usually applied for the analyses of polyamine spider toxins. The HPLC-ESI-MS spectrum of the chromatographic peak of **1** showed the expected signal for the protonated molecule $[M+H]^+$ at *m*/*z* 664 (base peak) and a weak signal relating to ions of the type $[M+Na]^+$ (*m*/*z* 686, 7%, *Figure 1a*). Also registered were two further signals at *m*/*z* 648 (4%) and *m*/*z* 646 (1%) corresponding to ions of the type $[M+H–16]^+$ and $[M+H–18]^+$, respectively. Usually, ions with such a low relative abundance would not be further considered. These signals, however, became relevant when APCI was used instead of ESI. The spectrum obtained by HPLC-APCI-MS (*Figure 1b*) showed in addition to the expected signal for the protonated molecule $[M+H]^+$ at *m*/*z* 664 (76%) — no $[M+Na]^+$ ions were registered — the two previously mentioned ions $[M+H–16]^+$ at *m*/*z* 648 (base peak) and $[M+H–18]^+$ at *m*/*z* 646 (18%) with significant intensities. A

third signal that cannot be ignored as well was found at *m*/*z* 662 (27%), corresponding to $[M+H-2]^+$ ions. Since it was shown by HPLC and by NMR that the sample compound was pure, these three additional ions have to be generated by in-source decomposition of **1,** and are not due to impurities.

A term *r* with the following equation is introduced to estimate the extent of the overall decomposition of **1** occurring in different experiments:

$$r = \frac{\sum I_{DP_i}}{I_{QMI} + \sum I_{DP_i}} = \frac{I_{[M+H-2]^+} + I_{[M+H-16]^+} + I_{[M+H-18]^+}}{I_{[M+H]^+} + I_{[M+H-2]^+} + I_{[M+H-16]^+} + I_{[M+H-18]^+}}$$

with I_{DP_i} = ion abundance of the decomposition products and I_{QMI} = ion abundance of the protonated molecule. Although *r* is not the actual molecular ratio of the three decomposition products and the initial concentration of **1**, it can still be regarded as a qualitative measure to describe the extent of decomposition of **1**, allowing, therefore, the characterization of different experiments.

The structures of the three ions detected at *m*/*z* 648, 662, and 646 — and thus the structures of the artifacts formed in the ion source — were deduced from the data acquired by HPLC-APCI-MS/MS and their measured accurate masses obtained by high-resolution ESI-MS of sample compound **1**. The measured exact masses of $[M+H]^+$, $[M+H-16]^+$, and $[M+H-18]^+$ revealed that the artifacts $[M+H-16]^+$ and $[M+H-18]^+$ were generated by formal losses of O and H_2O from **1**, respectively. No high-resolution MS data was available for the signal at *m*/*z* 662 ($[M+H-2]^+$). However, the loss of H_2 from the parent compound **1** appears to be the most reasonable process that could lead to an artifact responsible for the respective signal.

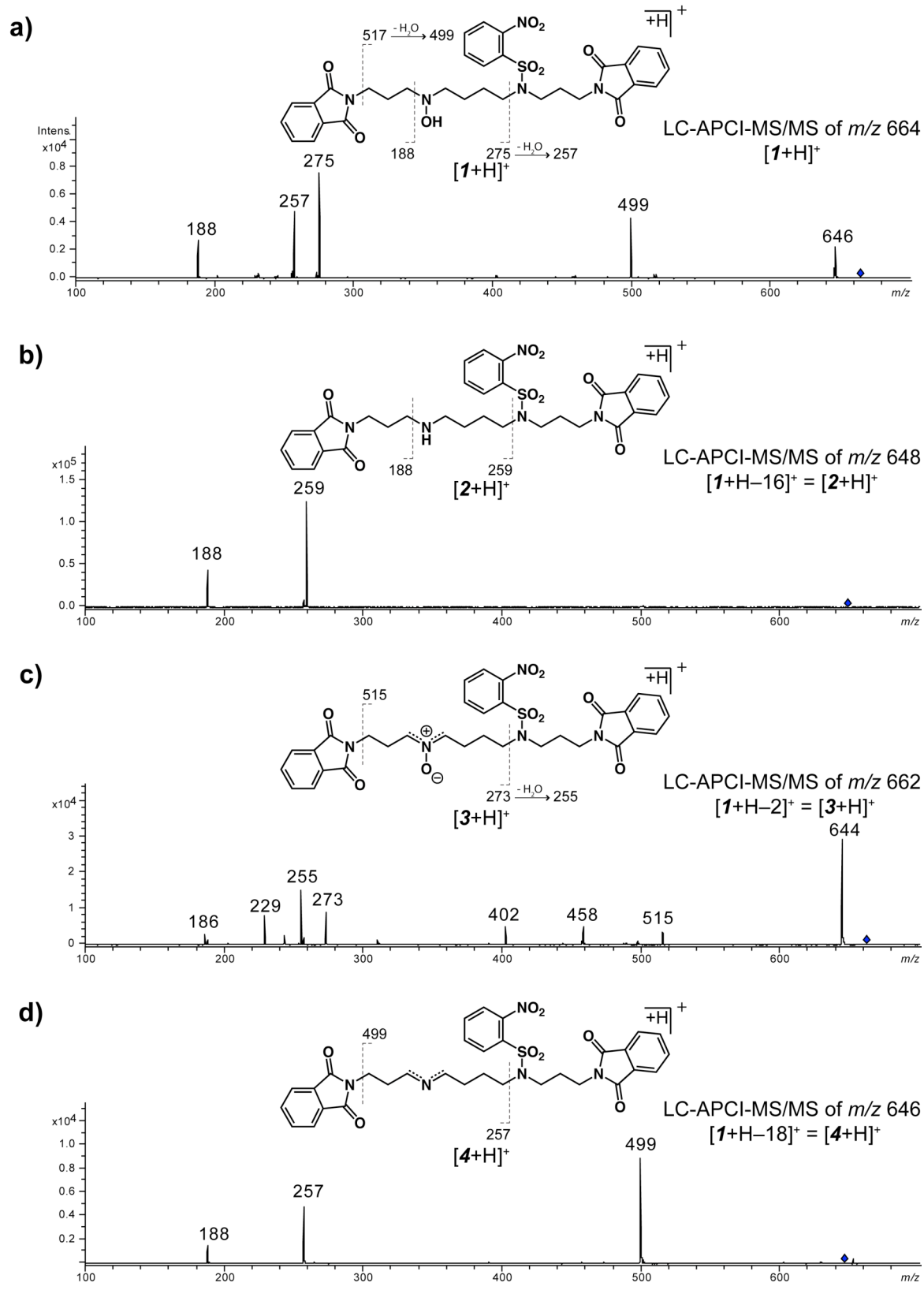

***Figure 2**. HPLC-APCI-MS/MS of (**a**) [**1**+H]$^+$, (**b**) [**1**+H–16]$^+$ = [**2**+H]$^+$, (**c**) [**1**+H–2]$^+$ = [**3**+H]$^+$, and (**d**) [**1**+H–18]$^+$ = [**4**+H]$^+$ ions with proposed structures and assignments of relevant fragment ions.*

The MS/MS spectra characterized the structures of the artifacts formed in the ion source as amine **2**, nitrone **3**, and imine **4** (in protonated forms, *Figure 2*). The loss of oxygen to form product **2** can occur either at the N-OH position or at the NO_2/SO_2 groups of the nosyl portion. The data revealed, however, that reduction took place at the hydroxylamine position only. While fragment ions at *m/z* 275 were observed for compound **1**, the respective signal — which should be the same if deoxygenation would occur at the NO_2 or SO_2 groups — was not found in the MS/MS of **2** (*Figure 2b* and *Scheme 1a*). Instead, a signal was registered at *m/z* 259, which is consistent with an amine instead of a hydroxylamine functionality in the "left-part" of the molecule (*Scheme 1b*). The fact that no ion response at *m/z* 275 was observed concluded that deoxygenation occurred solely at the N-OH group. Therefore, the concurrent previously described APCI deoxygenation of NO_2 to NO did not take place [1]. The eliminations of H_2 (formation of **3**) and of H_2O (formation of **4**) from sample compound **1** also occurred with the N-OH functional group rather than with other groups contained in the molecule. Analogously to **2**, the MS/MS of artifacts **3** and **4** showed no ion signals at *m/z* 275 but signals at *m/z* 273 and *m/z* 257, respectively, which are diagnostic for decomposition located in the "left-part" of the molecules (*Figure 2c* and *d*).

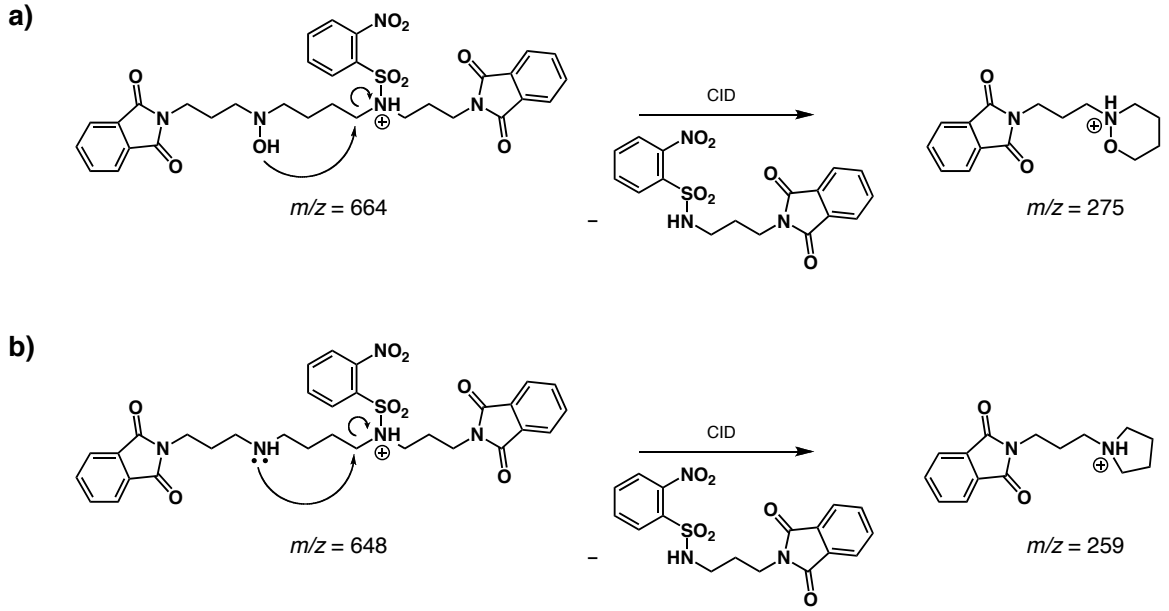

***Scheme 1**. Formation of diagnostic fragment ions at (**a**) m/z 275 and (**b**) m/z 259 from the precursor ions [**1**+H]⁺ and [**2**+H]⁺, respectively.*

The concurrent APCI decomposition of the aromatic NO_2 group of **1** to the respective amine did not occur, since the corresponding signal for the reduction product $[M+H-30]^+$ at *m*/*z* 634 was not detected. Thus, only decomposition of the N-OH but not of the aromatic nitro group was observed by APCI-MS of **1**. Hence, the decomposition of *N*-hydroxylated compounds during APCI is much more prominent compared to the previously described decomposition of aromatic nitro compounds [1].

1.2.1.1 Dependence of the APCI Decomposition of Hydroxylamines on the Sample Concentration

The online coupling of HPLC to MS allows fast acquisition of MS data of an analyte directly after column chromatography. Thus, mass spectra of different concentrated analyte solutions can be measured when reasonably broad chromatographic peaks were obtained. HPLC-APCI-MS of **1** (1 μg) afforded a chromatographic peak sufficiently broad to allow it splitting into several segments of 0.1 min, which represent different concentrated analyte solutions. The averaged concentration of each segment was estimated on the basis of the relative segment areas (*Figure 3*). The two segments with low analyte concentration at the beginning and at the end of the peak (approx. 1.8 and 0.8 μM) showed rather high degrees of decomposition (r = 0.86 @ rt 20.6–20.7 min and r = 0.90 @ rt 21.7–21.8 min, respectively). Still prominent but significantly less decomposition was observed with the segment taken at the peak maximum (r = 0.65 @ 21.0–21.1 min). The effect that less decomposition was observed when more highly concentrated solutions were investigated is general and was also recognized in other measurements, *e.g.*, in those performed with natural samples of polyamine spider toxins. This result suggests, in accordance with previously described studies, that APCI decompositions are surface-supported processes, which are controlled in their extent by the limited surface of the APCI interface [8].

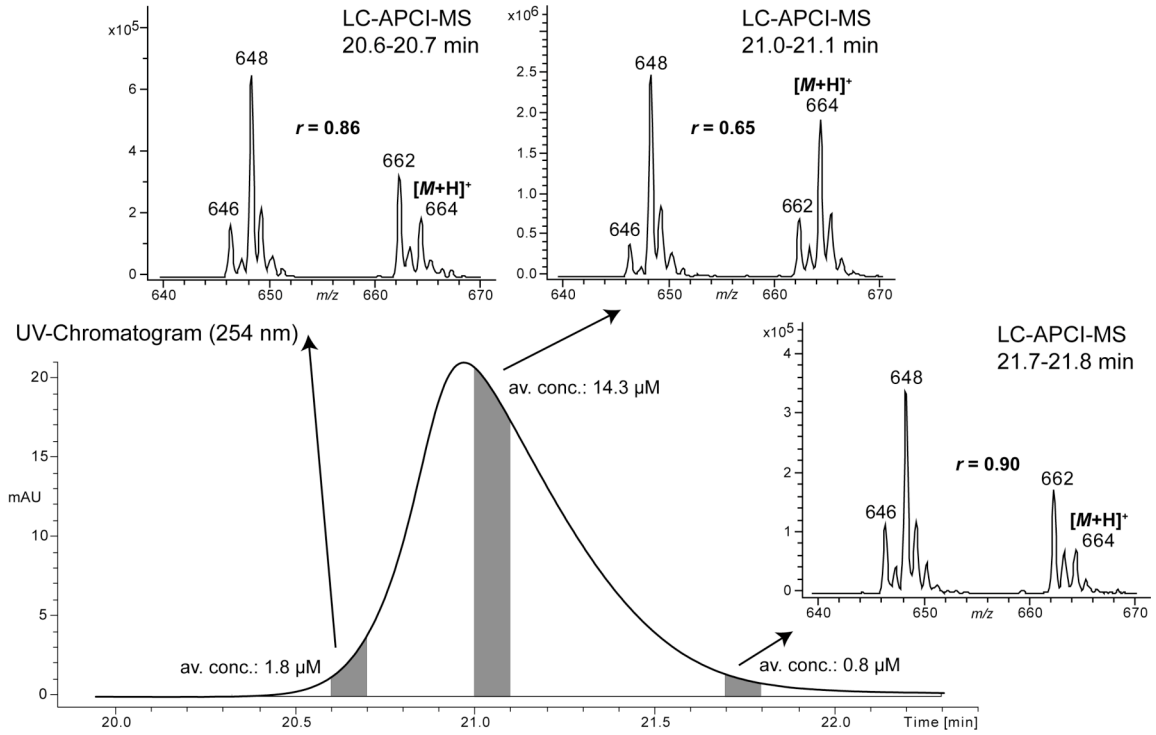

***Figure 3**. Concentration dependence of the APCI reduction of hydroxylamines shown with segments of a chromatographic peak of **1**.*

1.2.1.2 Dependence of the APCI decomposition of Hydroxylamines on the Acidity of the Solvent

Direct infusion APCI-MS experiments were performed to study the pH dependence of the APCI decomposition. Compound **1** was dissolved either in pure MeCN/H_2O (1:1) or in MeCN/H_2O (1:1) admixed with TFA, HCOOH, or TFA followed by NH_3 until neutralized, respectively (*Figure 4*). It is readily recognized from the spectra shown in *Figure 4* that increased acidity of the sample solutions led to more pronounced decomposition. While almost no decomposition of compound **1** was observed when the sample was introduced into the APCI-MS dissolved in the mixture of MeCN/H_2O (1:1) (r = 0.1, spectrum a, *Figure 4*), the decomposition rate of **1** increased markedly in presence of HCOOH or TFA. (r = 0.38 and 0.54, respectively, spectra b and c, *Figure 4*). Thus, the highest decomposition rate was observed with 0.1% TFA as the additive, which are the standard conditions used for the chromatographic separation of spider toxins. *Vice versa*, decomposition of **1** can be inhibited upon addition of base (r = 0.04, *Figure 4d*). Only little decomposition was observed, when NH_3 was added to the acidic solution of

experiment c (MeCN/H_2O (1:1) + 0.1% TFA) prior analysis. This experiment shows that the decomposition of **1** occurs in fact in the ion source and not already before its entry into the instrument.

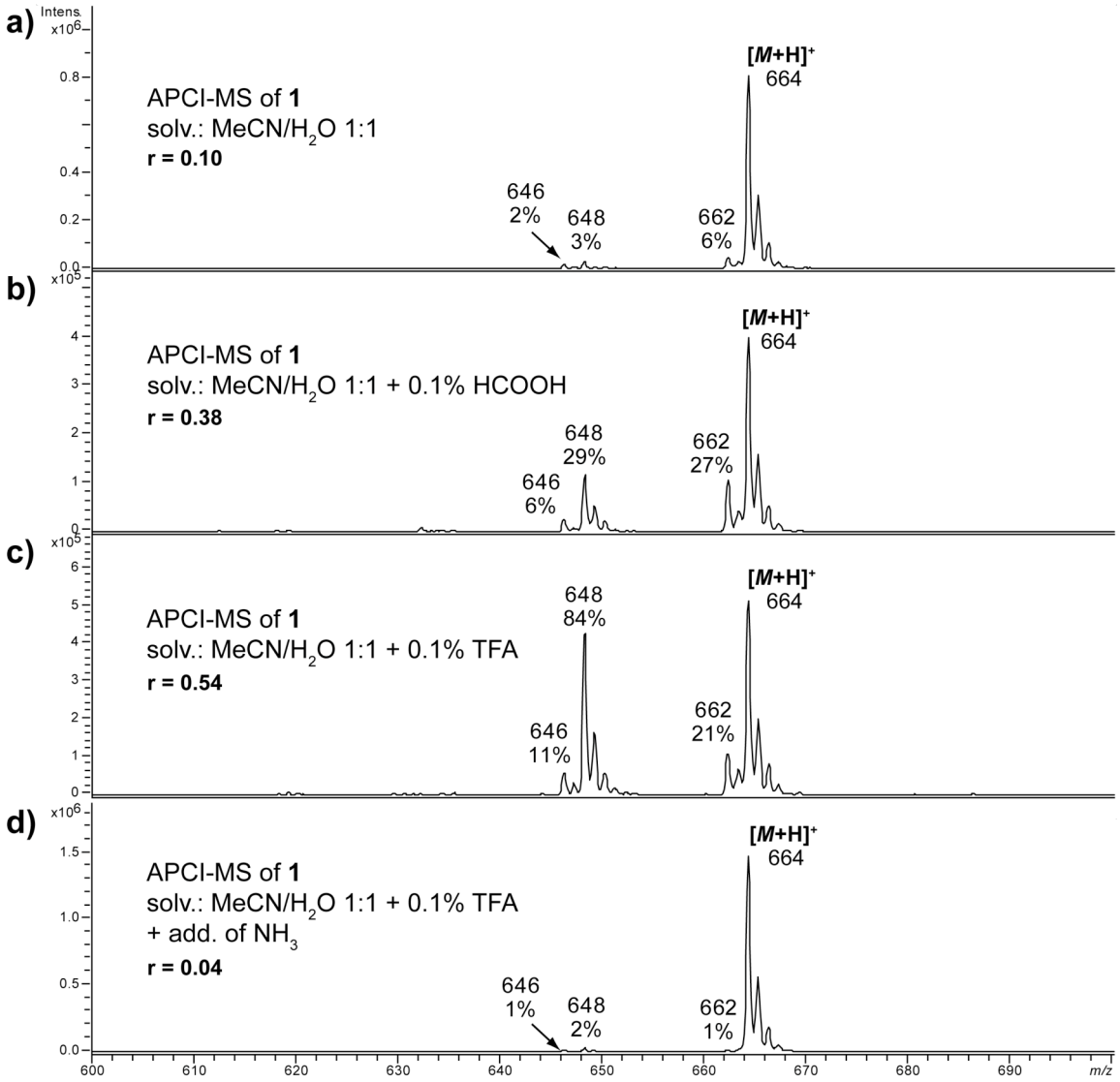

***Figure 4**. Direct infusion APCI-MS experiments performed with compound **1** dissolved (**a**) in pure MeCN/H_2O (1:1), or in MeCN/H_2O (1:1) admixed with (**b**) HCOOH, (**c**) TFA, or (**d**) TFA followed by addition of NH_3 until neutralized.*

The pH-dependence of the APCI decomposition of hydroxylamines can be taken as a means to identify the N-OH functionality of a molecule. If a compound shows $[M+H-H_2]^+$ and, particularly, $[M+H-O]^+$ signals in APCI-MS spectra ($[M+H-H_2O]^+$ ions are not diagnostic since elimination of H_2O is too common a process in MS), and if the formation of these ions can be enforced or inhibited by addition of acid or base to the sample solution prior

to its introduction into the instrument, the presence of the N-OH group in the molecule is rather likely. It should also be possible to distinguish between artifacts and real sample compounds by inhibition of the APCI decomposition. On the other hand, if no ions of the type $[M+H-H_2]^+$ and $[M+H-O]^+$ can be found for a compound — not even when the sample solution is acidified —, an N-OH group is most likely not present in the sample molecules. In the following, the pH-dependence of the APCI decomposition of hydroxylamines is used for the unequivocal recognition of native polyamine toxins of the spider *Agelenopsis aperta* and for the identification of the N-OH group as a functionality contained in mayfoline, a cyclic polyamine derivative of the shrub *Maytenus buxifolia* [14].

1.2.2 HPLC-APCI-MS Analysis of the Venom from the Spider *Agelenopsis aperta*

Over the last decade, HPLC-MS and -MS/MS became the methods of choice for the investigation of polyamine spider toxins — compounds of interest in connection with several diseases [15-19]. In our laboratories, HPLC-APCI-MS and -MS/MS was used for the study of the fragmentation behavior of acylpolyamines and the characterization of polyamine toxins contained in various spider venom [9-12,20]. Some years ago, acylpolyamines of the venoms of *A. aperta* [10] and of *Paracoelotes birulai* [9] were characterized by means of this analytical setup.

In these two spider species, also several *N*-hydroxylated polyamines derivatives were found. While most of the constituents have been fully characterized and structurally elucidated, some structures could not be completely assigned. For instance, it was claimed that "three pairs of compounds… with the same quasi-molecular ion at *m*/*z* 433 and close but, nevertheless, different t_R, had identical MS/MS data", and it was concluded, that the respective two compounds would differ in the position of the hydroxy group in the chromophoric head moiety — a structural information that is not accessible from MS data. In the mean time, synthetic access to several of the proposed structural variations was gained. While the synthetic 4-hydroxy-1*H*-

indole-3-acetamide (4-OH-IndAc) derivatives found their match in the natural samples, the other isomers hydroxylated at position 5 and 6 of the indole portion could not be connected to any of the natural compounds [21]. The discovery that hydroxylamines get reduced upon APCI, particularly under the acidic conditions that are used for the HPLC of spider venom, encouraged us for the re-investigation of the venom of *A. aperta*, since the several undisclosed toxins might have been in reality artifacts. This is actually the case.

The 2D-plot (a) in *Figure 5* summarizes the ion responses of all constituents of the acylpolyamine fraction of *A. aperta* investigated by HPLC-APCI-MS. Through the coupling of the HPLC to a mass spectrometer, protonated molecules of co-eluting components or artifacts differing in molecular masses were further separated by mass selection, thus adding the second dimension to the separation. The spots in the chromatogram thus represent ion responses registered in dependence on retention times (abscissa) and *m*/*z* values (ordinate).

It is striking to note the signal doublets and triplets characterized by the same t_R and by *m*/*z* values differing by 16 u on inspections of the 2D-plot. Scrutiny of the MS/MS of the respective ions revealed that the triplets represent ions of di-, mono-, and non-*N*-hydroxylated polyamine derivatives and the doublets of mono- and non-*N*-hydroxylated polyamine derivatives, in each case sharing the polyamine backbones. Applying the acquired knowledge of the APCI reduction of hydroxylamines, the signals of the "deoxygenated" structures were most likely due to APCI artifacts than the response of real sample compounds. This hypothesis is supported by the fact that matching signals were found for some of the potential APCI reduction products that showed very similar MS/MS but were recorded at different retention times. For instance, the MS/MS of signal A (singlet) — shown to be the response to a mixture of the three isomeric, non-*N*-hydroxylated pentamine derivatives **5**–**7** (*Scheme 2)* [21] — was almost the same as that of peak at *m*/*z* 433 of doublet B. This fits nicely to the hypothesis that the signal at *m*/*z* 433 of doublet B is due

to artifacts formed during APCI by deoxygenation of the toxins **8**+**9** registered as the signal at *m*/*z* 449 of doublet B.[1] Similar correlations were found with other signal doublets and also with signal triplets, where di-*N*-hydroxylated polyamine derivatives are registered together with corresponding mono- and non-*N*-hydroxylated polyamine derivatives. In the case of the signal triplets, however, no exact matches of the MS/MS spectra of the assumed mono-deoxygenated APCI artifacts and native deoxygenation products were found. This is reasonable since mono-deoxygenation of a di-*N*-hydroxylated polyamine toxin during APCI would be expected to produce non-selectively a mixture of regioisomeric mono-*N*-hydroxylated derivatives while the natural mono-*N*-hydroxylated products were found to be consistently hydroxylated at the first N-atom subsequent to the N-acyl group, only.

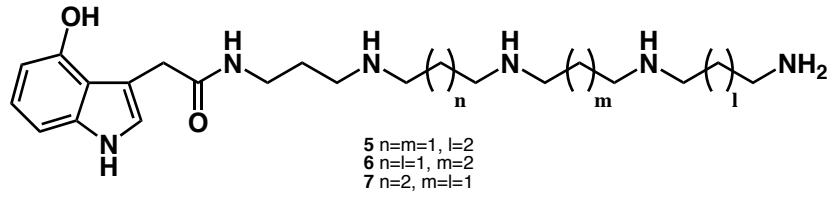

5 n=m=1, l=2
6 n=l=1, m=2
7 n=2, m=l=1

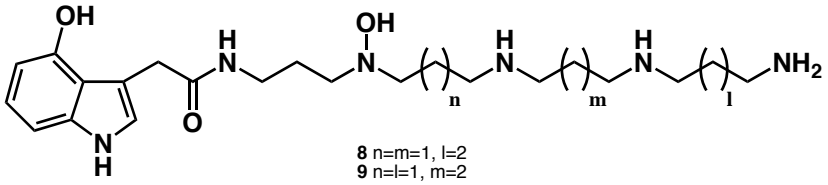

8 n=m=1, l=2
9 n=l=1, m=2

Scheme 2: *Structures of investigated acylpolyamines from* A. aperta.

[1] The MS/MS of the two mass spectral peaks at *m*/*z* 433 of signal A and B are slightly different, because diagnostic fragment ions of compound **7** are only detected by MS/MS of the protonated molecules of the naturally occurring compounds **5** – **7**. This sounds reasonable because of the fact that only the two isomers **5** and **6** but not **7** can be generated during the APCI-reduction of the toxins **8** and **9**. The difference, however, is not significant, since compound **7** is represented only in low concentration compared to the co-eluting isomers **5** and **6** in the natural sample, and therefore, the diagnostic fragment ions generated from **7** are low abundant.

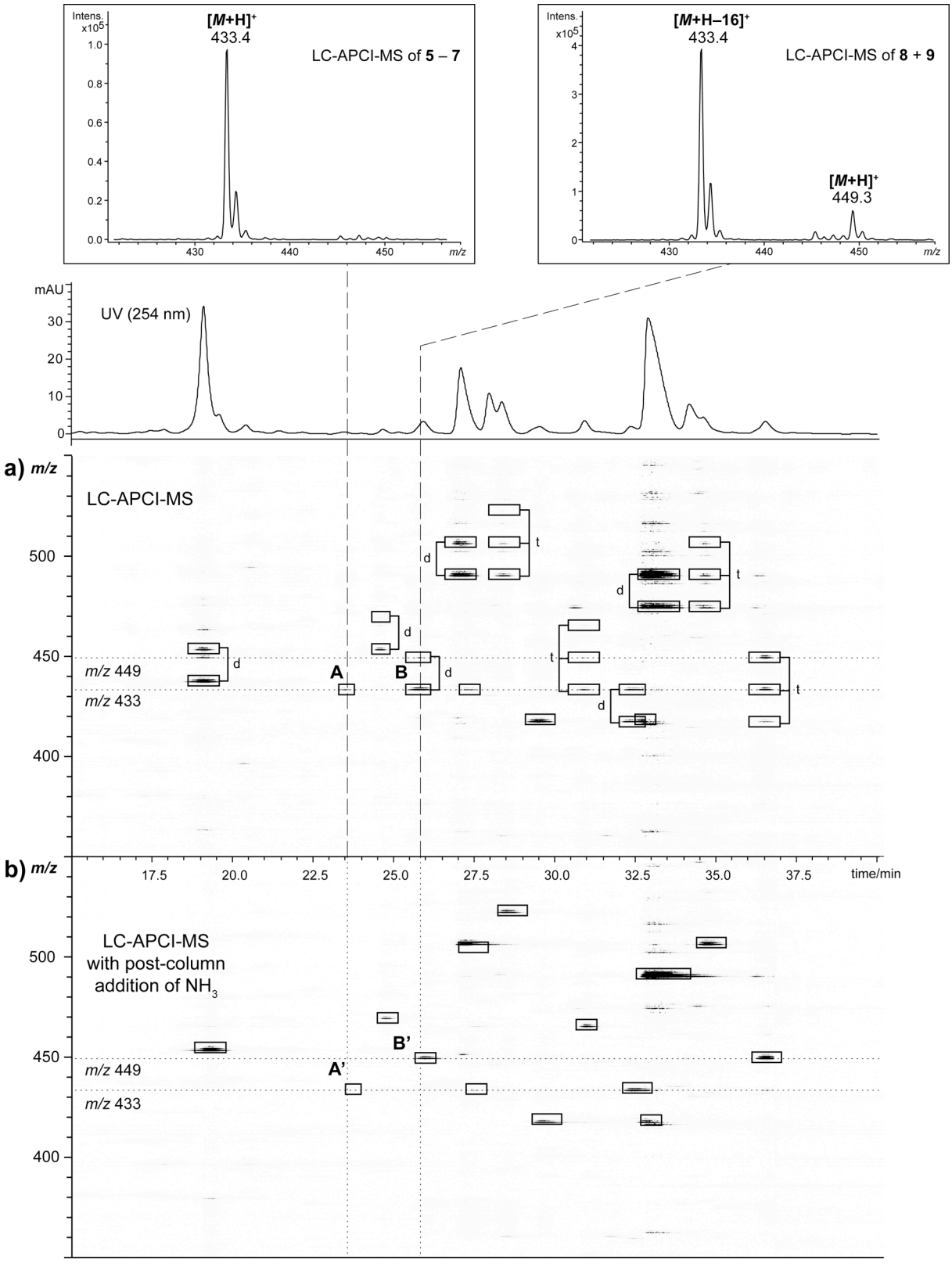

***Figure 5**. 2D-plot of an HPLC-APCI-MS run of A. aperta venom and the corresponding UV-chromatogram detected at λ = 254 nm using (**a**) MeCN/H_2O + 0.1% TFA as the mobile phase and (**b**) the same conditions but with post-column addition of NH_3. d designates a signal doublet and t a signal triplet.*

To prove that the doublets and triplets recorded in the 2D-chromatogram arise in fact from mono- or di-*N*-hydroxylated parent compounds, an HPLC-APCI-MS of the toxin mixture was acquired with the same (acidic) chromatographic conditions used before — which was necessary to effect the chromatographic separation —, however, with post-column addition of NH_3 to inhibit the APCI decompositions. The respective 2D-plot is shown in *Figure 5b*. It is readily recognized that the doublets and triplets found in *Figure 5b* largely disappeared, which allows the conclusion that the several vanished peaks arose from artifacts rather than from native compounds.

Evidently, analogously to the synthetic *N*-hydroxylated compound **1** – also *N*-hydroxylated acylpolyamines of spider venom underwent in-source decomposition during HPLC-APCI-MS experiments. The re-analysis of the venom of *A. aperta* revealed that compounds generated by APCI-decomposition were previously misinterpreted as constituents of the venom. As an example, AG505, which is an *N*(4)-mono-hydroxylated hexamine derivative, and AG489b, the corresponding non-hydroxylated polyamine analog, were considered as co-eluting constituents of the venom. As a matter of fact, however, AG489b was generated by APCI-reduction of AG505, and, therefore, is not a native constituent of the venom. Together with AG489b also AG432b, AG432c, AG432e, AG448b, AG452a, AG432h, and AG432i were unmasked to be artifacts that arose during the APCI-MS measurement.

The eye-catching doublet- and triplet-patterns recognized in the 2D-chromatogram (a) in *Figure 5* can be taken as a count for the number of N-OH groups in a molecule. Thus, two 2D-plots of *N*-hydroxylated (or potentially *N*-hydroxylated) compounds — the analytes introduced into the APCI source once in acidic and once in basic solvents — can, therefore, not only reveal the presence of N-OH groups in a unknown compound but also its number. Since *C*-hydroxy groups are not reduced during APCI-MS – for instance, the APCI-MS of the non-*N*-hydroxylated derivatives **5–7** did not show signals for deoxygenated products – APCI can also be used to distinguish *N*- from *C*-hydroxylation, analogously to the method reported to differentiate *N*-oxides from *C*-hydroxylated compounds [3].

1.2.3 APCI-MS Analysis of Mayfoline

Mayfoline (*Figure 6*) is a cyclic *N*-hydroxylated spermidine alkaloid isolated from the shrub *Maytenus buxifolia* [14]. It was synthesized some years ago by Hesse *et al.* [22] who also provided a sample of the compound for our investigation. Mayfoline was expected to show the same type of APCI decomposition as the model compound **1** and the polyamine spider toxins described above due to the *N*-hydroxy functionality. However, only little decomposition was observed (r = 0.21, *Figure 6a*) when a sample of the natural product was analyzed by HPLC-APCI-MS under the usual conditions applied for the separation of polyamine derivatives (MeCN/H_2O grad. + 0.1% TFA). The expected artificial signals $[M+H-H_2]^+$ and $[M+H-O]^+$ (and $[M+H-H_2O]^+$) were still found but with unexpected low relative intensities of 7% and 12% (8%), despite the high acidity of the solution that was introduced into the APCI source. When a sample of mayfoline was brought into the APCI-MS in neutral solvent (MeCN/H_2O 1:1), even a spectrum with a single signal only, the protonated molecule, was recorded. Thus, mayfoline represents an *N*-hydroxylated compound with little tendency to undergo APCI reduction, and it has to be expected that this compound is not alone with this property.

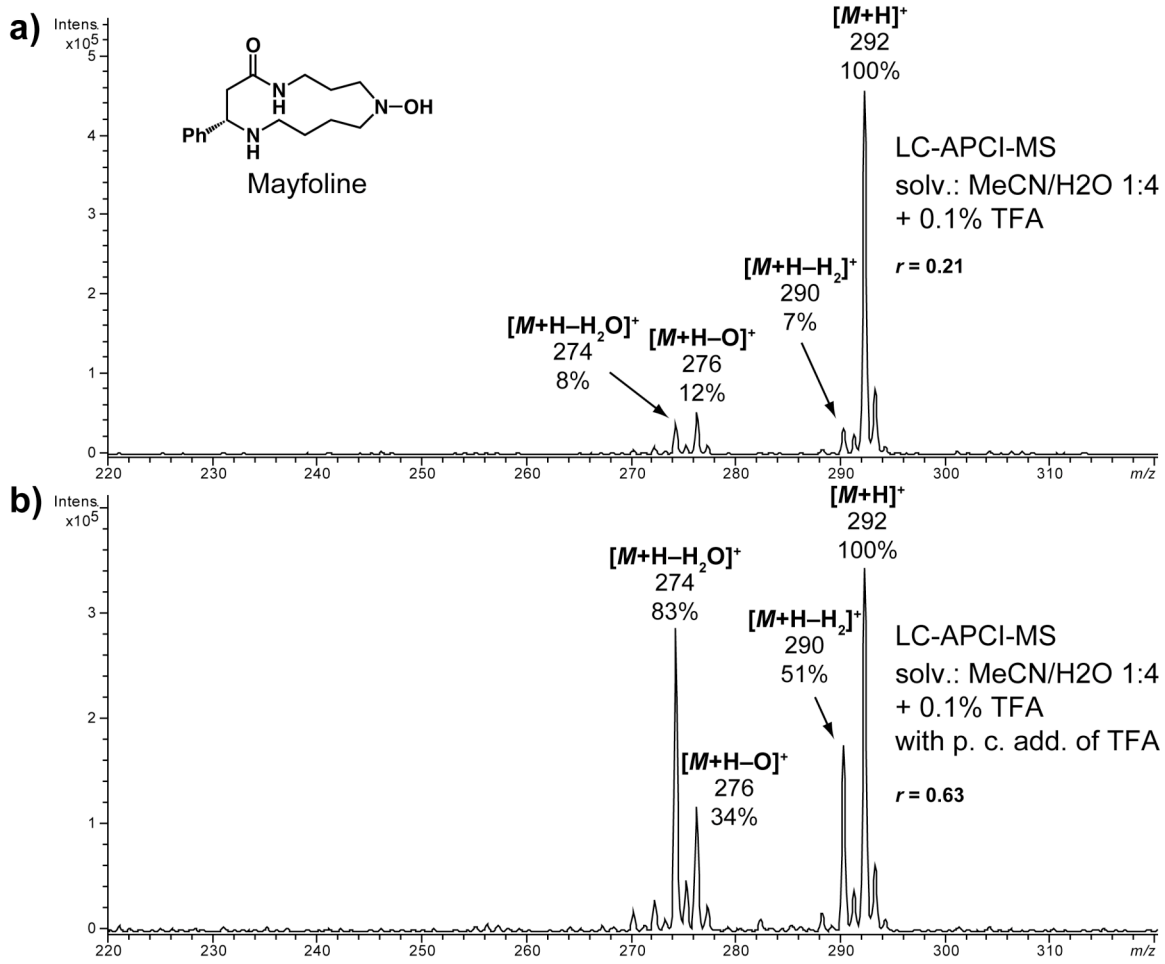

***Figure 6**. HPLC-APCI-MS of mayfoline (**a**) with MeCN/$H_2$0 grad. + 0.1% TFA @ 180 µl min^{-1} and (**b**) with MeCN/$H_2$0 grad. + 0.1% TFA @ 180 µl min^{-1} and post-column addition of MeCN/H_2O/TFA (2:6:2, 20 µl min^{-1}).*

Since APCI deoxygenation was intended to be taken as a conclusive argument for the identification of the N-OH functionality within a sample molecule, it was tested if APCI deoxygenation of mayfoline can be enforced to such a degree that the respective ions are unquestionably recognized. This, in fact, could be affected by the post-column addition of the highly acidic mixture of MeCN/H_2O/TFA (2:6:2) to the analyte flow. Under these conditions, the MS revealed the signals of the decomposition products at *m/z* 290 ($[M+H–H_2]^+$, 51%), *m/z* 276 ($[M+H–O]^+$, 34%), and *m/z* 274 ($[M+H–H_2O]^+$, 83%) with significantly higher intensities (*Figure 6b*). It is to mention at this point that no analogous decomposition (actually no decomposition at all) was observed with a sample of synthetic deoxymayfoline (=(2S)-*1*-hydroxy-2-phenyl-1,5,9-triazacyclo–tridecan-4-one) treated the same way (data not shown).

1.3 Conclusions

The investigation of the various *N*-hydroxylated amines above revealed that N-OH-containing compounds characteristically form artifacts upon APCI. The corresponding decomposition reactions are strongly pH-dependent — to a lesser degree concentration-dependent — and also dependent on the exact molecular structures of the analytes. For all compounds investigated, however, APCI decomposition could be enforced by the addition of sufficient acid to the analyte solution and suppressed by the addition of base.

The knowledge of this rather easily proceeding in-source decomposition of *N*-hydroxylated amines can avoid misinterpretation of MS data that could arise from unknown mixtures, which contain *N*-hydroxylated analytes (particularly of HPLC-MS data for which no additional analytic information is available). The pH-dependence of the APCI decomposition can be applied in two ways: it can be used to (1) distinguish unavoidable artifacts from native compounds — as shown with the investigation of the spider venom of *A. aperta* — or (2) for the conclusive identification of N-OH functionalities within a compound.

1.4 Experimental Part

1.4.1 Chemicals and Sample Preparation

HPLC supra grade acetonitrile (MeCN) was purchased from Scharlau (Barcelona, Spain), trifluoroacetic acid (TFA) and formic acid (HCOOH) from Fluka (Buchs, Switzerland), and aqueous solution of NH_3 (25%) from Merck (Darmstadt, Germany) in the respective highest qualities. HPLC grade H_2O (< 5ppb) was obtained by purification of deionized H_2O with a MilliQ gradient apparatus (Millipore, Milford, MA, USA). [4-Hydroxy-9-(2-nitro-benzenesulfonyl)-4,9-diazadodecane]-1,12-diphthalimide (**1**) was synthesized on solid support and purified by preparative HPLC [13]. Synthetic (–)-(2S)-9-hydroxy-2-phenyl-1,5,9-triazacyclotridecan-4-one (= mayfoline) was obtained

from Hesse [22]. Lyophilized venom of *A. aperta* was purchased from Fauna Laboratories Ltd. (Almaty, Kazakhstan).

1.4.2 Liquid Chromatography and Mass Spectrometry

General: HPLC-MS analyses were performed on a Hewlett-Packard 1100 HPLC system (Hewlett-Packard Co., Palo Alto, CA, USA) fitted with a HTS PAL autosampler (CTC Analytics, Zwingen, Switzerland), a Hewlett-Packard 1100 binary pump, and a Hewlett-Packard 1100 diode array detector (DAD). The reversed-phase column used was an Interchim Uptisphere RP C_{18} column (UP3HDO-20QS, 3 μm, 2.3 × 200 mm, Interchim, Montluçon, France). Either a step gradient or isocratic conditions at flow rates between 150 and 180 μl min^{-1} were applied with solvents A and B (solvent A: H_2O + 0.1% TFA, solvent B: MeCN + 0.1% TFA).

The HPLC system was connected to an EsquireLC quadrupole ion trap mass spectrometer (Bruker Daltonik GmbH, Bremen, Germany), equipped with either an ESI or APCI Hewlett-Packard Atmospheric Pressure Ion (API) source. Conditions for ESI: nebulizer gas (N_2, 40 psi), dry gas (N_2, 9 l min^{-1}), dry temperature (300 °C), HV capillary (4500 V), HV EndPlate (–600 V). Conditions for APCI: nebulizer gas (N_2, 21 psi), dry gas (N_2, 7 l min^{-1}), dry temperature (300 °C), APCI temperature (300 °C), HV corona (2870 V), HV capillary (3713 V), HV EndPlate (–600 V). The MS-parameters (target mass, compound stability, and trap drive) were optimized for each measurement to obtain highest ion response and minimal in-source fragmentation. The MS acquisitions were performed in positive ion mode at normal resolution (0.6 u at half peak height) and under ion charge control conditions (ICC, target: 10'000). Full scan MS and MS/MS were averaged over 5 to 8 single spectra and acquired with a mass window between *m/z* 50 and 1000. For all MS/MS experiments, the isolation width was set to 1 Da, the fragmentation cut-off to "fast calc", and the fragmentation amplitude to 1 in the "SmartFrag" mode.

High-resolution Fourier transform (FT) mass spectral data were obtained with a LTQ-Orbitrap XL mass spectrometer (Thermo Electron, Bremen, Germany)

equipped with a standard ESI source. Parameters: spray voltage (5 kV), tube lens voltage (120 V), capillary voltage (38 V), temperature (275 °C). The mass spectrometer was calibrated for mass accuracy immediately before each measurement according to the manufacturers instructions, the relative mass error being typically lower than 3 ppm (externally). The high-resolution FT-MS data were additionally calibrated internally during the measurements with established lock masses (429.088735 and 445.120025). Data was acquired within a mass range of *m/z* 150 to 1000. The AGC target setting for FT-MS experiments was set to 50000. Spectra were acquired with a resolving power of 60000 (full width at half-maximum height, FWHM) at *m/z* 400, and 10 spectra were averaged.

*Synthetic compound **1***: For HPLC-MS analyses, 5 µl of a stock solution of **1** (200 µg) in MeCN/H_2O (1:1, 1 ml) was injected at isocratic conditions with 40% of B and a flow rate of 0.18 ml min^{-1}. Direct infusion APCI experiments were carried out by pumping 200 µl min^{-1} of a 30fold diluted stock solution of **1** into the mass spectrometer with a syringe infusion pump (Cole-Parmer Instrument Company, Vernon Hills, IL, USA). For FT-MS experiments, a 10fold diluted stock solution of **1** was introduced at 6 µl min^{-1} using the same syringe infusion pump.

Spider venom: Crude lyophilized *A. aperta* venom (100 µg) was dissolved in MeCN/H_2O (1:3, 50 µl) + 0.1% TFA, and an aliquot of 5 µl was injected into the HPLC-MS system. A linear gradient from 5 to 20% B over 40 min at a flow rate of 150 µl min^{-1} was applied. The post-column addition of NH_3 to the eluent was performed by the addition of an aqueous solution of NH_3 (10%) at a rate of 20 µl min^{-1} through a Tee located in-between the exit of the column and the entry of the APCI interface.

Mayfoline: Mayfoline (6.34 µg) was dissolved in MeCN/H_2O (1:4, 1 ml), and an aliquot of 5 µl was injected into the HPLC-MS system under isocratic conditions with 20% B and a flow rate of 180 µl min^{-1}. The post-column addition of TFA to the sample was performed by the addition of a mixture of

MeCN/H_2O/TFA (2:6:2) at a rate of 40 µl min^{-1} through a Tee located in-between the exit of the column and the entry of the APCI interface.

1.5 References

[1] T. Karancsi, P. Slegel, *J. Mass Spectrom.* **1999**, *34*, 975.

[2] E. A. Straube, W. Dekant, W. Voelkel, *J. Am. Soc. Mass Spectrom.* **2004**, *15*, 1853.

[3] R. Ramanathan, A. D. Su, N. Alvarez, N. Blumenkrantz, S. K. Chowdhury, K. Alton, J. Patrick, *Anal. Chem.* **2000**, *72*, 1352.

[4] W. Tong, S. K. Chowdhury, J.-C. Chen, R. Zhong, K. B. Alton, J. E. Patrick, *Rapid Commun. Mass Spectrom.* **2001**, *15*, 2085.

[5] S.-N. Lin, S. L. Walsh, D. E. Moody, R. L. Foltz, *Anal. Chem.* **2003**, *75*, 4335.

[6] D. M. Peiris, W. Lam, S. Michael, R. Ramanathan, *J. Mass Spectrom.* **2004**, *39*, 600.

[7] S. Ma, S. K. Chowdhury, K. B. Alton, *Anal. Chem.* **2005**, *77*, 3676.

[8] V. Kertesz, G. J. Van Berkel, *J. Am. Soc. Mass Spectrom.* **2002**, *13*, 109.

[9] S. Chesnov, L. Bigler, M. Hesse, *Helv. Chim. Acta* **2000**, *83*, 3295.

[10] S. Chesnov, L. Bigler, M. Hesse, *Helv. Chim. Acta* **2001**, *84*, 2178.

[11] S. Chesnov, L. Bigler, M. Hesse, *Eur. J. Mass Spectrom.* **2002**, *8*, 1.

[12] N. Manov, M. Tzouros, S. Chesnov, L. Bigler, S. Bienz, *Helv. Chim. Acta* **2002**, *85*, 2827.

[13] M. Méret, S. Bienz, *Eur. J. Org. Chem.* **2008**, in press.

[14] H. Ripperger, *Phytochemistry* **1980**, *19*, 162.

[15] A. Antonello, R. Banzi, M. L. Bolognesi, A. Minarini, M. Rosini, V. Tumiatti, C. Melchiorre, *Med. Res. Rev.* **2003**, *23*, 200.

[16] M. L. Bolognesi, V. Andrisano, M. Bartolini, R. Banzi, C. Melchiorre, *J. Med. Chem.* **2005**, *48*, 24.

[17] C. Gomes-Trolin, I. Nygren, S.-M. Aquilonius, H. Askmark, *Exp. Neurol.* **2002**, *177*, 515.

[18] M.-J. Paik, S. Lee, K.-H. Cho, K.-R. Kim, *Anal. Chim. Acta* **2006**, *576*, 55.

[19] V. Tumiatti, V. Andrisano, R. Banzi, M. Bartolini, A. Minarini, M. Rosini, C. Melchiorre, *J. Med. Chem.* **2004**, *47*, 6490.

[20] M. Tzouros, N. Manov, S. Bienz, L. Bigler, *J. Am. Soc. Mass Spectrom.* **2004**, *15*, 1636.

[21] N. Manov, *unpublished work*.

[22] P. Kuehne, A. Linden, M. Hesse, *Helv. Chim. Acta* **1996**, *79*, 1085.

CHAPTER 2

Structure Elucidation of Acylpolyamines from the Venom of the Spider *Larinioides folium*

Abstract

Lyophilized *Larinioides folium* venom was analyzed by HPLC-ESI-MS and -MS/MS, nanoLC coupled with high-resolution and high mass accuracy Fourier transform MS and MS/MS, on-column H/D exchange HPLC-MS and amino acid analysis of venom fractions. By this extended analytical setup, the structures of 40 acylpolyamines — most of them found for the first time in natural sources — were elucidated. The toxins share a common structure, they are all composed of a α,ω-aminopolyazaalkane backbone and an aromatic acyl head group connected through an asparagine linker. Overall, nine different aromatic acyl groups and six different polyamine backbones were found, whereas four aromatic acyl groups were found for the first time as structural parts in spider venom.

2.1 Introduction

Polyamines and their derivatives are widely found throughout the animal and plant kingdom [1,2]. They exhibit a variety of interesting and important biological activities [3,4]. Therefore, scientists are looking for more sensitive analytical procedures for identification and structure elucidation of unknown lead compounds from natural sources and efficient methods for their synthesis.

Particularly acylpolyamines found in spider venom have attracted the attention of the scientific community in the past decades [5,6]. Initially, only the major constituents of such venoms could be revealed by means of the classical analytic procedure of isolation and purification, followed by the investigation of the pure compounds by IR-, UV-, and NMR-spectroscopy as well as mass spectrometry. With the advent of more sensitive and selective analytical methods — in particular of the modern mass spectrometric approaches — also minor constituents of the complex venoms became amenable for detection and structural elucidation.

High-performance liquid chromatography (HPLC), on-line coupled with mass spectrometry (MS) and tandem mass spectrometry (MS/MS) is a meanwhile well-established methodology for the direct analysis of acylpolyamines in spider venoms without prior isolation of the sample components [7]. The power of this method was demonstrated, *e.g.*, by the structural elucidation of acylpolyamines from the venom of the spider *Agelenopsis aperta* [8,9]. The new procedure revealed a supplementary of 25 minor components in addition to the 8 major constituents of this venom that were identified and characterized earlier [6].

While successful for the analysis of the spider toxins of *A. aperta* [8,9] and *P. birulai* [10], the method proved insufficient, however, for the investigation of the toxins of the spider *Larinioides folium* (*Araneidae*). The chemical structures of the venom constituents from this spider are more complex than those of the

other species. Therefore, the analytical setup had to be supplemented with on-column H/D-exchange HPLC-MS, high mass accuracy and high-resolution (HR) MS, and amino acid analysis of venom fractions. This extended analytical procedure, which we have described in a short communication [11], finally allowed for the detection and structural elucidation of an overall of 37 new acylpolyamine derivatives.

Meanwhile, the method was refined by the use of nano LC (nLC) connected to a LTQ Orbitrap XL™, a hybrid linear quadrupole ion trap (LIT) orbitrap mass spectrometer [12,13]. This arrangement allowed acquiring on-line HR MS and MS/MS data at high accurate masses thanks to the orbitrap, a *Fourier* transform (FT) mass analyzer. Additionally, the amount of spider venom loaded onto the column could be decreased by a factor of 500 due to the higher sensitivity of nLC compared to HPLC. Furthermore, the "higher energy collisional dissociation" (HCD) cell added to the LIT allowed overcoming problems related to the "low-*m*/*z*-cutoff" observed with quadrupole ion traps.

With this approach, the structures of the 37 compounds found in *L. folium* were confirmed and three additional toxins characterized. In the following, the structural elucidation of the characterized 40 toxins from *L. folium* venom by the use of the new analytical setups is shown and discussed in detail.

2.2 Results and Discussion

2.2.1 Structural Diversity and Initial Classification of the Toxins

As mentioned above, the polyamine derivatives found in *L. folium* are of higher complexity than those we had investigated before [8-10]. The toxins contain in addition to the α,ω-aminopolyazaalkane backbones and the chromophoric acyl head groups, which are common for all spider toxins, also asparagine as a linker unit in-between these two moieties and methylated N-atoms (see *Figure 1*). These additional structural features, already known in literature for toxins from other spiders [5,6], led to analytical challenges that could no longer be solved with the experimental setup used so far. The analysis of the venom of *L. folium* was additionally impeded by the high structural diversity of the investigated polyamine toxins and the related high complexity of sample.

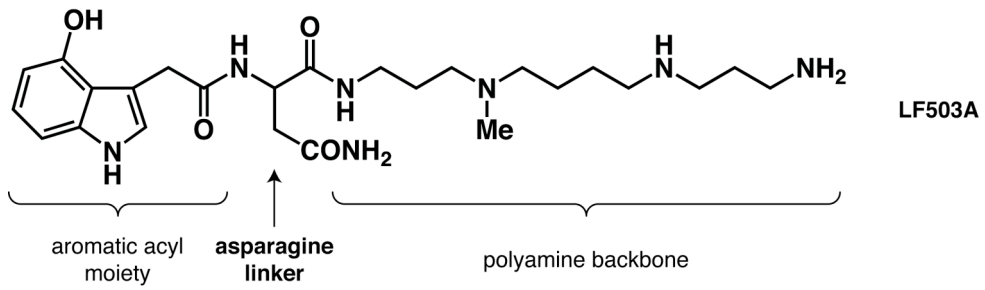

***Figure 1**. General structure of acylpolyamines contained in* L. folium *exemplified by **LF503A**.*

The high complexity of the polyamine fraction of the venom is well illustrated by the 2D chromatogram displayed in *Figure 2*. The chromatogram was obtained with a setup of HPLC-UV(DAD)-ESI-MS. It is to mention at this point that nLC provided a similar elution profile with a slightly but unsignificantly lower chromatographic resolution. Within the acylpolyamine fraction, the several toxins were either completely or partially separated by chromatography. Through the coupling of the HPLC-UV(DAD)/nLC to a mass spectrometer, quasi-molecular ions of co-eluting components differing in

molecular masses were further separated by mass selection, thus adding the second dimension to the separation. The spots in the chromatogram thus represent responses to quasi-molecular ions of the type $[M+H]^+$ recorded in dependence on retention times (abscissa) and *m/z* values (ordinate). The combination of HPLC-UV(DAD)/nLC to mass spectrometry allowed the acquisition of UV, MS and MS/MS data, which for the 40 encircled sample spots are compiled in the *Tables 1 – 7*.

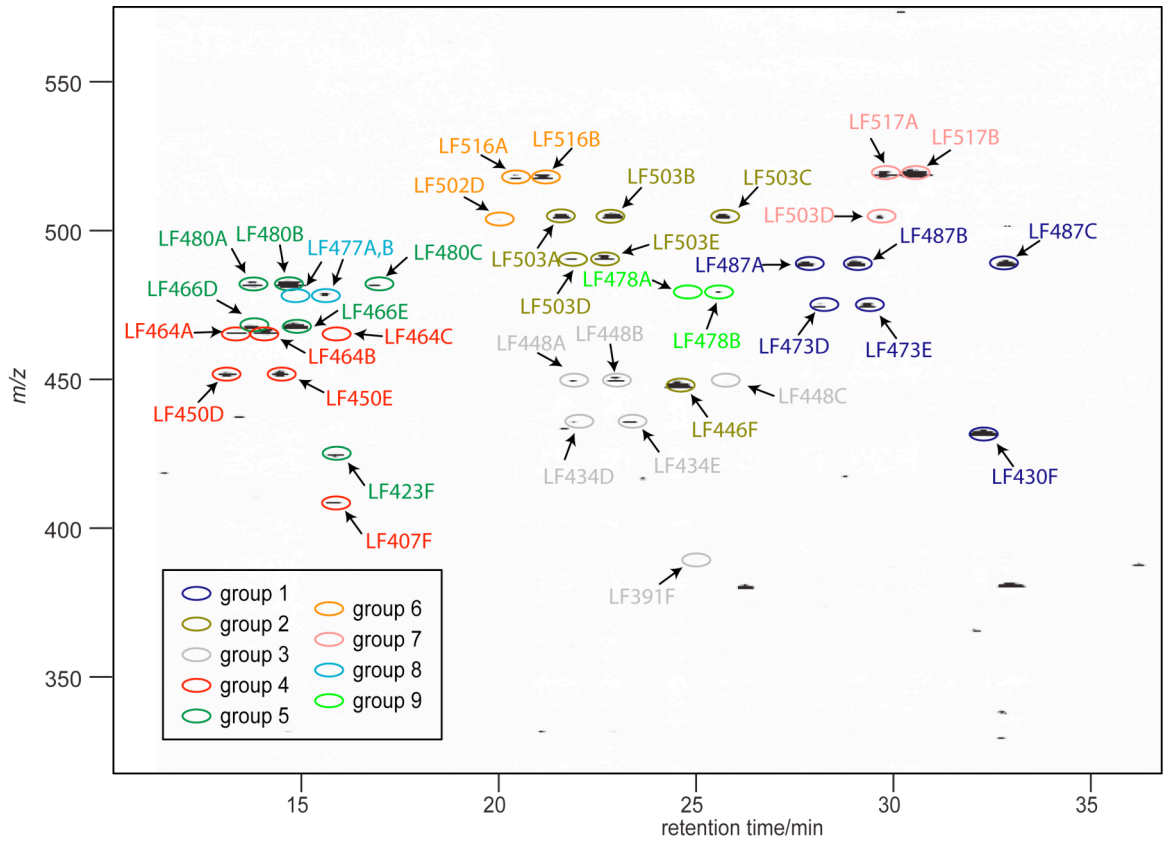

***Figure 2**. 2D-plot of the HPLC-MS analysis of lyophilized* L. folium *venom. The structures of the 40 encircled signals could be elucidated and they were classified by a color scheme according to groups with the same aromatic head portion.*

The initial examination of the spectra revealed that the several toxins are related to each other through their aromatic head groups and their polyamine frameworks. Nine different chromophoric head groups and six different polyamine backbones were recognized. Thereby four types of chromophoric head groups were found for the first time as structural parts in polyamine spider toxins. These are phenylacetic acid (group 3, PhAc), tryptophan (group 6, Trp), phenylalanine (group 8, Phe) and phenyllactic acid (group 9, PhLac).

Table 1. *Structures, retention times (rt), relative amounts, number of exchangeable protons and high-resolution ESI-MS data of acylpolyamines found in* L. folium *venom.*

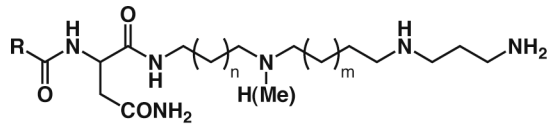

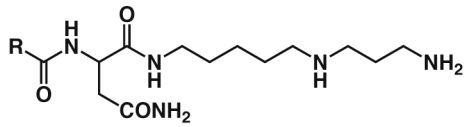

group	R	head portion	name	backbone[a]	rt [min]	r. a.[b] [%]	exch. protons	elem. comp. $[M+H]^+$	$[M+H]^+_{theo}$ *m/z*	$[M+H]^+_{exp.}$ *m/z*	Δm [ppm]
1	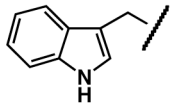	IndAc	**LF487A**	PA3(Me)43	27.6	21	8	$C_{25}H_{42}N_7O_3$	488.3344	488.3344	≤0.1
			LF487B	PA353	28.8	29	9	$C_{25}H_{42}N_7O_3$	488.3344	488.3341	–0.6
			LF487C	PA533	32.3	28	9	$C_{25}H_{42}N_7O_3$	488.3344	488.3342	–0.3
			LF473D	PA343	27.9	8	9	$C_{24}H_{40}N_7O_3$	474.3187	474.3184	–0.7
			LF473E	PA433	29.0	18	9	$C_{24}H_{40}N_7O_3$	474.3187	474.3189	0.4
			LF430F	PA53	31.8	64	8	$C_{22}H_{35}N_6O_3$	431.2765	431.2765	≤0.1
2	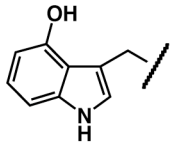	4-OH-InAc	**LF503A**	PA3(Me)43	21.6	22	9	$C_{25}H_{42}N_7O_4$	504.3293	504.3285	–1.6
			LF503B	PA353	22.9	33	10	$C_{25}H_{42}N_7O_4$	504.3293	504.3286	–1.4
			LF503C	PA533	25.6	18	10	$C_{25}H_{42}N_7O_4$	504.3293	504.3286	–1.4
			LF489D	PA343	21.9	6	10	$C_{24}H_{40}N_7O_4$	490.3136	490.3134	–0.4
			LF489E	PA433	22.7	20	10	$C_{24}H_{40}N_7O_4$	490.3136	490.3137	≤0.1
			LF446F	PA53	24.4	73	9	$C_{22}H_{35}N_6O_4$	447.2714	447.2708	–1.4
3	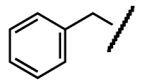	PhAc	**LF448A**	PA3(Me)43	21.9	4	7	$C_{23}H_{41}N_6O_3$	449.3235	449.3229	–1.2
			LF448B	PA353	22.9	15	8	$C_{23}H_{41}N_6O_3$	449.3235	449.3225	–2.1
			LF448C	PA533	26.3	2	8	$C_{23}H_{41}N_6O_3$	449.3235	449.3233	–0.3
			LF434D	PA343	21.9	4	8	$C_{22}H_{39}N_6O_3$	435.3078	435.3077	–0.2
			LF434E	PA433	23.2	9	8	$C_{22}H_{39}N_6O_3$	435.3078	435.3074	–0.9
			LF391F	PA53	25.3	2	7	$C_{20}H_{34}N_5O_3$	392.2656	392.2654	–0.6
4	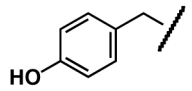	4-OH-PhAc	**LF464A**	PA3(Me)43	13.5	14	8	$C_{23}H_{41}N_6O_4$	465.3184	465.3182	–0.3
			LF464B	PA353	14.1	33	9	$C_{23}H_{41}N_6O_4$	465.3184	465.3188	0.8
			LF464C	PA533	16.9	2	9	$C_{23}H_{41}N_6O_4$	465.3184	465.3188	1.0
			LF450D	PA343	13.3	19	9	$C_{22}H_{39}N_6O_4$	451.3027	451.3024	–0.6
			LF450E	PA433	14.5	22	9	$C_{22}H_{39}N_6O_4$	451.3027	451.3028	0.2
			LF407F	PA53	15.7	8	8	$C_{20}H_{34}N_5O_4$	408.2605	408.2617	2.9

[a] PA stands for polyamine, the figures designate the number of methylene units in-between the N-atoms.

[b] The values given represent the concentration in % relative to the most abundant acylpolyamine contained in the venom and were estimated on the basis of the peak integrals in their EIC obtained by HPLC-ESI-MS.

Table 1 *(cont.). Structures, retention times (rt), relative amounts, number of exchangeable protons and high-resolution ESI-MS data of acylpolyamines found in* L. folium *venom.*

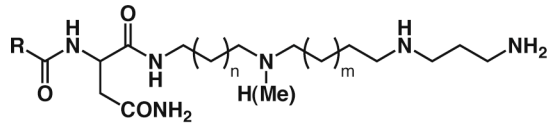

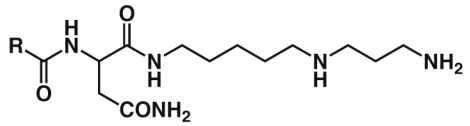

group	R	head portion	name	backbone[a]	rt [min]	r. a.[b] [%]	exch. protons	elem. comp. $[M+H]^+$	$[M+H]^+_{theo}$ *m/z*	$[M+H]^+_{exp.}$ *m/z*	Δm [ppm]
5	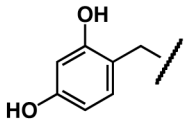	2,4-$(OH)_2$-PhAc	**LF480A**	PA3(Me)43	13.9	21	9	$C_{23}H_{41}N_6O_5$	481.3133	481.3128	–0.9
			LF480B	PA353	14.6	70	10	$C_{23}H_{41}N_6O_5$	481.3133	481.3131	–0.4
			LF480C	PA533	16.7	9	10	$C_{23}H_{41}N_6O_5$	481.3133	481.3135	0.3
			LF466D	PA343	13.9	14	10	$C_{22}H_{39}N_6O_5$	467.2977	467.2973	–0.8
			LF466E	PA433	14.8	53	10	$C_{22}H_{39}N_6O_5$	467.2977	467.2978	0.3
			LF423F	PA53	15.7	14	9	$C_{20}H_{34}N_5O_5$	424.2555	424.2557	0.7
6	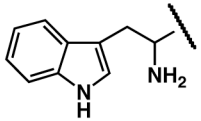	Trp	**LF516A**	PA3(Me)43	20.6	8	10	$C_{26}H_{45}N_8O_3$	517.3609	517.3611	0.4
			LF516B	PA353	21.2	27	11	$C_{26}H_{45}N_8O_3$	517.3609	517.3600	–1.7
			LF502D	PA343	20.2	2	11	$C_{25}H_{43}N_8O_3$	503.3453	503.3453	≤0.1
7	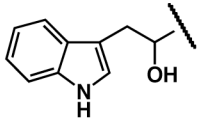	IndLac	**LF517A**	PA3(Me)43	29.4	27	9	$C_{26}H_{44}N_7O_4$	518.3449	518.3449	≤0.1
			LF517B	PA353	30.0	100	10	$C_{26}H_{44}N_7O_4$	518.3449	518.3451	0.3
			LF503D	PA343	29.3	8	10	$C_{25}H_{42}N_7O_4$	504.3293	504.3292	–0.2
8	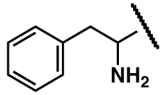	Phe	**LF477A**	PA3(Me)43	14.5	3	9	$C_{24}H_{44}N_7O_3$	478.3500	478.3490	–2.2
			LF477B	PA353	15.5	9	10	$C_{24}H_{44}N_7O_3$	478.3500	478.3499	–0.3
9	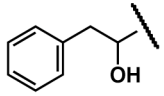	PhLac	**LF478A**	PA3(Me)43	24.5	1	8	$C_{24}H_{43}N_6O_4$	479.3340	479.3339	–0.3
			LF478B	PA353	25.4	4	9	$C_{24}H_{43}N_6O_4$	479.3340	479.3326	–3.1

[a] PA stands for polyamine, the figures designate the number of methylene units in-between the *N*-atoms.

[b] The values given represent the concentration in % relative to the most abundant acylpolyamine contained in the venom and were estimated on the basis of the peak integrals in their EIC obtained by HPLC-ESI-MS.

The pairwise combination of these two structural portions would potentially allow for an overall of 54 different acylpolyamines, wherefrom 40 were in fact detected in the venom. Concerning the non-detected compounds, it seems that the biosynthesis is limited to specific polyamines only. It is striking to see that all toxins containing a propionic acid (groups 6 – 9) instead of an acetic acid (groups 1 – 4) in the aromatic acyl portion start with a PA3 unit in the backbone.

The identified toxins were named LF according to the source organism *L. folium*, followed by their molecular mass and a suffix A–F. The suffixes A–F are standing for the type of polyamine backbone contained in the molecules. The chromophoric units of the compounds are not encoded in the names. They are, however, visualized in the 2D plot (*Figure 2*) by a color scheme, grouping the toxins that possess the same head groups with the same color. The 40 toxins of *L. folium* are thus arranged in *Figure 2* in nine differently colored groups of toxins (corresponding to the shared chromophoric units) consisting of up to six members (differentiated by the suffixes and thus the polyamine portions). The distribution pattern of the several spots within a colored group of toxins is repetitive, already suggesting the structural similarities of the respective analytes (see discussion later).

Considering the general construction of the compounds, the structural elucidation of the polyamine toxins appears to be straightforward, involving simply the identification of the acyl head moieties, the amino acid linkers, and the polyamine backbones. It proved, however, to be a rather delicate process, since the arguments for the structural proof of the several parts are interrelated and not in all cases conclusive on the basis of the spectral data alone. In some cases, reasoning by analogy and consideration of rational biosynthetic pathways was necessary. In the following, the structural elucidation of the three fundamental units is discussed in separate sections, and, where required, cross-reference to other parts of the discussion is given.

2.2.2 Amino Acid Linker

An initial examination of the MS/MS data revealed that the toxins of *L. folium* possess besides the mandatory polyamine backbones and the chromophoric head portions — recognized by their typical fragmentations and the UV spectra, respectively — an additional structural unit interconnecting these two groups. For most compounds, but not for all, fragment ions of the type ***f*** and ***g*** (*Figures 3* and *4*) with a mass difference of 114 amu were found. This mass difference is consistent with the presence of an asparagine (Asn) linker, a structural unit, which has been found in several spider toxins before [6]. To prove Asn as a constituent of the toxin molecules, the full venom was separated by HPLC into 11 fractions, which were subsequently submitted to hydrolysis and amino acid analysis. These analyses revealed that all hydrolysates contained aspartic acid (Asp), which confirmed Asn as the linker.

The assignment of Asn as a molecular portion, however, is solely unambiguous for toxins of fractions that contain no additional components. For most fractions, though, this is not the case. Nevertheless, we are confident that Asn is a molecular moiety of all the 40 described spider toxins.

Definite proof for its presence is available for **LF517B**, which is the sole constituent of the chromatographic fraction F11. Sound evidence is certainly also available for all compounds that deliver the fragment ions ***f*** and/or ***f***–NH_3 together with ***g*** upon CID. This is the case for all acylpolyamines that contain the polyamine portions PA353 (polyamine backbone of type B), PA533 (type C), PA433 (type E), and PA53 (type F). The mass difference between the fragment ions ***f*** and ***g*** allows, according to the HR MS, solely for a molecular portion of $C_4H_6N_2O_2$ as the interlinking unit. This is again consistent with Asn. Certainly, a structural unit isomeric to Asn could also be proposed as an alternative. But because Asp was established as the dominant component in all hydrolysates of the toxins and because no molecular portion isomeric to Asn has been found by us or has ever been found as a constituent of a polyamine

toxin in any other spider species before, we ruled out any alternative structural unit.

More problematic with regard to the amino acid linker are the polyamine toxins with the proposed polyamine portions PA3(Me)43 (type A) and PA343 (D). These compounds were not fully separated by HPLC. They always eluted in A/D-pairs of compounds sharing the chromophoric head moiety. They do not show the ***f*** and ***g*** fragment ions and thus do not directly reveal the chemical formula of the molecular portions interlinking the polyamine and the chromophoric head groups. Most of these alkaloids, however, gave rise to fragment ions of type ***d*** and ***e*** as well as ***j***, also observed with most of the previously described compounds. These fragments disclose the chemical formula of the molecular moieties that are composed of the linking amino acid and the first portion of the polyamine backbone. For all alkaloids of type A and D showing these fragments, $C_7H_{13}N_3O_2$ was found as the chemical formula of this interlinking portion. This elemental composition is consistent with an Asn-PA3 unit, and such a structural moiety is more than only reasonable for the toxins due to the following reason: It is well known that polyamine spider toxins are constructed from several portions like polyamine backbones, chromophoric head groups, and interlinking amino acids in an almost random way [6]. For a given species, the toxins were always related to each other through the polyamine backbone, the chromophoric head group, the amino acid linker, or combinations thereof. Since Asn was secured as the amino acid linker for most of the toxins of *L. folium* venom and no other amino acid linker was found therein, it is most likely that Asn is also the linking amino acid for the toxins containing the polyamine backbones of type A and D.

The weakest evidence for Asn as amino acid linker is available for the alkaloids **LF434D** and **LF464A**. For these compounds, only fragment ions were found that were relevant for the structure of the polyamine backbone. For instance, the signals for the fragments of type ***b***, ***d***, and ***h*** gave no direct hint for Asn as a component of the sample molecules. However, since we are confident to know the polyamine portions as well as the chromophoric head

moieties of both alkaloids **LF434D** and **LF464A** (see discussion below), the molecular compositions of the fragment ions ***b***, ***d*** and ***h*** allowed to deduce Asn as the interlinking amino acid for these molecules as well.

2.2.3 Polyamine Backbones

With our previous investigations we have shown that CID of acylpolyamines follows some rather simple and characteristic rules and that MS/MS patterns of acylpolyamines usually reflect directly the types of polyamine backbones contained in the molecules [8-10]. Other structural parts like aromatic acyl moieties do not markedly influence fragmentations. Hence, similar MS/MS patterns suggest that the respective sample molecules share the same polyamine backbones. Scrutiny of the MS/MS data of the 40 labeled signals in the 2D plot revealed six distinct MS/MS patterns only. Hence it was assumed, and finally also found, that the toxins contain six different types of polyamine backbones only.

The structural elucidation of these backbones is based on the fragmentation rules determined before, supplemented with the results of HR MS and H/D-exchange HPLC-MS. The major fragmentations of polyamine derivatives are explained by intramolecular substitutions of protonated amines according to process (a) in *Scheme 1*. Substitution reactions proceed *via* favored transition states, *e.g.*, five-membered cyclic structures. Such fragmentations were found to be particularly pronounced that led to strong signals dominating the spectra. Dissociation of the quasi-molecular ions also occurs according to process (b), but to a minor extent, and only if no dominating alternative fragmentations take place. This transformation corresponds to the loss of a terminal aminoalkyl group with concurrent proton transfer analogously to the reaction described to account for the formation of the b_n/y_n ion series in peptide fragmentation [14]. Often, also the free protonated polyamine is detected.

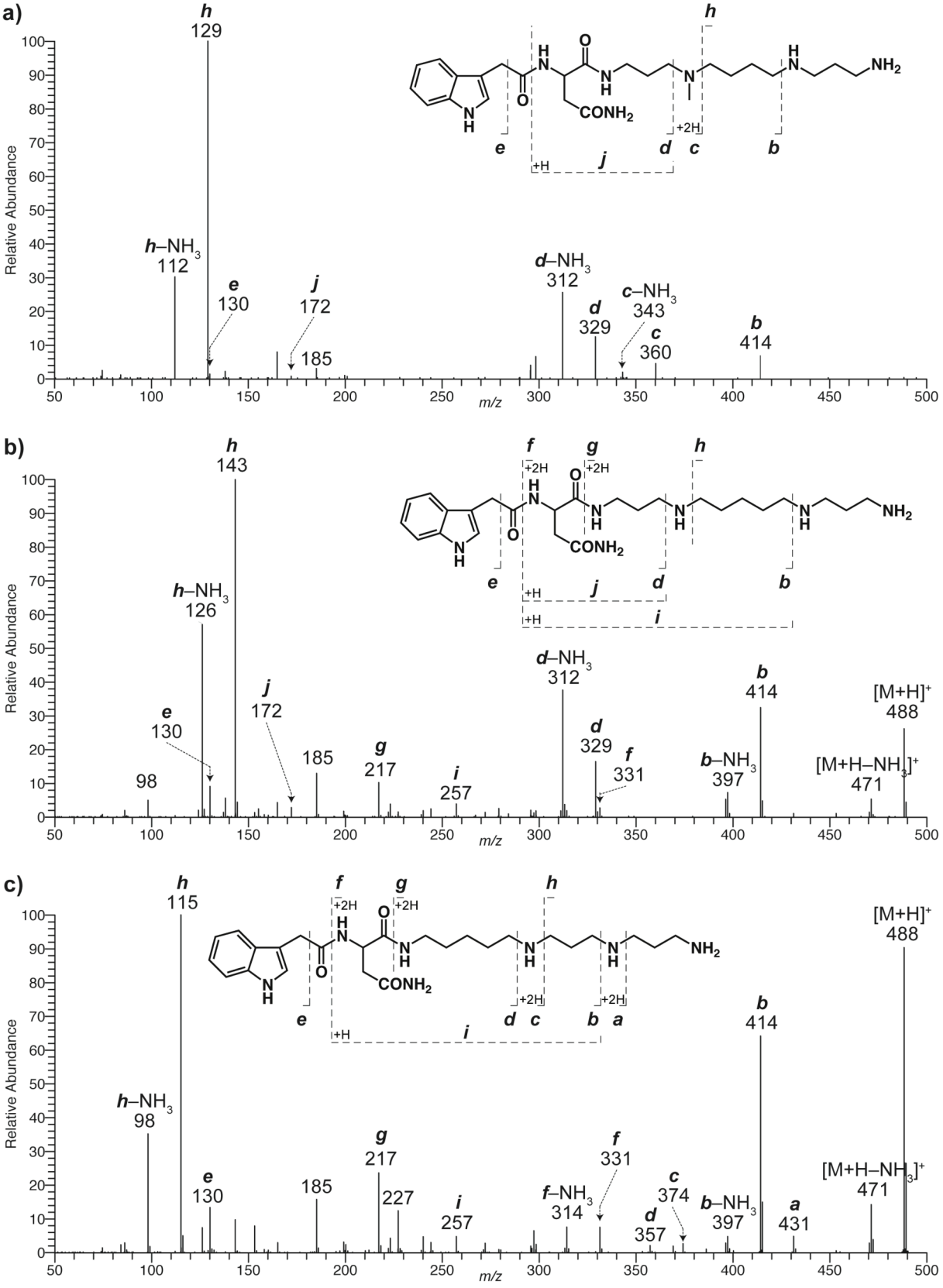

***Figure 3**. nLC-ESI-HCD-MS/MS of [M+H]⁺ of (**a**) **LF487A**,(**b**) **LF487B** and (**c**) **LF487C**.*

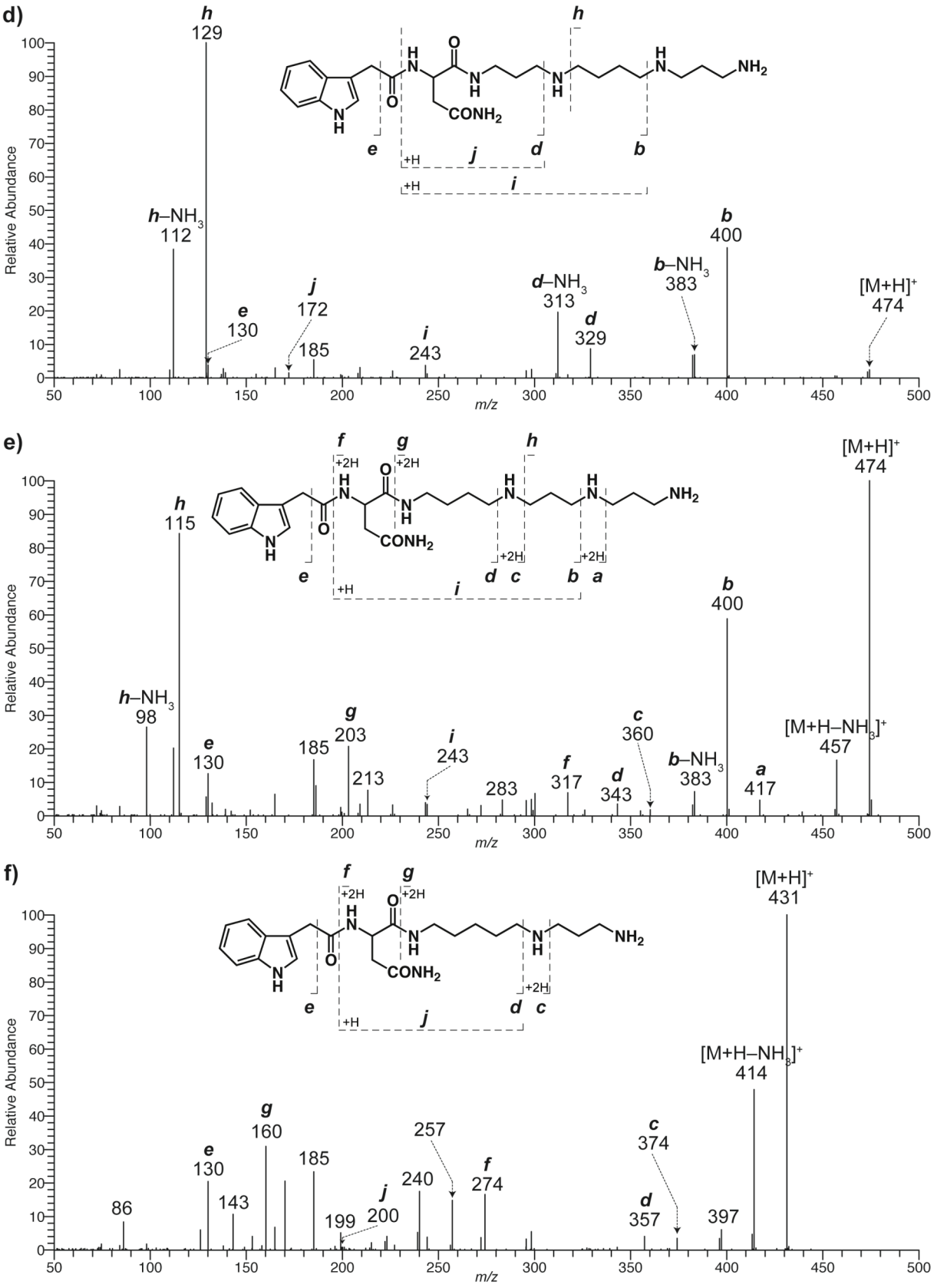

Figure 3 *(cont.). nLC-ESI-HCD-MS/MS of* [M+H]$^+$ *of (**d**)* ***LF473D****,(**e**)* ***LF473E****, and (**f**)* ***LF430F****.*

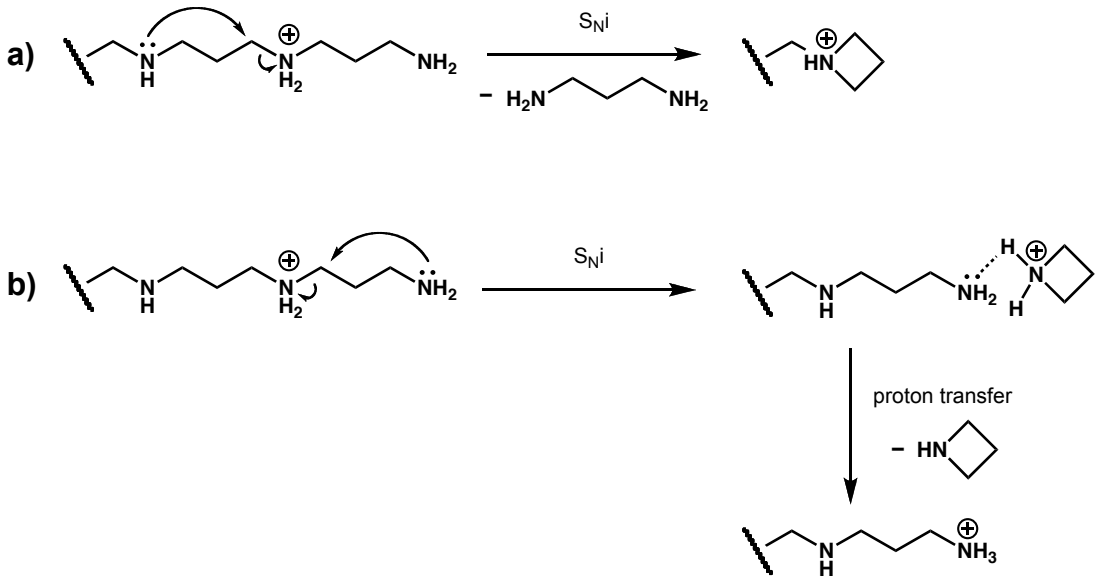

***Scheme 1**. Proposed fragmentation reactions leading to the two main types of fragment ions through (**a**) intramolecular substitution and (**b**) intramolecular substitution and subsequent proton transfer.*

The structural elucidation of the six polyamine backbones contained in the 40 toxins of *L. folium* is easiest illustrated by means of a set of compounds possessing the same head groups. This is, *e.g.*, the case for the group of **LF487A**, **LF487B**, **LF487C**, **LF473D**, **LF473E**, and **LF430F** (group 1 in *Table 1*, *Table 2*), which was chosen because the structure of their shared head moiety is well secured. The compounds together with their nLC-ESI-HCD-MS/MS spectra are shown in *Figure 3*.

The structural elucidation of the polyamine backbones started from the amino endings (from the "right-end") of the molecules. Fragment ions of type ***b*** (or ***d*** for the triamine derivative **LF430F**) were observed for all compounds, proving the common PA3 termini of the molecules. The corresponding fragment ions of type ***a*** and ***c*** were also found for **LF487C**, **LF473E**, and **LF430F**. This not only supports the assignment of the terminal PA3 units for these compounds, but also indicates the absence of PA4 or PA5 moieties as an internal molecular portion of the polyamine backbones of the samples. Protonated molecules of compounds with internal PA4 and/or PA5 units typically undergo dominating alternative fragmentation, not showing the ions of the shortened polyamine derivative. On the basis of this argument, the absence of fragment ions of type ***a*** can likewise be taken as a hint, that the remaining toxins,

LF487A, **LF487B**, and **LF473D**, do possess an internal PA4 or PA5 portion.

This interpretation was confirmed by the fragmentations observed around the N-atoms located next to the left within the polyamine backbones. For all toxins — except for **LF430F** whose last N-atom is acylated and thus not prone for the corresponding decompositions — fragment ions of type ***c***, ***d***, and ***h*** were recorded either in the MS/MS obtained upon HCD or, for some fragments of type ***c***, upon CID in the QIT only. The elemental compositions of these fragments redundantly revealed the chemical formula of the respective terminal triamine portions, thus allowing the structural assignments of PA33, PA43, PA(Me)43, and PA53 for these groups. A novelty for us with regard to the interpretation of fragments of type ***c*** and ***d*** was encountered with toxin **LF487A** possessing the PA(Me)43 terminus. In this case, the mass difference between the fragments ***c*** and ***d*** did not correspond to NH but to NMe. H/D exchange LC-MS was performed to secure that the fragments ***c*** and ***d*** did not arise from two co-eluting isomers with a PA43 (giving rise to fragment ***c*** at *m*/*z* at 367) and a PA53 (***d*** at *m*/*z* 345) termini. This experiment, delivering information on H/D-exchange properties of all the investigated toxins, revealed an overall of nine readily exchangeable protons for **LF487A**. This is consistent only with a structure that contains a tertiary amine in the polyamine backbone, and not with the alternatively considered structures possessing secondary amines instead.

For the remaining portion of the polyamine backbones, fragments of type ***g*** were acknowledged. With the exact masses of these fragments, the polyamine portions contained in **LF487B**, **LF487C**, **LF473E**, and **LF430F** were completed to PA353, PA533, PA433, and PA53, respectively. For **LF487A** and **LF473D**, fragment ions of type ***g*** were not observed, and thus direct proof for the remaining portions of the polyamine backbones of these compounds was not available from MS data. However, the mass differences of fragment ions ***e*** and ***d*** together with the mass of the fragment ion ***i*** are consistent with an Asn-PA3 unit as the moiety in-between the chromophoric head group and the residual of the polyamine backbone. Since Asn is considered to be the amino acid interlinking the chromophoric head groups and the polyamine portions of the

toxins (see above), PA3 remains as the only reasonable missing unit of the polyamine backbone. This assignment is rational also for biosynthetic reasons. Polyamine backbones of spider toxins have consistently been found to be constructed of a single PA4 or PA5 portion, connected to a number of PA3 units (1–4 units). The PA4 and PA5 moieties most likely arose biosynthetically from ornithine and lysine, respectively, and were presumably repetitively aminopropylated at either end by decarboxylated S-adenosylmethionine [15].

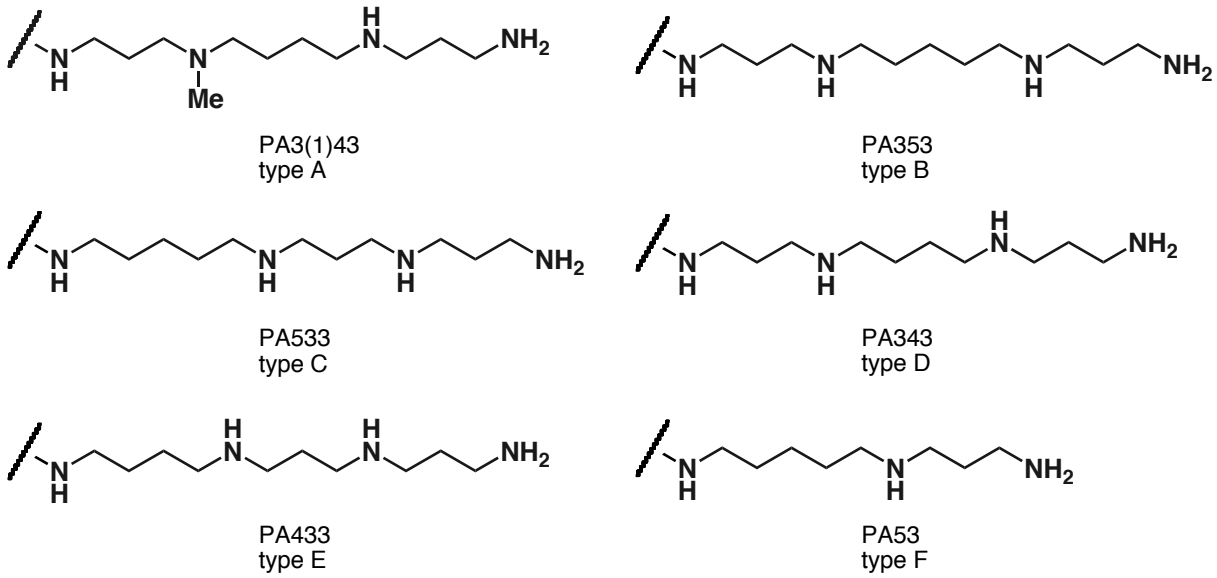

***Figure 4**. Structures of polyamine backbones found in* L. folium *polyamine toxins.*

The analysis of the six compounds **LF487A**, **LF487B**, **LF487C**, **LF473D**, **LF473E**, and **LF430F**, thus, revealed that the six polyamine backbones shown in *Figure 4* are contained in the toxins of *L. folium*. Since the same fragmentation patterns as observed for this prototype compounds were repetitively found for the remaining toxins of *L. folium*, the attribution of the respective polyamine backbones was readily possible to the several compounds.

Completion of the masses of the polyamine backbones to the overall masses of the several toxins finally revealed that nine groups of toxins exist, which evidently consist of compounds that share their head moieties. It was further found that the relative chromatographic behavior of the components within a group is closely dependent on the type of polyamine portion contained in the molecules. This results in such a characteristic distribution of the signals in the 2D-plot that the chromatographic behavior of a compound could be taken as

an argument for its structural identity. For instance for the toxins **LF464A** and **LF434D**, to which spectroscopic evidence is scarce, the chromatographic behavior suggests strongly that these compounds possess the same polyamine backbones as the corresponding chromatographic members of the other groups, and also the same chromophoric group as the other members of the own group.

2.2.4 Chromophoric Head Groups

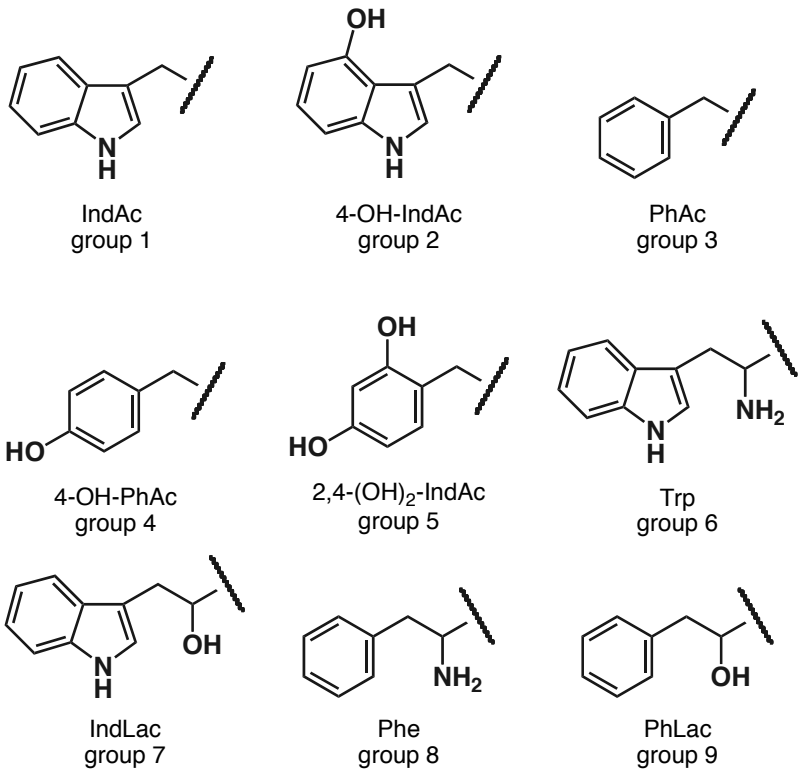

***Figure 5**. Structures of aromatic acyl portions found in* L. folium *polyamine toxins.*

The identification of the chromophoric acyl head groups of the polyamine toxins of *L. folium* is primarily based on the UV absorption spectra of the compounds and the accurate masses of the fragment ions determining the head units. While the latter were obtained directly from data of the HCD-MS/MS experiments, the former were collected by an on-line coupled UV diode array detector (DAD). Since UV data, in contrast to mass spectrometric data, are only meaningful when they arise from pure analytes, complete chromatographic separation of the venom components was necessary to

obtain the required UV information. This was not realized for all toxins. However, as mentioned above, the 40 polyamine toxins of *L. folium* can be divided into nine groups of compounds that share their head moieties (*Figure 5)*. Thus, elucidation of the chromophoric acyl portion of one member of each of these groups would already be sufficient to identify the head moieties of all compounds. This was rather helpful for the determination of the head groups of the majority of the compounds.

Individual UV data were accessible for all toxins of group 1 (**LF487A**, **LF487B**, **LF487C**, **LF498d**, **LF498e**, and **LF430F**) and group 2 (**LF503A**, **LF503B**, **LF503C**, **LF473D**, **LF473E**, and **LF446F**). Though not all compounds were baseline-separated by HPLC, it was still possible to acquire spectra from pure analytes either on top or in ascending and/or descending slopes of the chromatographic peaks. The spectra of all compounds were the same for the individual compound within the two groups of compounds and indicative for the indole (λ_{max} = 280, 288, shoulder at λ = 270) or 4-hydroxyindole chromophores (λ_{max} = 268, 284, 292). The structural moieties defined by the chromophores (C_8H_6N and C_8H_6NO), together with the molecular formula of the fragment ions of type ***e*** (C_9H_8N/C_9H_8NO), or simply the formula that were calculated as the remains of the molecules after removal of the known polyamine backbones and the Asn linker, left little structural flexibility for the respective overall acyl head groups. Definitely, the head groups had to be indole acetyl and 4-hydroxyindole acetyl groups. Since IndAc and 4-OH-IndAc, which are connected through C(3) of the indole moieties to the acetyl groups (*Table 1*), have previously found as head moieties in related spider toxins, these two specific isomers are proposed to be contained in the toxins of *L. folium* as well.

Similarly, 4-OH-PhAc and 2,4-$(OH)_2$PhAc were deduced as the head moieties of the toxins of the groups 4 and 5, respectively. **LF464B** was the only compound of which a UV spectrum could be acquired. This spectrum is consistent with cresol (= methylphenol, λ_{max} = 274 nm). The remaining components (**LF464A**, **LF464C**, **LF450D**, **LF450E**, and **LF407F**) were either too low in concentration to deliver reasonable spectra or were not separable from

compounds possessing different chromophores. For the compounds of group 5, too, only an incomplete set of UV spectra was accessible. But still for five of the six components (**LF480A**, **LF480B**, **LF466D**, **LF466E**, and **LF423F**; the remaining toxin **LF480C** was not fully separated from other components of the venom), UV spectra consistent with 1-alkyl-2,4-dihydroxybenzene were found (λ_{max} = 278 nm). The elemental composition of the head groups, again obtained from HR MS data, allowed analogously to above only (hydroxyphenyl)acetyl and (dihydroxyphenyl)acetyl groups to be assigned for the two classes of compounds. And since the 4-OH-PhAc and the 2,4-$(OH)_2$-PhAc groups (*Table 1*) were already well-known constituents of other spider toxins [5,6], these two groups were assigned as the most likely head moieties of the toxins.

More problematic was the assignment of the acyl head groups for the rest of the toxins. Except for the IndLac group, which was found as chromophoric head group in polyamine toxins **MG30** from the venom of the spider *Macrothele gigas* [16] and **Het389**/**Het403** from *Hebestatis theveniti* [17], the remaining acyl moieties are without precedence as components in spider toxins. Additionally, spectroscopic data is rather scarce for some of the compounds as well.

For the compounds of group 3 (**LF448A**, **LF448B**, **LF448C**, **LF434D**, **LF434E** and **LF391F**), PhAc is proposed as their head portion (*Table 1*). For none of the six members of this group a UV spectrum was attainable. The compounds were too minor in concentration for this purpose, and co-eluting foreign substances falsified the acquired spectra. The head moiety, however, had to be composed of C_8H_7O as revealed by the HR MS data. This left the PhAc group as the most likely structure for the fragment, considering the hydroxylated PhAc groups as archetypes.

The compounds of group 6 (**LF516A**, **LF516B**, and **LF502D**) and 7 (**LF517A**, **LF517B**, and **LF503D**) most possibly contain Trp and IndLac (*Table 1*), respectively, as their chromophoric head groups. For all of these compounds, UV spectra characteristic of indole ((λ_{max} = 280, 288, shoulder at λ = 270) were found. The elemental compositions of the complete head groups, possessing

an additional $CHNH_2$ or CHOH moiety as compared to the previously found IndAc group, suggested Trp or IndLac or their β-aminated or β-hydroxylated propionic acid isomers as the missing structures. The β-functionalized compounds were excluded on the basis of HCD fragments observed at *m*/*z* 130, standing for methyleniumindole ($C_9H_8N^+$) (*Scheme 2*).

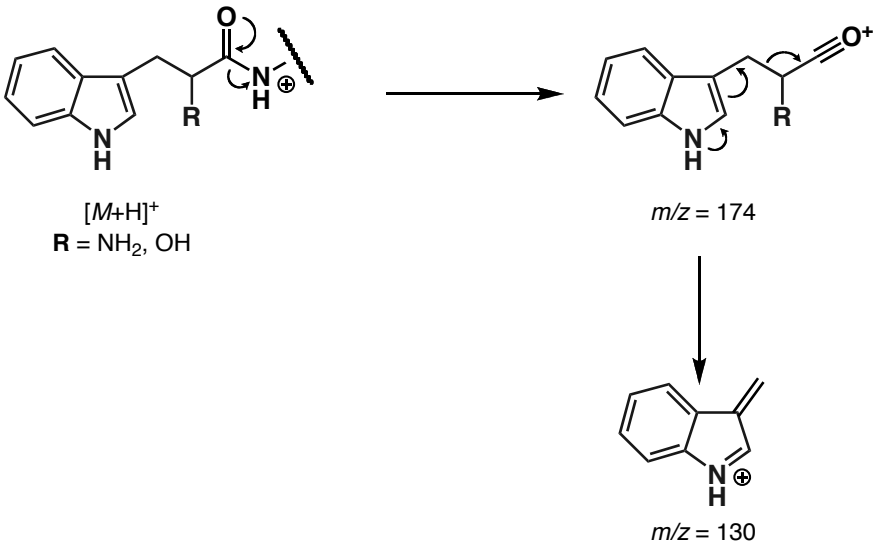

***Scheme 2**. Proposed fragmentation mechanism for the generation of ions at* m/z *130 of Trp- and IndLac derivatives.*

For the final four toxins of the groups 8 (**LF477A** and **LF477B**) and 9 (**LF478A** and **LF478B**) no reliable UV data is available. The content of these toxins in the sample was too low, and the spectra obtained from the chromatographic peaks of the compounds were affected by partially co-eluting and highly UV-absorbing additional analytes. The elemental compositions of the head moieties, however, pointed to Phe and PhLac, possessing — as Trp and IndLac in comparison to IndAc — an additional $CHNH_2$ or CHOH portion as compared to the previously found PhAc group. Unlike to the previous case, however, no signal for the tropylium ion (*m*/*z* 91), the fragment corresponding to the above mentioned methyleniumindole, was found for these toxins. Thus no evidence for the α-amino or α-hydroxy propionate was available. Nevertheless, we are confident that the head portions of the remaining toxins are Phe and PhLac. This for three major reasons: (1) Phe was found in the amino acid analysis of fraction 3 in substantial amounts, (2) Phe and PhLac are biosynthetically realistic structures, and (3) the Phe and PhLac-containing

toxins can be biosynthetically explained in analogy to the Trp- and IndLac-containing analogs. Furthermore, the compounds of groups 6/7 and 8/9 share the peculiarity that they contain only polyamine backbones which are connected through a PA3 unit to the head portions. This is most possibly the result of biosynthetic discrimination of the other potential precursor molecules and suggests a close structural relationship of the respective acyl moieties — which is the case for Trp, IndLac, Phe, and PhLac.

2.3 Conclusion

It was shown with our investigations that the combination of on-line coupled nLC-MS, using an hybrid LIT orbitrap MS system with attached HCD collision cell allows to reach new frontiers for the direct analysis of low abundant natural products arising as components in complex mixtures. This method, together with HPLC-UV(DAD)-MS, delivers high-resolution and high mass accuracy MS and MS/MS data of smallest amounts of analytes as well as UV spectra. The structures of 40 new toxins contained in the venom of the spider *L. folium* were elucidated. Amino acid analyses and on-line H/D-exchange experiments supported the conclusions drawn from the UV/MS data. The new instrumental setup is highly sensitive and, due to the high accuracy of the mass analysis, allows for the attribution of molecular formula to any detected ion signal. This is certainly most helpful for structural assignments.

The method, however, is still limited with regard to the investigation of co-eluting compounds (missing UV spectra) or with regard to compounds that do not reveal their full structures by UV/MS data alone. In fact, the *de novo* structural elucidation of the new toxins of *L. folium* would have been impossible with just the new arrangement: our considerations did not solely rely on the acquired analytical data but also on structural precedence of other spider toxins and on biogenetic considerations. For instance, the polymethylene characters of the interlinking alkylidene moieties in-between the several N-atoms of the polyamine backbones cannot be proven by the collected MS data. We had to trust that the new polyamine toxins possess non-branched carbon chains in-between the N-atoms as all the other previously

investigated polyamine toxins, too — which is reasonable on the basis of chemotaxonomic considerations as well as with regard to the biosynthesis of polyamine derivatives. Experience with fragmentation patterns of related compounds, which were structurally secured either by additional spectroscopic data or by synthesis, were helpful for the safe attribution of the structural units as well. "Irregularities" in fragmentation behavior would certainly have attracted our attention. Nevertheless, definite and unconditional proof for the proposed structures could only be gained, if additional data for the compounds could be obtained, *e.g.*, NMR data, which would require the accumulation of more and pure sample material. In the course of our synthetic endeavors we plan to access such material by solid-supported chemistry.

***Table 2**. Types, nominal masses and relative intensities of relevant HCD-MS/MS signals of type A compounds.*

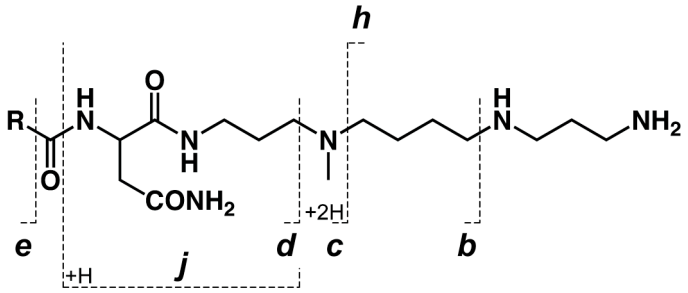

name (group) head portion	*m/z* (relative abundance)						
	$[M+H]^+$	***b***	***c*** ***c***–NH_3	***d*** ***d***–NH_3	***e***	***h*** ***h***–NH_3 ***h***–NH_3–C_2H_4	***j*** ***j***–NH_3 ***j***–$2NH_3$
LF487A (1) IndAc	—	414 (7)	360 (5) 343 (2)	329 (12) 312 (26)	130 (1)	129 (100) 112 (30) 84 (1)	172 (1) — 138 (2)
LF503A (2) 4-OH-IndAc	504 (1)	430 (7)	376 (5) 359 (2)	345 (12) 328 (23)	146 (2)	129 (100) 112 (31) 84 (2)	172 (4) 155 (2) 138 (3)
LF448A (3) PhAc	449 (1)	375 (10)	321 (4) 304 (2)	290 (15) 273 (29)	—	129 (100) 112 (36) 84 (2)	172 (1) 155 (1) 138 (2)
LF464A (4) 4-OH-PhAc	—	391 (8)	337 (3) —	306 (13) 289 (28)	—	129 (100) 112 (33) 84 (1)	— — —
LF480A (5) 2,4-$(OH)_2$-PhAc	481 (1)	407 (9)	353 (4) 336 (1)	322 (9) 305 (19)	—	129 (100) 112 (31) 84 (2)	172 (8) 155 (3) 138 (1)
LF516A (6) Trp	—	443 (5)	389 (4) 372 (1)	358 (9) 341 (14)	159 (2)	129 (100) 112 (31) 84 (2)	172 (7) 155 (2) 138 (1)
LF517A (7) IndLac	518 (1)	444 (6)	390 (4) 373 (2)	359 (12) 342 (22)	—	129 (100) 112 (32) 84 (2)	172 (1) 155 (1) 138 (2)
LF477A (8) Phe	—	404 (7)	350 (3) —	319 (11) 302 (18)	—	129 (100) 112 (28) —	172 (1) — —
LF478A (9) PhLac	479 (1)	405 (8)	351 (3) 334 (2)	320 (14) 303 (27)	—	129 (100) 112 (34) 84 (3)	172 (1) 155 (1) 138 (2)

***Table 3**. Types, nominal masses and relative intensities of relevant HCD-MS/MS signals of type B compounds.*

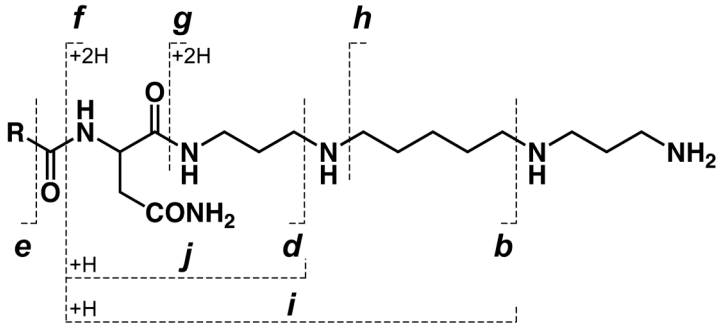

name (group) head portion	*m/z* (relative abundance)								
	$[M+H]^+$ $[M+H-NH_3]^+$ $[M+H-H_2O]^+$	***b*** ***b***–NH_3 ***b***–H_2O	***d*** ***d***–NH_3 ***d***–H_2O	***e***	***f*** ***f***–NH_3 ***f***–$2NH_3$	***g***	***h*** ***h***–NH_3 ***h***–NH_3–C_2H_4	***i*** ***i***–NH_3 ***i***–$2NH_3$	***j*** ***j***–NH_3 ***j***–$2NH_3$
LF487B (1) IndAc	488 (26) 471 (5) 470 (1)	414 (32) 397 (7) 396 (5)	329 (16) 312 (38) 311 (2)	130 (9)	331 (3) 314 (2) 297 (1)	217 (10)	143 (100) 126 (57) 98 (5)	257 (4) 240 (2) 223 (4)	172 (3) 155 (2) 138 (6)
LF503B (2) 4-OH-IndAc	504 (26) 487 (6) 486 (2)	430 (24) 413 (6) 412 (4)	345 (13) 328 (24) 327 (2)	146 (12)	331 (6) 314 (3) 297 (2)	217 (15)	143 (100) 126 (51) 98 (5)	257 (7) 240 (3) 223 (4)	172 (6) 155 (4) 138 (5)
LF448B (3) PhAc	449 (30) 432 (5) 431 (1)	375 (44) 358 (7) 357 (7)	290 (18) 273 (46) 272 (2)	—	— 314 (2) 297 (1)	217 (8)	143 (100) 126 (65) 98 (7)	257 (2) 240 (2) 223 (3)	172 (2) 155 (3) 138 (5)
LF464B (4) 4-OH-PhAc	465 (31) 448 (6) 447 (1)	391 (44) 374 (8) 373 (7)	306 (18) 289 (46) 288 (2)	107 (2)	331 (1) 314 (1) 297 (1)	217 (7)	143 (100) 126 (64) 98 (6)	257 (2) 240 (2) 223 (3)	172 (2) 155 (3) 138 (5)
LF480B (5) 2,4-$(OH)_2$PhAc	481 (32) 464 (3) —	407 (34) 390 (6) 389 (6)	322 (10) 305 (24) 304 (3)	—	331 (6) 314 (3) —	217 (9)	143 (100) 126 (57) 98 (4)	257 (7) 240 (2) 223 (1)	172 (10) 155 (7) 138 (4)
LF516B (6) Trp	517 (24) 500 (4) —	443 (22) 426 (5) 425 (2)	358 (8) 341 (14) 324 (2)	159 (13)	331 (13) 314 (4) 297 (1)	217 (13)	143 (100) 126 (46) 98 (7)	257 (15) 240 (3) 223 (2)	172 (11) 155 (4) 138 (3)
LF517B (7) IndLac	518 (21) 501 (5) —	444 (29) 427 (7) 426 (3)	359 (14) 342 (28) 341 (2)	160 (2)	331 (2) 314 (2) 297 (2)	217 (8)	143 (100) 126 (57) 98 (6)	257 (3) 240 (2) 223 (4)	172 (3) 155 (3) 138 (5)
LF477B (8) Phe	478 (35) 461 (5) —	404 (36) 387 (5) 386 (3)	319 (14) 302 (26) —	120 (9)	331 (8) 314 (1) —	217 (8)	143 (100) 126 (47) 98 (4)	257 (10) 240 (2) 223 (2)	172 (9) 155 (4) 138 (1)
LF478B (9) PhLac	479 (30) 462 (5) —	405 (44) 388 (8) 387 (5)	320 (20) 303 (47) 302 (2)	—	— 314 (1) 297 (1)	217 (7)	143 (100) 126 (61) 98 (6)	257 (3) 240 (2) 223 (4)	172 (2) 155 (3) 138 (5)

***Table 4**. Types, nominal masses and relative intensities of relevant HCD-MS/MS signals of type C compounds.*

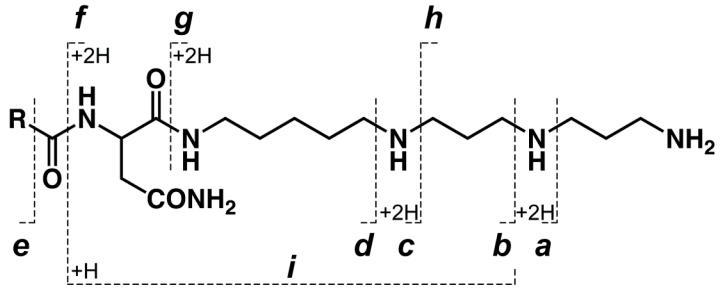

name (group) head portion	*m/z* (relative abundance)								
	$[M+H]^+$ $[M+H–NH_3]^+$ $[M+H–H_2O]^+$	***a***	***b*** ***b***–NH_3 ***b***–H_2O	***c*** ***d***	***e***	***f*** ***f***–NH_3 ***f***–H_2O	***g*** ***g***–NH_3	***h*** ***h***–NH_3	***i*** ***i***–NH_3 ***i***–$2NH_3$
LF487C (1) IndAc	488 (90) 471 (14) 470 (3)	431 (5)	414 (64) 397 (5) 396 (3)	374 (3) 357 (2)	130 (13)	331 (7) 314 (8) 297 (6)	217 (24) 200 (2)	115 (100) 98 (35)	257 (5) 240 (5) 223 (4)
LF503C (2) 4-OH-IndAc	504 (100) 487 (15) 486 (3)	447 (4)	430 (52) 413 (5) 412 (3)	390 (3) 373 (2)	146 (20)	331 (20) 314 (11) 297 (9)	217 (38) 200 (3)	115 (97) 98 (30)	257 (10) 240 (5) 223 (4)
LF448C (3) PhAc	449 (100) 432 (15) 431 (2)	392 (5)	375 (76) 358 (3) 357 (3)	335 (2) 318 (1)	—	331 (2) 314 (4) 297 (3)	217 (12) —	115 (74) 98 (26)	257 (2) 240 (3) 223 (3)
LF464C (4) 4-OH-PhAc	465 (100) 448 (15) 447 (2)	408 (5)	391 (78) 374 (4) 373 (4)	— —	107 (1)	331 (3) 314 (4) 297 (3)	217 (14) —	115 (85) 98 (31)	257 (3) 240 (4) 223 (2)
LF480C (5) 2,4-$(OH)_2$PhAc	481 (93) 464 (13) 463 (4)	424 (5)	407 (64) 390 (5) 389 (4)	— —	—	331 (28) 314 (11) 297 (4)	217 (25) 200 (3)	115 (100) 98 (35)	257 (19) 240 (7) 223 (3)

***Table 5**. Types, nominal masses and relative intensities of relevant HCD-MS/MS signals of type D compounds.*

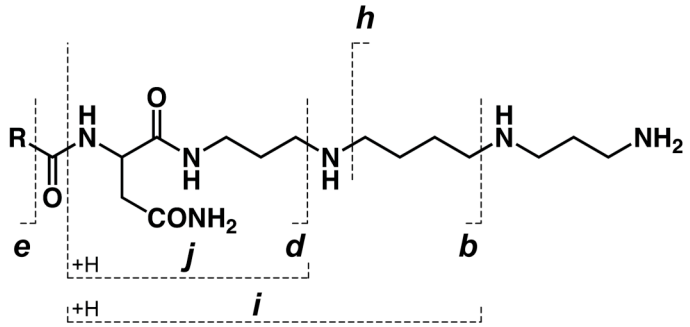

name (group) head portion	*m/z* (relative abundance)						
	$[M+H]^+$	***b*** ***b***–NH_3 ***b***–H_2O	***d*** ***d***–NH_3 ***d***–H_2O	***e***	***h*** ***h***–NH_3 ***h***–NH_3–C_2H_4	***i*** ***i***–NH_3 ***i***–$2NH_3$	***j*** ***j***–NH_3 ***j***–$2NH_3$
LF473D (1) IndAc	474(2)	400 (39) 383 (7) 382 (7)	329 (9) 312 (20) 311 (1)	130 (4)	129 (100) 112 (38) 84 (2)	243 (4) 226 (2) 209 (3)	172 (1) 155 (1) 138 (3)
LF489D (2) 4-OH-IndAc	490 (3)	416 (32) 399 (5) 398 (6)	345 (7) 328 (12) 327 (1)	146 (5)	129 (100) 112 (34) 84 (2)	243 (6) 226 (2) 209 (3)	172 (3) 155 (2) 138 (2)
LF434D (3) PhAc	—	361 (42) 344 (5) 343 (6)	290 (7) 273 (18) —	—	129 (100) 112 (38) 84 (2)	— — —	— — 138 (3)
LF450D (4) 4-OH-PhAc	451 (2)	377 (31) 360 (4) 359 (5)	306 (6) 289 (13) 288 (1)	—	129 (100) 112 (39) 84 (2)	243 (1) 226 (1) 209 (1)	172 (2) 155 (1) 138 (2)
LF466D (5) 2,4-$(OH)_2$-PhAc	467 (3)	393 (41) 376 (1) 375 (6)	— 305 (11) —	—	129 (100) 112 (34) 84 (2)	243 (4) — —	172 (3) — 138 (1)
LF502D (6) Trp	—	429 (30) 412 (5) 411 (3)	358 (5) 341 (8) —	159 (6)	129 (100) 112 (33) 84 (2)	243 (14) 226 (2) 209 (2)	172 (5) 155 (1) 138 (1)
LF503D (7) IndLac	504 (3)	430 (40) 413 (7) 412 (5)	359 (8) 342 (16) 341 (1)	160 (1)	129 (100) 112 (36) 84 (2)	243 (3) 226 (2) 209 (3)	172 (1) 155 (2) 138 (2)

***Table 6**. Types, nominal masses and relative intensities of relevant HCD-MS/MS signals of type E compounds.*

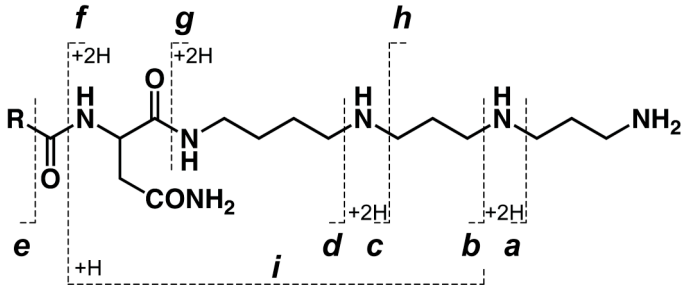

name (group) head portion	*m/z* (relative abundance)								
	$[M+H]^+$ $[M+H-NH_3]^+$ $[M+H-H_2O]^+$	***a***	***b*** ***b***–NH_3 ***b***–H_2O	***c*** ***d*** ***d***–NH_3	***e***	***f*** ***f***–NH_3 ***f***–H_2O	***g*** ***g***–NH_3	***h*** ***h***–NH_3	***i*** ***i***–NH_3 ***i***–$2NH_3$
LF473E (1) IndAc	474 (100) 457 (17) 456 (2)	417 (5)	400 (59) 383 (7) 382 (3)	360 (2) 343 (4) 326 (2)	130 (13)	317 (7) 300 (7) 283 (5)	203 (21) 186 (9)	115 (84) 98 (26)	243 (4) 226 (3) 209 (3)
LF489E (2) 4-OH-IndAc	490 (100) 473 (16) 472 (3)	433 (4)	416 (45) 399 (6) 398 (3)	376 (2) 359 (4) —	146 (20)	317 (19) 300 (9) 283 (7)	203 (33) 186 (13)	115 (88) 98 (24)	243 (9) 226 (3) 209 (3)
LF434E (3) PhAc	435 (100) 418 (15) 417 (2)	378 (5)	361 (68) 344 (6) 343 (4)	321 (1) 304 (3) 287 (2)	—	317 (3) 300 (5) 283 (3)	203 (15) 186 (6)	115 (84) 98 (29)	243 (2) 226 (3) 209 (2)
LF450E (4) 4-OH-PhAc	451 (100) 434 (15) —	394 (3)	377 (67) 360 (5) 359 (3)	— 320 (2) 303 (1)	—	317 (2) 300 (4) 283 (2)	203 (13) 186 (5)	115 (81) 98 (27)	243 (2) 226 (3) 209 (2)
LF466E (5) 2,4-$(OH)_2$-PhAc	467 (100) 450 (15) 449 (3)	410 (4)	393 (56) 376 (4) 375 (4)	— 336 (2) 319 (1)	123 (1)	317 (26) 300 (10) 283 (4)	203 (22) 186 (9)	115 (86) 98 (28)	243 (14) 226 (4) 209 (2)

***Table 7**. Types, nominal masses and relative intensities of relevant HCD-MS/MS signals of type F compounds.*

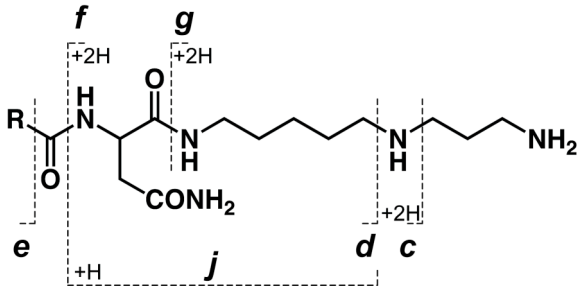

name (group) head portion	*m/z* (relative abundance)					
	$[M+H]^+$ $[M+H-NH_3]^+$ $[M+H-H_2O]^+$	***c*** ***d***	***e***	***f*** ***f***–NH_3 ***f***–H_2O	***g*** ***g***–NH_3 ***g***–$2NH_3$	***j*** ***j***–NH_3
LF430F (1) IndAc	431 (100) 414 (48) 413 (5)	374 (3) 357 (4)	130 (20)	274 (17) 257 (15) 240 (17)	160 (31) 143 (11) 126 (6)	200 (1) —
LF446F (2) 4-OH-IndAc	447 (100) 430 (40) 429 (2)	390 (2) 373 (3)	146 (35)	274 (37) 257 (27) 240 (24)	160 (50) 143 (13) 126 (7)	200 (1) —
LF391F (3) PhAc	392 (100) 375 (50) 374 (4)	335 (4) 318 (4)	91 (1)	274 (5) 257 (8) 240 (11)	160 (20) 143 (7) 126 (5)	— 183 (1)
LF407F (4) 4-OH-PhAc	408 (100) 391 (54) 390 (5)	351 (4) 334 (5)	107 (5)	274 (9) 257 (11) 240 (15)	160 (25) 143 (9) 126 (7)	200 (1) 183 (1)
LF423F (5) 2,4-$(OH)_2$-PhAc	424 (100) 407 (44) 406 (8)	367 (3) 350 (4)	123 (4)	274 (52) 257 (36) 240 (21)	160 (45) 143 (18) 126 (13)	200 (2) —

2.4 Experimental

2.4.1 Material

HPLC supra grade acetonitrile was purchased from Scharlau (Barcelona, Spain), trifluoroacetic acid (TFA) from Fluka (Buchs, Switzerland), and D_2O 99.9% and d_1-TFA 99.5% from Cambridge Isotope Laboratories, Inc. (Andover, Ma, USA). HPLC grade H_2O (< 5 ppm) was obtained by purification of deionized water with a MilliQ gradient apparatus (Millipore, Milford, MA, USA).

2.4.2 Venom Preparation

Lyophilized *L. folium* venom was purchased from Fauna Laboratories, Ltd (Almaty, Kazakhstan) and dissolved (~ 100 μg) in MeCN/H_2O + 0.1% TFA (1:3, 50 μl) or MeCN/D_2O + 0.1% d_1-TFA (1:3, 50 μl) for the LC-MS experiments in deuterated solvent. The venom and the stock solution was stored at -20 °C prior to use.

2.4.3 HPLC-UV(DAD)-ESI-MS and -MS/MS

LC-MS analyses were performed on a Hewlett-Packard 1100 HPLC system (Hewlett-Packard Co., Palo Alto, CA, U.S.A.) fitted with a HTS PAL autosampler (CTC Analytics, Zwingen, Switzerland), a Hewlett-Packard 1100 binary pump, and a Hewlett-Packard 1100 photodiode-array detector (DAD). The reversed-phase column used was an Interchim Uptisphere RP C_{18} column (UP3HDO-20QS, 3 μm, 2.3 × 200 mm, Interchim, Montluçon, France). After 5 μl injection, compounds eluted with a step gradient from 5 to 20% B (solvent A: H_2O + 0.1% TFA, solvent B: MeCN + 0.1 % TFA) over 40 min at a flow rate of 150 μl min^{-1}. UV/VIS spectra of the eluent were acquired between 190 and 600 nm every 1 second directly after the column. The HPLC system was connected to an Esquire-LC quadrupole ion trap mass spectrometer (Bruker

Daltonik GmbH, Bremen, Germany), equipped with a Hewlett-Packard ESI Atmospheric Pressure Ion (API) source. The MS-parameters were optimized to get highest response with a minimum of in-source fragmentation. The parameters were: Nebulizer gas (N_2) 40 psi, dry gas (N_2) 9.5 l min^{-1}, dry temperature 300 °C, HV capillary: 4500 V, HV EndPlate offset: –600 V, target mass: 400, compound stability: 80%, trap drive: 120%. The MS acquisitions were performed in positive ion mode at normal resolution (0.6 u at half peak height), and under ion charge control conditions (ICC, target 10'000). Full scan MS were recorded in the mass range from *m/z* 50 to 600 and averaged over 6 single spectra. MS/MS acquisitions were obtained in the mass range from *m/z* 50-600. The isolation width was between 2 and 4 u, the fragmentation cut-off set by "fast calc", and the fragmentation amplitude set at 1V in the "SmartFrag" mode.

2.4.4 On-Column H/D Exchange HPLC-ESI-MS

The H/D exchange experiments were performed using identical conditions than for the HPLC-UV-ESI-MS and MS/MS experiments replacing water and TFA with deuterium oxide and d-TFA, respectively.

2.4.5 nLC-LTQ Orbitrap XL MS and -MS/MS analysis

HR measurements were performed using a Eksigent nano LC system (Eksigent Technologies, Dublin. CA, USA) online coupled to a LTQ Orbitrap XL™ (Thermo, Bremen, Germany) equipped with a nanoelectrospray ion source (nESI). Chromatographic separation was obtained with a 11 cm fused silica emitter, 75 μm inner diameter (BGB Analytik, Böckten, Switzerland), packed in-house with Uptisphere RP C_{18} resin (UP120-3HDO, 3 μm, Interchim, Montluçon, France).

1 μl sample (0.04 mg ml^{-1} lyophilized venom in MeCN/H_2O 1:99 + 0.05% TFA) was loaded onto the column. After loading, compounds eluted with isocratic conditions (3% B over 5 min) followed by a linear gradient (3 to 22% B in 35

min) at a flow rate of 200 nl min^{-1} (solvent A: H_2O/MeCN 99:1 + 0.05% TFA, solvent B: H_2O/MeCN 2:8 + 0.05% TFA).

The nanospray ion source interface was operated as follows: capillary temperature 200 °C, source voltage 1.7 kV, capillary voltage 49 V, tube lens 125 V.

The mass spectrometer was calibrated immediately before the measurements according to manufacturers instructions. Furthermore, masses were calibrated internally during measurements using lock masses (429.088735 and 445.120025), resulting in a relative mass error of the measured masses lower then 2 ppm for MS and 5 ppm for MS/MS data.

The LTQ Orbitrap XL was operated in parallel mode, allowing the acquisition of an Fourier transform (FT) MS spectrum in the orbitrap concurrent with the acquisition of two low resolution MS/MS spectra in the ion trap, followed by the acquisition of two FT-MS/MS spectra in the orbitrap. FT-MS spectra were acquired with a resolving power of 60000 full-width at half maximum (FWHM) at *m*/*z* 400 in a mass range from *m*/*z* 120 to 1000. Data dependent™ MS/MS spectra of the two most intense ions of the FT-MS spectrum were acquired after collision-induced dissociation (CID) and detection in the linear ion trap (IT-MS/MS, low resolution) as well as after "higher-energy collisional dissociation" (HCD) in the octopole collision cell and subsequent analysis in the orbitrap (FT-MS/MS, high resolution). For the IT-CID-MS/MS, the isolation width was set to 2 *m*/*z* and the normalized collision energy to 30. FT-HCD-MS/MS data were acquired with a resolution of 7500 FWHM at *m*/*z* 400, with an isolation width of 2 *m*/*z*, and a normalized collision energy of 35. The automatic gain control (AGC) target settings for the allowed number of ions in the mass analyzers were set to 5e5 for FT-MS, 1e4 for IT-MS/MS and 2e5 for FT-MS/MS experiments.

2.4.6 Amino Acid Analysis

The venom was fractionated using the same chromatographic conditions as applied for the HPLC-MS analysis and 20 µl of the venom sample was injected. The following fractions were collected: F2: 13 – 14.4 min (contains **LF450D**, **LF450E**, **LF464A**, **LF464B**, **LF466D**, **LF480A**), F3: 14.4 – 15.8 min (contains **LF407F**, **LF423F**, **LF466E**, **LF477A**, **LF477B**, **LF480B**), F4: 15.8 – 20.1 min (contains **LF464C**, **LF480C**, **LF502D**, not submitted for amino acid analysis, too diluted), F5: 20.1 – 22.1 min (contains **LF434D**, **LF448A**, **LF489D**, **LF503D**, **LF516A**, **LF516B**), F6: 22.1 – 23.2 min (contains **LF434E**, **LF448B**, **LF489E**, **LF503B**), F7: 23.2-24.8 (contains **LF446F**, **LF478A** + unknown compound), F8: 24.8 – 26.7 min (contains **LF391F**, **LF448C**, **LF478B**, **LF503C** + unknown compound), F9: 26.7 – 28.0 min (contains **LF473D**, **LF487A**), F10: 28.0 – 29.2 min (contains **LF473E**, **LF487B**, **LF503D**, **LF517A**), F11: 29.2 – 30.5 min (contains **LF517B**), F12 (contains **LF430F** + **LF487C** + unknown compound). For the hydrolysis, 150 or 200 µl of the fractions were lyophilized and hydrolyzed with 6M HCl in vapour for 22 hours at 110 °C. The hydrolyzed sample was dissolved in 20 µl of 50 mM HCl containing the internal standards norvaline and sarcosine. The solutions were centrifuged, and 1 µl was injected for derivatization (with OPA/FMOC chemistry) and amino acid analysis (performed on a Amino Quant amino acid analyzer, Agilent).

2.5 References

[1] S. Bienz, P. Bisegger, A. Guggisberg, M. Hesse, *Nat. Prod. Rep.* **2005**, *22*, 647.

[2] S. Bienz, R. Detterbeck, C. Ensch, A. Guggisberg, U. Häusermann, C. Meisterhans, B. Wendt, C. Werner, M. Hesse, in *The Alkaloids, Vol. 58* (Ed.: G. A. Cordell), Academic Press, New York, **2002**, pp. 83.

[3] A. L. Mueller, R. Roeloffs, H. Jackson, in *The Alkaloids, Vol. 46* (Ed.: G. A. Cordell), Academic Press, New York, **1995**, pp. 63.

[4] G. Karigiannis, D. Papaioannou, *Eur. J. Org. Chem.* **2000**, 1841.

[5] M. S. Palma, T. Nakajima, *Toxin Rev.* **2005**, *24*, 209.

[6] A. Schäfer, H. Benz, W. Fiedler, A. Guggisberg, S. Bienz, M. Hesse, in *The Alkaloids, Vol. 45* (Ed.: G. A. Cordell), Academic Press, New York, **1994**, pp. 1.

[7] S. Chesnov, L. Bigler, M. Hesse, *Eur. J. Mass Spectrom.* **2002**, *8*, 1.

[8] S. Chesnov, L. Bigler, M. Hesse, *Helv. Chim. Acta* **2001**, *84*, 2178.

[9] N. Manov, M. Tzouros, S. Chesnov, L. Bigler, S. Bienz, *Helv. Chim. Acta* **2002**, *85*, 2827.

[10] S. Chesnov, L. Bigler, M. Hesse, *Helv. Chim. Acta* **2000**, *83*, 3295.

[11] S. Eichenberger, L. Bigler, S. Bienz, *Chimia* **2007**, *61*, 161.

[12] Q. Hu, R. J. Noll, H. Li, A. Makarov, M. Hardman, R. G. Cooks, *J. Mass Spectrom.* **2005**, *40*, 430.

[13] A. Makarov, E. Denisov, A. Kholomeev, W. Balschun, O. Lange, K. Strupat, S. Horning, *Anal. Chem.* **2006**, *78*, 2113.

[14] B. Paizs, S. Suhai, *Mass Spectrom. Rev.* **2005**, *24*, 508.

[15] A. E. Pegg, *Biochem. J.* **1986**, *234*, 249.

[16] N. Yamaji, M. Horikawa, G. Corzo, H. Naoki, J. Haupt, T. Nakajima, T. Iwashita, *Tetrahedron Lett.* **2004**, *45*, 5371.

[17] W. S. Skinner, P. A. Dennis, A. Lui, R. L. Carney, G. B. Quistad, *Toxicon* **1990**, *28*, 541.

CHAPTER 3

Structure Elucidation of Acylpolyamines from *Ozyptila lugubris*, *Lachesana sp.*, and *Drassodes sp.* Spider Venom

Abstract

Lyophilized *Ozyptila lugubris*, *Lachesana sp.*, and *Drassodes sp.* venom was analyzed with the same extended analytical setup as used for the investigations of *Larinioides folium* venom, *i.e.* by HPLC-ESI-MS, nanoLC coupled with high-resolution Fourier transform MS, on-column H/D exchange HPLC-MS and amino acid analysis of venom fractions. By this extended analytical setup, the structures of 20 acylpolyamines — most of them found for the first time in natural sources — could be elucidated. Three structurally different types of acylpolyamines were found, whereas within the same venom, only one structural type was found. The toxins of *D. sp.* are of particular interest since they are members of the rather rare case of bis-acylated polyamines.

3.1 Introduction

Polyamines and their derivatives are widely found throughout the animal and plant kingdom (for reviews, see [1,2]). Since they exhibit a variety of interesting and important biological activities [3,4], not only new and efficient methods for their synthesis but also more sensitive and selective methods for the identification and structural elucidation of new examples from natural sources are searched for.

Particularly acylpolyamines of spider venoms have attracted the attention of the scientific community in the past decades [5,6]. A most sensitive and meanwhile well-established methodology for the direct analysis of acylpolyamines in spider venoms — without prior isolation of the sample compounds — is high-performance liquid chromatography (HPLC), on-line coupled with mass spectrometry (MS) and tandem mass spectrometry (MS/MS) [7,8]. The power of this method was demonstrated, *e.g.*, by the structural elucidation of acylpolyamines contained in the venom of the spiders *Agelenopsis aperta* [9] and *Paracoelotes birulai* [10]. While well suited for the study of the rather structurally simple compounds found in these spiders, this method proved to be insufficient for the investigation of the more complex polyamine toxins of the spider *Larinioides folium*. Thus, the analytical setup had to be extended with of on-column H/D-exchange HPLC-MS, amino acid analysis of venom fractions, and nano LC (nLC) connected to high-resolution Fourier transform (FT) MS with an LTQ Orbitrap XL [11,12]. This analytical procedure finally provided access to adequate information to dispel most of the remaining uncertainties, allowing the structural elucidation of most of the polyamine toxins contained in this venom.

The same extended analytical setup was also appropriate for the study of the polyamine toxins contained in the venom of the spiders *Ozyptila lugubris*, *Lachesana sp.*, and *Drassodes sp*. In the following, the structural diversity of the acylpolyamine toxins produced by these three spider species is shown, and the structural elucidation of the compounds is discussed in detail.

3.2 Results and Discussion

3.2.1 General Structures of the Toxins

The venoms of the three spiders *O. lugubris*, *L. sp.*, and *D. sp.* contain three major types of polyamine derivatives, each type being characteristic for each of the spider species. Figure 1 shows the three toxins **OZ375**, **LH446**, and **DR442**[1] as respective examples of these compound classes.

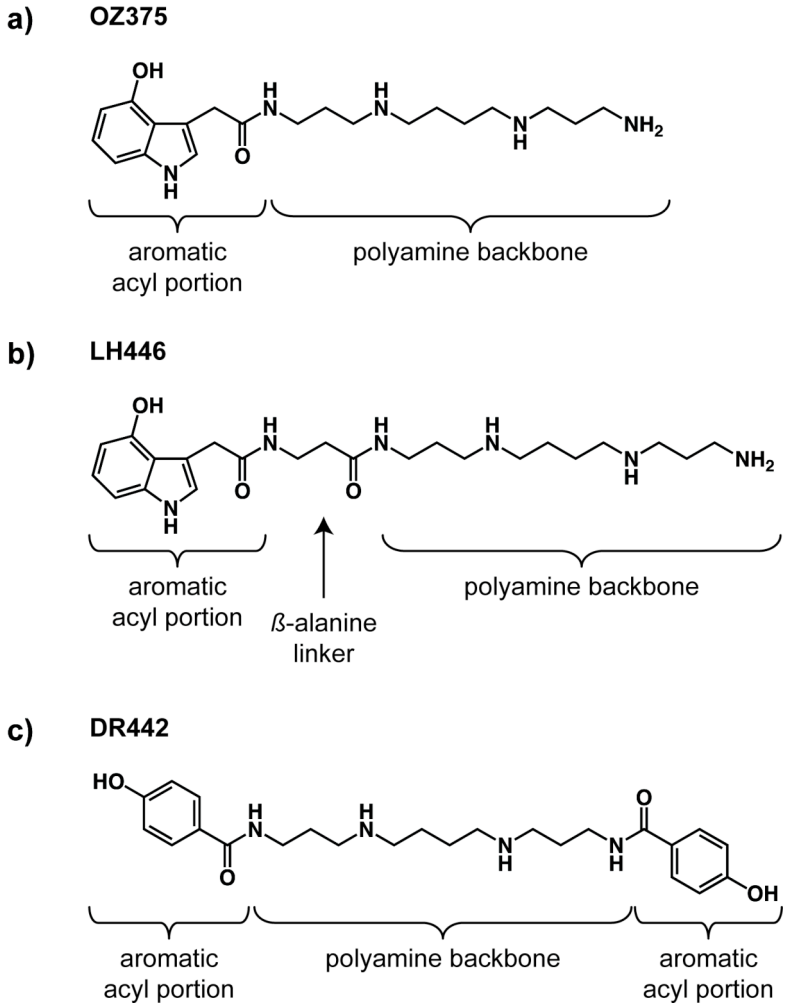

***Figure 1**. Spider-specific general structures of the acylpolyamines found in* O. lugubris, L. sp., *and* D. sp. venom, *exemplified with **OZ389**, **LH446**, and **DR442**, respectively. For the complete set of toxins see Tables 1, 3, and 5.*

[1] The toxins were named according to the genus of the source organism (OZ for *Ozyptila*; LH for *Lachesana*; DR for Drassodes), followed by their nominal mass and, if isomeric compounds are present in the venom, by a suffix A, B, according to their polyamine backbone.

All three types of compounds contain a polyamine backbone and a chromophoric acyl group, the two well-known and meanwhile for polyamine spider toxins as mandatory regarded molecular portions. While **OZ375** and the related toxins of *O. lugubris* are composed of these two units alone, **LH446** and **DR442** are more complex in structure. The former compound and the related toxins of *L. sp.* possess, in addition to the polyamine core and the acyl moiety, a β-alanine unit interlinking these two portions. Such interlinking β-alanine groups have already been found as building blocks in polyamine toxins of other spiders. **DR442** and its structure-related compounds from *D. sp.*, however, are structurally rather unique. Unlike most of the spider toxins that have been found so far, their polyamine cores bear two terminal acyl groups and thus lack the ordinarily found basic terminus of the compounds.

With regard to the polyamine portions contained in the molecules, only non-functionalized backbones were found. In addition to the PA343 (= spermine) unit, being the polyamine portion of the toxins shown in Figure 1, PA353 (= *sym*-homospermine) was found as an additional tetraamine derivative together with the triamines PA34 (= spermidine) and PA35 (= homospermidine) and the diamine PA5 (= cadaverine).[1] (*Figure 2*) The various polyamine blocks, however, were not found as constituents within toxins of all three spider species. Only the venom of *D. sp.* contained compounds with the complete set of the polyamines, while PA5 derivatives were missing in the venom of *O. lugubris*, and the venomous cocktail of *L. sp.* contained only compounds possessing the PA343 and PA353 units.

The polyamine portions of the spider toxins, eventually the polyamine portions extended with β-alanine, were found to be acylated with an overall of four aromatic acyl portions (*Figure 2*). These are 1*H*-indole-3-acetyl (= IndAc), 4-hydroxy-1*H*-indole-3-acetyl (= 4-OH-IndAc), 4-hydroxybenzoyl (= 4-OH-Bz), and dihydroxybenzoyl (= $(OH)_2$-Bz; unknown location of the hydroxy

[1] With regard to the abbreviated polyamine nomenclature, see [2].

groups). The two IndAc building blocks were found in the toxins of *O. lugubris* and *L. sp.* and the two Bz groups in *D. sp.*

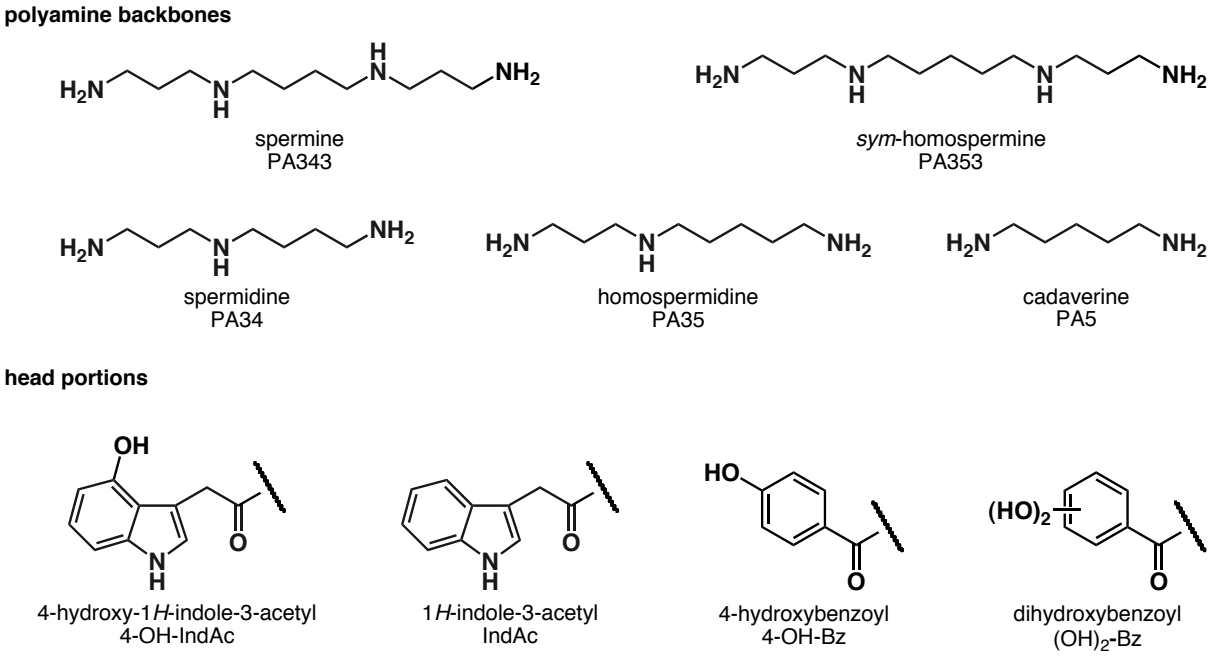

***Figure 2**. Polyamine backbones and head portions found in the acylpolyamines from* O. lugubris*,* L. sp.*, and* D. sp.

A random combination of the various building blocks found for the three spiders would allow for a high structural diversity for the respective toxins. However, possibly due to discrimination during the biosynthesis and the limited sensitivity of the analytical method, some of the potential spider toxins were not found in the venoms. The complete sets of the toxins are described in *Tables 1*, *3*, and *5*.

3.2.2 General Analytical Procedure

The venom of *O. lugubris*, *L. sp.*, and *D. sp.* was investigated with an analytical setup similar to the one used for the study of the polyamine toxins from *L. folium* (*Chapter 2*). In a first pass, the venoms were analyzed by HPLC-UV(DAD)-ESI-MS and MS/MS on a quadrupole ion trap mass spectrometer, then by nano LC (nLC)-MS and -MS/MS performed on a LTQ Orbitrap XL mass spectrometer, a hybrid linear quadrupole ion trap high-resolution *Fourier* transform (FT) orbitrap mass spectrometer equipped with an additional

octopole collision cell. The first analysis included UV data of the compounds along with low-resolution MS and MS/MS data. The second pass revealed high-resoluton MS and MS/MS data at high mass accuracy and, thus, allowed direct determination of elemental compositions of the detected ions. Furthermore, the higher sensitivity of nLC provided better quality of MS and MS/MS data when compared to the HPLC-ESI-MS setup. In a third analytical step, on-column H/D exchange HPLC-MS was performed, providing information about the number of exchangeable protons of the analytes.

These datasets were sufficient, to a certain extent even redundant, for the elucidation of the structures of the polyamine toxins derived from the spiders *O. lugubris* and *D. sp*. However, they were not yet sufficient for the structural elucidation of the toxins contained in *L. sp.* For these compounds, the analytical procedure had to be complemented with amino acid analyses of venom fractions, as it was necessary in the study of the toxins from the spider *L. folium* (see *Chapter 2*).

The relative amounts of the compounds were estimated on the basis of the peak integrations of the extracted ion chromatograms (EIC) obtained by the HPLC-ESI-MS method. The corresponding estimates based on the peak areas of the respective EIC from the nLC method proved inadequate because it was found that at higher concentrations of the polyamine samples saturation in the ion response occurred, which led to systematic errors.

The analytical data acquired according to the setup shown above is summarized in the *Tables 1–6*. They are discussed below in turn for the toxins originating from the three different spider species.

3.2.3 Polyamine Toxins from *Ozyptila lugubris* Venom

3.2.3.1 Structural Diversity

The polyamine toxins found in the venom of *O. lugubris* have the simplest structures of the compounds investigated in this study. They are composed solely of a polyamine backbone connected at one end to an aromatic acyl moiety (*e.g.*, **OZ375** in *Figure 1*; the remaining structures are found in *Table 1*). All four polyamine backbones mentioned above have been found as molecular portions in the compounds. Together with the two chromophoric units, IndAc and 4-OH-IndAc, twelve toxins would theoretically be possible. Of these compounds, eight were in fact found: all six possible structures with the 4-OH-IndAc head moiety and two structures with the non-hydroxylated chromophoric unit IndAc. The latter two examples correspond, with regard to the polyamine backbones, to the two major constituents containing the 4-OH-IndAc group (see chromatograms in *Figure 3* and data in *Table 1*). Since the IndAc derivatives occur only in approximately 5–8% of the amount of the 4-OH-IndAc compounds, the "missing" IndAc toxins most probably were not found due to the detection limits of the analytical setup rather than due to their real absence from the venom.

3.2.3.2 Structure Elucidation

Figure 3 shows three examples of the HPLC traces obtained with the venom of *O. lugubris* using the setup of HPLC-UV(DAD)-ESI-MS. Trace (a) shows the UV chromatogram (detection at 254 nm) and traces (b) to (d) MS traces. (b) Represents the base peak chromatogram (BPC); (c) and (d) two extracted ion chromatograms (EIC), obtained by extracting the ions with *m*/*z* corresponding to quasi-molecular ions of the 4-OH-IndAc and IndAc derivatives, respectively.

The figure clearly shows that the various compounds are well separated in the two dimensions of retention time and *m/z*, which allowed independent MS analyses. It also shows, however, that the acquisition of the individual UV spectra is not possible for all of the toxins. **OZ332B** and **OZ359** are almost co-eluting compounds, with **OZ359** being present in only a small concentration, which did not produce a "pure" UV spectrum for **OZ359**. In the case of **OZ332A** and **OZ318A**, the concentration of the analyte was simply too low for the acquisition of a meaningful spectrum.

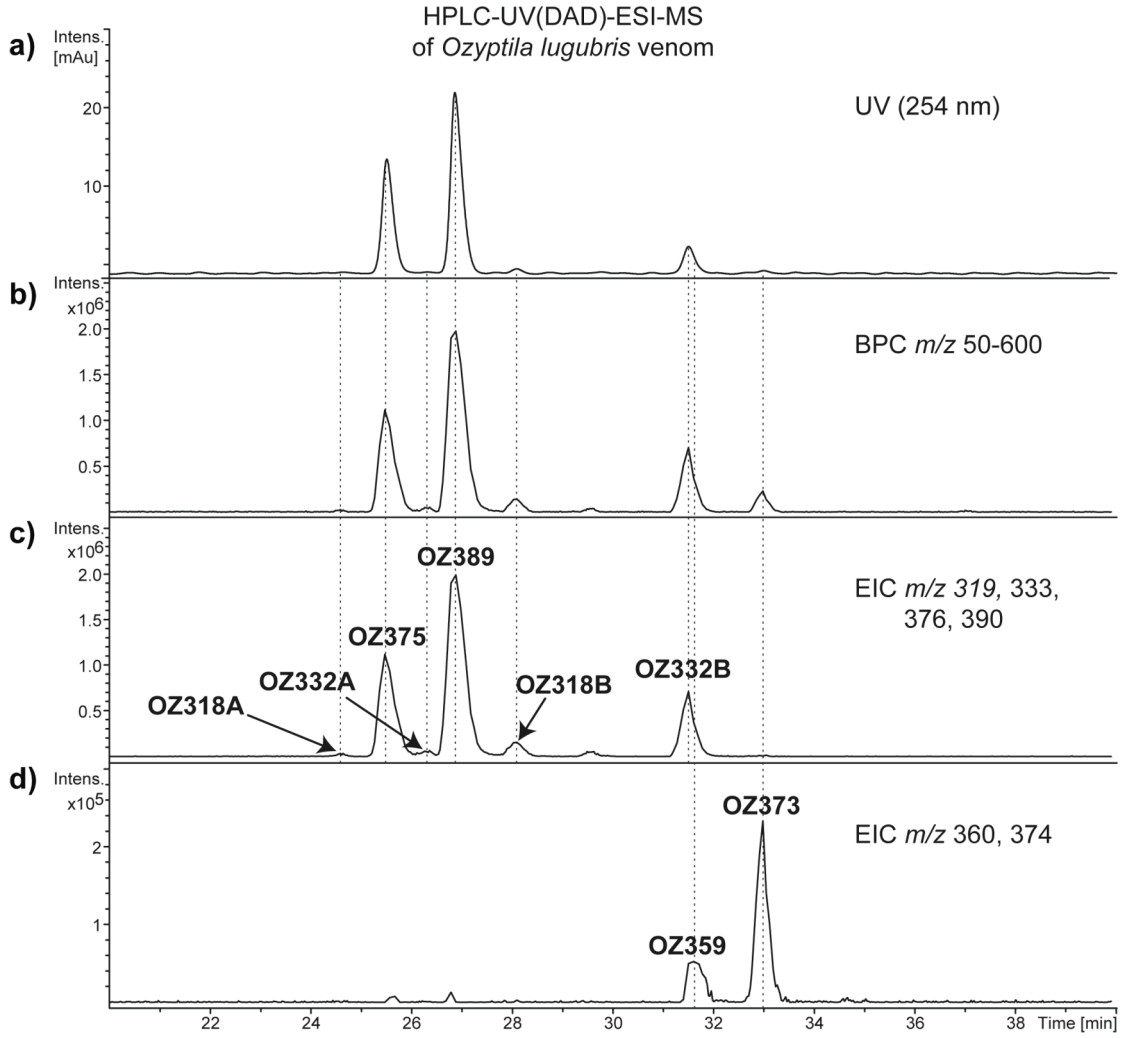

***Figure 3**. Relevant UV- and MS-trace chromatograms of an HPLC-UV(DAD)-ESI-MS run of* O. lugubris *venom: (**a**) UV-chromatogram at 254 nm, (**b**) BPC at m/z 50 – 600, and EIC of (**c**) ions at m/z 319, 333, 376, and 390 and (**d**) ions at m/z 360 and 374.*

***Table 1**. Structures, retention times (rt), relative amounts, number of exchangeable protons and high-resolution ESI-MS data of acylpolyamines found in* O. lugubris *venom.*

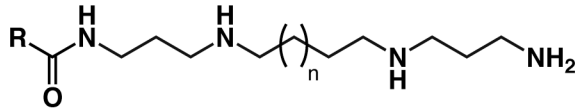

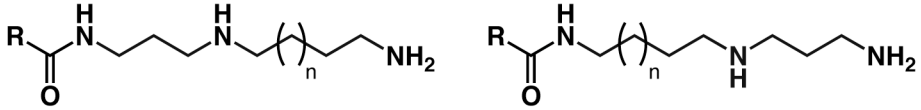

R head portion	name	backbone[a]	rt [min]	r. a.[b] [%]	exch. protons	elem. comp. $[M+H]^+$	$[M+H]^+_{theo}$ m/z	$[M+H]^+_{exp.}$ m/z	Δm [ppm]
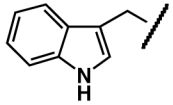 IndAc	**OZ359**	PA343	31.6	3	6	$C_{20}H_{34}N_5O$	360.27579	360.27571	–0.2
	OZ373	PA353	33	8	6	$C_{21}H_{36}N_5O$	374.29144	374.29132	–0.3
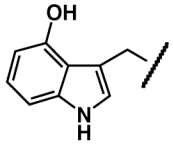 4-OH-IndAc	**OZ375**	PA343	25.5	48	7	$C_{20}H_{34}N_5O_2$	376.27070	376.27070	0.0
	OZ389	PA353	26.9	100	7	$C_{21}H_{36}N_5O_2$	390.28635	390.28644	0.2
	OZ318A	PA34	24.6	1	—	$C_{17}H_{27}N_4O_2$	319.21285	319.21270	–0.5
	OZ318B	PA43	28.1	6	6	$C_{17}H_{27}N_4O_2$	319.21285	319.21300	0.5
	OZ332A	PA35	26.4	2	—	$C_{18}H_{29}N_4O_2$	333.22850	333.22856	0.2
	OZ332B	PA53	31.5	27	6	$C_{18}H_{29}N_4O_2$	333.22850	333.22868	0.5

[a] PA stands for polyamine, the figures designate the number of methylene units in-between the N-atoms.
[b] The values given represent the concentration in % relative to the most abundant acylpolyamine contained in the venom and were estimated on the basis of the peak integrals in their EIC obtained by HPLC-ESI-MS.

***Table 2**. Types, nominal masses and relative intensities of relevant HCD-MS/MS signals of acylpolyamines contained in O. lugubris.*

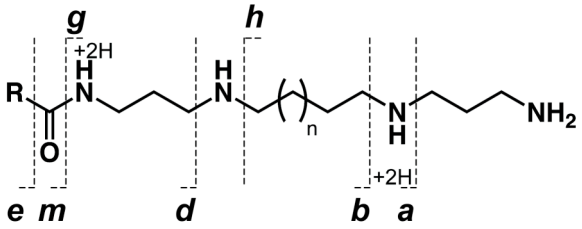

backbone[a]	**name** head portion	*m/z* (relative abundance)					
		[M+H]$^+$ [M+H–NH_3]$^+$ [M+H–H_2O]$^+$	***a*** ***b***	***d*** ***d***–C_2H_4	***m*** ***e***	***g***	***h*** ***h***–NH_3 ***h***–NH_3–C_2H_4
PA343	**OZ359** IndAc	360 (9) — —	— 286 (71)	215 (82) —	— 130 (1)	—	129 (100) 112 (39) 84 (2)
	OZ375 4-OH-IndAc	376 (10) — 358 (1)	— 302 (63)	231 (80) —	— 146 (2)	203 (1)	129 (100) 112 (34) 84 (1)
PA353	**OZ373** IndAc	374 (43) 357 (3) 356 (3)	317 (1) 300 (43)	215 (100) —	— 130 (2)	217 (4)	143 (59) 126 (36) 98 (3)
	OZ389 4-OH-IndAc	390 (38) 373 (3) 372 (6)	333 (1) 316 (33)	231 (100) 203 (1)	174 (1) 146 (3)	217 (11)	143 (62) 126 (32) 98 (3)

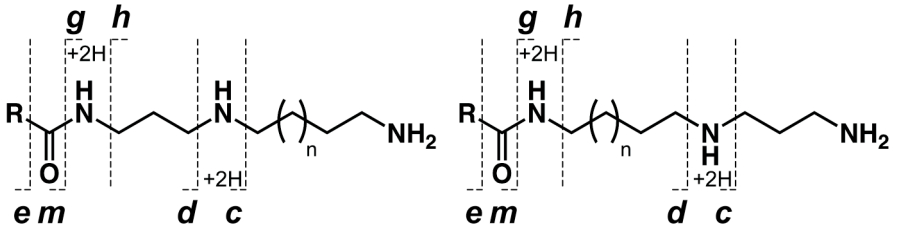

backbone[a]	**name** head portion	*m/z*[b] (relative abundance)				
		[M+H]$^+$ [M+H–NH_3]$^+$ [M+H–H_2O]$^+$	***c*** ***d*** ***d***–C_2H_4	***m*** ***e***	***g***	***h*** ***h***–NH_3 ***h***–NH_3–C_2H_4
PA34	**OZ318A** 4-OH-IndAc	319 (16) 302 (26) —	248 (9) 231 (100) 203 (1)	174 (1) 146 (3)[b]	146 (2)[b]	129 (2) 112 (1) —
PA35	**OZ332A** 4-OH-IndAc	333 (37) 316 (9) 315 (3)	248 (3) 231 (100) 203 (1)	174 (1) 146 (3)	160 (4)	143 (1) — —
PA43	**OZ318B** 4-OH-IndAc	319 (100) 302 (33) 301 (3)	262 (5) 245 (38) —	174 (2) 146 (8)[b]	146 (8)[b]	129 (10) 112 (8) —
PA53	**OZ332B** 4-OH-IndAc	333 (100) 316 (45) 315 (3)	276 (9) 259 (6) —	174 (2) 146 (6)	160 (11)	143 (4) 126 (4) 98 (1)

[a] PA stands for polyamine, the figures designate the numbers of methylene units in-between the N-atoms.

[b] In the case of **OZ318A** and **OZ318B**, fragment ions **e** and **g** have the same nominal but a different exact mass and are distinguished by HCD-MS/MS due to high resolution and accuracy.

Individual and significant UV spectra, however, were recorded for the compounds **OZ375**, **OZ389**, **OZ318B**, and **OZ323B** as well as for **OZ373**. The spectrum for the first four toxins was the same (λ_{max} = 268, 284, and 292) and was indicative of 4-hydroxyindole, a well-known structural moiety for spider toxins [6]. **OZ373**, on the other hand, showed a UV spectrum indicative of indole (λ_{max} = 280, 288; shoulder at λ = 270) as also found frequently with other spider toxins. Together with the HR-MS/MS fragments of type ***e***, ***g***, and ***m***, which are all or at least in part found for all these analytes, the 4-hydroxy-1*H*-indole-3-acetyl (4-OH-IndAc) and the 1*H*-indole-3-acetyl (IndAc) were redundantly secured as the molecular portions of the two types of compounds. Even though UV evidence was not available, the remaining chromophores were determined by the MS/MS spectra of their parent compounds. At least fragment ***e*** was found for all the remaining toxins — for **OZ318A** and **OZ332A** also the fragments of type ***g*** and ***m*** were recorded — allowing the deduction of the chemical formula of the head portions. Together with the fact that within a spider venom usually sets of polyamine toxins share the same head portion, evidence appears to be strong enough that this head group is IndAc for **OZ359** and 4-OH-IndAc for **OZ318A** and **OZ332A**.

The assignment of the polyamine backbones to the several toxins is based on the fragmentation behavior of the quasi-molecular ions upon CID and on the high-resolution high mass accuracy data that was collected by HCD-MS/MS of the analytes. The fragments of type ***g***, which were detected for all toxins except for **OZ359**, directly revealed the elemental compositions of the polyamine backbones of the sample molecules, corresponding to the structures shown in *Tables 1* and *2*. For **OZ359**, the elemental composition of the polyamine portion was deduced from the compositions of the quasi-molecular ion $[M + H]^+$ and of fragment ***e***.

With our previous investigations we have shown that MS/MS fragmentation of acylpolyamines follows some rather simple and characteristic rules and that MS/MS patterns of acylpolyamines usually reflect directly the types of

polyamine backbones contained in the molecules [9,10,13]. This observation was directly applied to reveal the polyamine frameworks of the several new toxins.

For the tetra-amine derivatives, two distinct fragmentation patterns were observed that were indicative for PA343 (**OZ359** and **OZ375**) and PA353 (**OZ373** and **OZ389**). Direct evidence for the 1,3-diaminopropyl termini of both types of backbones is found with the fragment ions of type ***b***, which correspond to the loss of 1,3-diaminopropane ($C_3H_{10}N_2$) from the quasi-molecular ions, presumably affected through intramolecular nucleophilic substitution reactions. The positions of the final N-atoms are evidenced redundantly by fragment ions of type ***d*** and ***h***, originating from fragmentations occurring "from the right" or "from the left" sides of the molecules.

In a similar way, the triamine backbones of the remaining four toxins were deduced as PA34/PA43 (**OZ318A** and **OZ318B)** and PA35/PA53 (**OZ332A** and **OZ332B**). For the toxins with suffix B, fragment ions of type ***d*** corresponding to the loss of $C_3H_{10}N_2$ (analogously to fragment ions of type ***b*** above) vouch again for the 1,3-diaminopropyl termini of these compounds, while the respective fragment ions ***d*** of the toxins with the suffix A, corresponding to the losses of $C_4H_{12}N_2$ (**OZ318A**) and $C_5H_{14}N_2$ (**OZ332A**), were proof for the 1,4-diaminobutyl and 1,5-diaminopentyl termini of the compounds.

3.2.4 Polyamine Toxins from *Lachesana sp.* Venom

3.2.4.1 Structural Diversity

Only four polyamine toxins were found in *L. sp.*, and they proved similar in structure to those of *O. lugubris*. As the latter, they possess the chromophoric head groups IndAc and 4-OH-IndAc, and they also share the tetra-amine tail portions PA343 and PA353. Unlike the toxins of *O. lugubris*, however, they contain also a linker in-between the head and tail moieties, namely β-alanine (see, *e.g.*, **LH446**, *Figure 1*; the remaining structures are found in *Table 3*). There is also a difference between the toxins of *L. sp.* and *O. lugubris* with regard to the relative quantities of the compounds within the venoms. While the relative amounts of the compounds possessing the PA353 and PA343 frameworks is approximately the same in both spider venoms (ca. 2:1), the relative amounts of the compounds with the IndAc head groups is much higher in the case of *L. sp.* (approximately 30%, see chromatogram in *Figure 4* and data in *Table 3*, as compared to approximately 7% in the case of *O. lugubris*,). Interestingly, no polyamine toxins were found with smaller polyamine portions than the described tetraamines. However, an additional compound that was not further characterized was registered in the UV chromatogram (rt = 33.4 min). As can be seen in the BPC in *Figure 4*, this venom constituent was not registered in the mass range used in this study (*m*/*z* 50–600) and is probably of a mass higher than 600 Da.

3.2.4.2 Structure Elucidation

Due to the additional β-alanine moiety, the structural elucidation of the *L. sp.* toxins was more complex that that of the toxins of *O. lugubris*. The chromophoric units of the toxins as well as their tetraamine polyamine portions, however, were identified in similar ways. As can be readily recognized with the chromatograms shown in *Figure 4*, the four compounds were separated well enough to allow the acquisition of individual UV and MS

data (see *Tables 3* and *4*). The UV spectra showed again the presence of the indole (λ_{max} = 280, 288; shoulder at λ = 270) and the 4-hydroxyindol moieties (λ_{max} = 268, 284, and 292) for the toxins **LH430**/**LH444** and **LH446**/**LH460**, respectively. Together with the fragment ions of type ***e***, found for all toxins except for **LH430**, and particularly with the fragment ions of type ***d*** and ***i***, found with higher intensities for all compounds and giving in the difference the elemental compositions of the complete head groups, the assignments of IndAc and 4-OH-IndAc as molecular portions of the toxins was secured. For the identification of the polyamine moieties, the same types of fragments as used in the structural deduction of the toxins of *O. lugubris* were diagnostic. The fragment ions of type ***b***, ***d***, and ***h*** clearly prove the polyamine part of the molecules to be PA343 for **LH430**/**LH446** and PA353 for **LH444**/**LH460**.

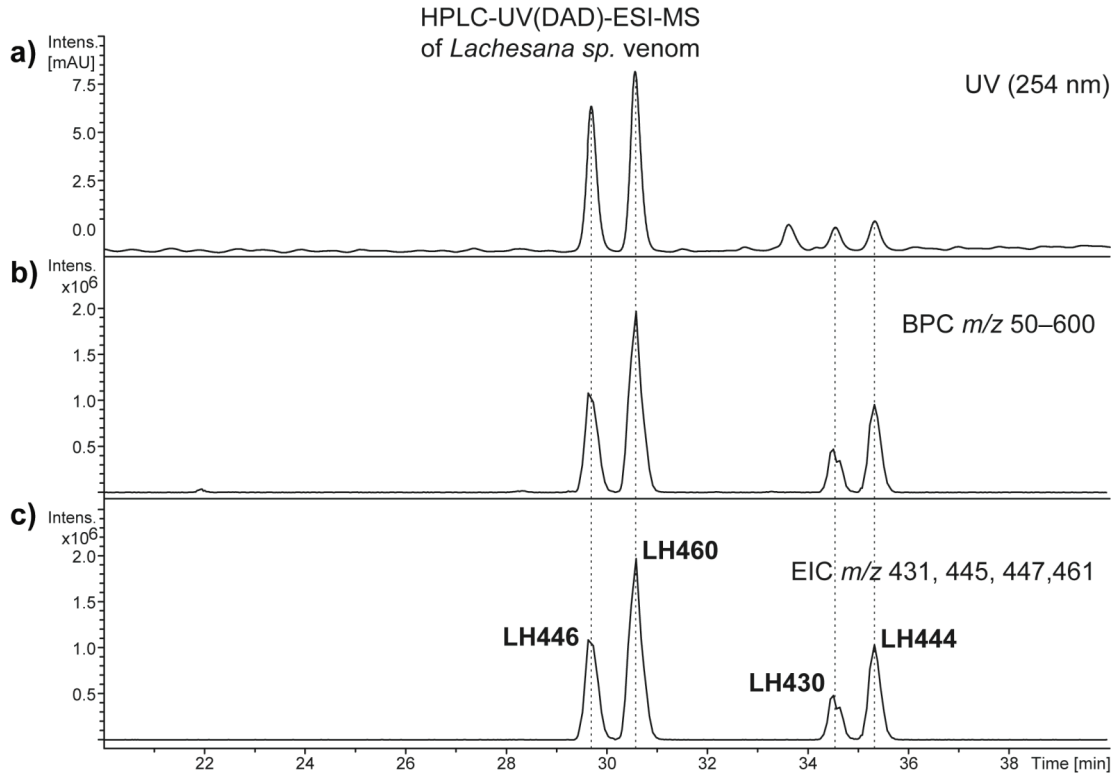

Figure 4*. Relevant UV-trace and ion response chromatograms of an HPLC-UV(DAD)-ESI-MS run of* L. venom: *(**a**) UV-chromatogram at 254 nm, (**b**) BPC at* m/z *50 – 600 and (**c**) EIC of ions at* m/z *431, 445, 447 and 461.*

The amino acid portion of the molecules were not directly amenable by UV and MS data. With the known overall elemental compositions of the toxins ($[M+H]^+$), the chromophoric head groups, and the polyamine portions,

however, the elemental composition of the remaining molecular fragment could be readily deduced as C_3H_5NO. For this chemical formula, several structural units could be proposed, among them an interlinking alanine or β-alanine moiety. To finally secure β-alanine as the interlinking moiety, hydrolysis and amino acid analysis was performed *pars pro toto* with purified **LH460**.

***Table 3**. Structures, retention times (rt), relative amounts, number of exchangeable protons and high-resolution ESI-MS data of acylpolyamines found in* Lachesana sp. *venom.*

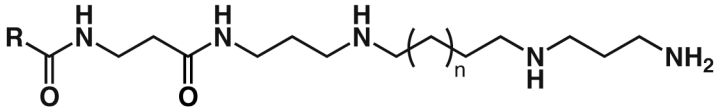

R head portion	name	backbone[a]	rt [min]	r. a.[b] [%]	exch. protons	elem. comp. $[M+H]^+$	$[M+H]^+_{theo}$ m/z	$[M+H]^+_{exp.}$ m/z	Δm [ppm]
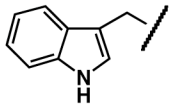 IndAc	**LH430**	PA343	34.5	24	7	$C_{23}H_{39}N_6O_2$	431.31290	431.31274	–0.4
	LH444	PA353	35.3	46	7	$C_{24}H_{41}N_6O_2$	445.32855	445.32835	–0.4
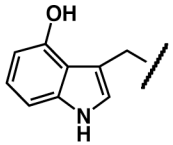 4-OH-IndAc	**LH446**	PA343	29.6	57	8	$C_{23}H_{39}N_6O_3$	447.30782	447.30734	–1.1
	LH460	PA353	30.6	100	8	$C_{24}H_{41}N_6O_3$	461.32347	461.32309	–0.8

[a] PA stands for polyamine, the figures designate the number of methylene units in-between the N-atoms.
[b] The values given represent the concentration in % relative to the most abundant acylpolyamine contained in the venom and were estimated on the basis of the peak integrals in their EIC obtained by HPLC-ESI-MS.

***Table 4**. Types, nominal masses and relative intensities of relevant HCD-MS/MS signals of acylpolyamines contained in L. sp.*

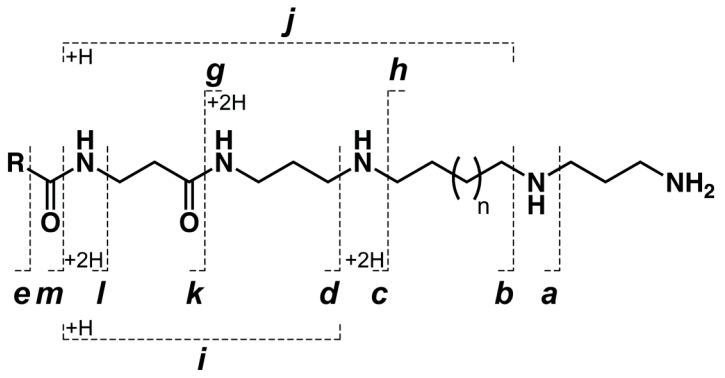

name	*m/z* (relative abundance)								
head portion	$[M+H]^+$	***a***	***c***	***k***	***l***	***g***	***h***	***i***	***j***
backbone[a]	$[M+H-H_2O]^+$	***b***	***c*–H_2O**		***m***		***h*–NH_3**	***i*–NH_3**	***j*–NH_3**
			d		***e***		***h*–NH_3–C_2H_4**		
LH430	431 (5)	—	—	229 (2)	—	—	129 (100)	—	200 (1)
IndAc	—	357 (56)	—		—		112 (35)[c]	112 (39)[c]	183 (10)
PA343			286 (22)		130 (1)		84 (2)		
LH446	447 (7)	—	319 (1)	245 (4)	191 (3)	—	129 (100)[c]	129 (1)[c]	200 (4)
4-OH-IndAc	—	373 (52)	301 (1)		174 (1)		112 (30)[c]	112 (31)[c]	183 (11)
PA343			302 (16)		146 (2)		84 (1)		
LH444	445 (56)[d]	—	—	—	—	217 (3)[d]	143 (72)[d]	—	—
IndAc	—	371 (38)[d]	—		—		126 (39)[d]	112 (62)[d]	197 (8)[d]
PA353			286 (30)[d]		—		—		
LH460	461 (53)	404 (2)	319 (1)	245 (9)	191 (6)	217 (7)	143 (100)	129 (4)	214 (6)
4-OH-IndAc	443 (4)	387 (39)	—		174 (3)		126 (50)	112 (73)	197 (14)
PA353			302 (29)		146 (5)		98 (4)		

[a] PA stands for polyamine, the figures designate the numbers of methylene units in-between the N-atoms.
[c] In the case of **LH430** and **LH446**, the ion pairs **h** and **l** as well as **h**–NH_3 and **i**–NH_3 have each the same nominal but different exact masses and are distinguishable by HCD-MS/MS due to high mass accuracy.
[d] Base peak of the measured HCD-MS/MS of **LH444** is a fragment ion at *m/z* 149 of the lock mass at *m/z* 445.12005. This lock mass ions were co-isolated and -fragmented during HCD of $[M+H]^+$ of **LH444** due to the broad isolation mass window of 2 Da.

3.2.5 Polyamine Toxins from *Drassodes sp.* Venom

3.2.5.1 Structural Diversity

Except for **DR222** and **DR238**, which are simple acyl derivatives of PA5, the toxins of *D. sp.* are terminally bis-acylated tri- and tetra-amines such as **DR442**, the example shown in *Figure 1*. Bis-acylated polyamines (with two non-basic acyl components) are rather unusual structures for spider toxins and to the best of our knowledge found only once before [14]. In *D. sp.*, an overall of six further examples were detected, varying in the polyamine portion and the chromophoric head groups.

Two acyl head groups, 4-OH-Bz and $(OH)_2$-Bz, were found as their building blocks. Together with the four polyamine portions PA34, PA35, PA343, and PA353, an overall of 14 different terminally bis-acylated toxins are principally possible. As in the case of *O. lugubris*, however, not the complete set of compounds was found in the venom of *D. sp.* and again, a certain discrimination of detection of compounds could be the result of the limited sensitivity of the analytical setup. It is evident from the data in *Table 5* (see also chromatograms in *Figure 5*) that the $(OH)_2$-Bz chromophore is much less abundant in the venom as compared to the 4-OH-Bz group. It would not be surprising, then, that for the "mixed" bis-acyl derivatives only the combinations with the most abundant polyamine portions (**DR458** and **DR472** with PA343 and PA353, respectively) would fall in the detection range of the instrumental setup. The "mixed" combinations with the less abundant polyamines, PA34 and PA35, and particularly also all bis-$(OH)_2$-Bz derivatives would then be expected to be present in even smaller amounts, and, thus, lie even more below the detection limits of the instrumentation.

3.2.5.2 Structure Elucidation

Even though the constructions of most of the *D. sp.* toxins are quite different

from those of the other spider species, the analysis of the compounds followed similar tracks as before. *Figure 5* illustrates the elution profiles, obtained by HPLC-UV(DAD) of the lyophilized *D. sp.* venom, and as in the cases before, the several signals seemed well enough separated to allow the acquisition of all relevant UV and MS data. However, there are same peculiarities with these chromatograms that are noteworthy.

Rather striking are the significant differences of the UV and the BPC traces with regard to the number of signals and the relative signal intensities. Especially remarkable are the low signal intensities of the quasimolecular ions $[M + H]^+$ of **DR222** and **DR238**, which contrast with the respective high UV responses. This effect might be the result of a lower efficiency in ion formation for these analytes as compared to the other acylpolyamines that are contained in the venom, and might already hint to the "primary amine natures" of the toxins (the rest of the toxins are secondary amines and as such more basic). A similar effect as with **DR222** and **DR238** is recognized with **DR385**. Also with this compound, low ion response is found in the BPC but high signal intensity in the UV trace. Here, the situation, however, was different. The UV absorption that is recognized in the UV chromatogram (no $\lambda_{max} > 220$ nm) was not due to the polyamine toxin but rather due to a co-eluting analyte, which showed multiply charged ions at *m*/*z* 1357 and 1018 upon MS acquisition in the *m*/*z* window 200–2200. This ions can be interpreted as the $[M + 3H]^{3+}$ and $[M + 4H]^{4+}$ ions of a compound, probably a peptide, with a molecular mass of 4069 Daltons. The remaining signals in the UV chromatogram without an MS response also derive from venom components of higher mass, lying outside the selected mass window of *m*/*z* 50–600.

With regard to the structural elucidation of the toxins of *D. sp.*, the UV data acquired for the several compounds was of lesser value than in the previous cases. This is due to the fact that with the "mixed" acylated toxins **DR458** and **DR472**, possessing two different chromophoric units as structural building blocks, by nature no "pure" UV spectrum could be obtained. The UV spectra, together with the HR mass analyses of the fragments of type ***m*/*m'*** (see *Table 6*), however, still allowed to a large extent the structural assignments of the

two chromophoric units.

MS/MS revealed that **DR238** is the only toxin of *D. sp.* that contains solely a single chromophoric carboxyl unit corresponding to the brutto formula $C_7H_5O_3$. The same mass for the carboxyl group was also found for **DR458** and **DR472**, however, together with the mass corresponding to $C_7H_5O_2$ for a second chromophoric head group. Thus, **DR238** was the only compound that could reveal with its UV spectrum the structure of the respective acyl head group. The UV spectrum of **DR238** (λ_{max} = 256, 289), in fact, was in good agreement with the spectra reported for 3,4-dihydroxybenzoyl derivatives of amines [15,16]. However, the differences to the UV spectra reported for the corresponding carboxylic acid was rather significant, which might be due to the different solvents used in the several investigations. On the basis of further UV data found in literature, the alternative isomers of $C_7H_5O_3$ could largely be excluded as structural possibilities for **DR238**. However, since the reported data are not directly comparable with each other and with our results, due to different experimental setups, we like to stay on the safe side with our assignment and offer solely the general structure $(OH)_2$-Bz for the head group contained in **DR238**, without the specification of the localization of the hydroxy groups.

The situation was less problematic for the toxins **DR222**, **DR385**, **DR399**, **DR442**, and **DR456** that contain solely the chromophoric head group with brutto formula $C_7H_5O_2$. Except for **DR385**, individual UV spectra could be acquired for all the compounds, which were all identical and characteristic for the 4-hydroxybenzoyl moiety (4-OH-Bz, λ_{max} = 254 nm, no additional absorptions at 298 or 302 nm that would be indicative for the 2- or 3-hydroxybenzoyl isomer, respectively). By reason of analogy, 4-OH-Bz was assigned to **DR385** as the head moiety as well.

In the case of the "mixed" toxins **DR458** and **DR472**, the UV spectrum was again the same as for the compounds containing solely the 4-OH-Bz head group. In fact, additional absorptions deriving from the $(OH)_2$-Bz acyl group were expected. Evidently, however, the extinction coefficients for these

additional bands were to low to compete with the major absorption of the 4-OH-Bz chromophore at λ_{max} = 254 nm. On the basis of previous experiences, however, we are confident that the same $(OH)_2$-Bz isomer as for **DR238** constitutes the dihydroxylated benzoyl head portion of these compounds.

Also the structures of the polyamine backbones of the *D. sp.* toxins were deduced analogously to the former investigation. The elemental compositions of these molecular parts were calculated on the basis of the measured exact masses of the $[M + H]^+$ quasi-molecular ions and the known acyl head groups, which revealed purely saturated aminoalkyl moieties for all compounds. The fragments of type ***a***/***a'***, ***b***/***b'***, ***c***/***c'***, and ***d***/***d'*** finally redundantly allowed the location of the internal N-atoms as given in the structures of *Table 5*.

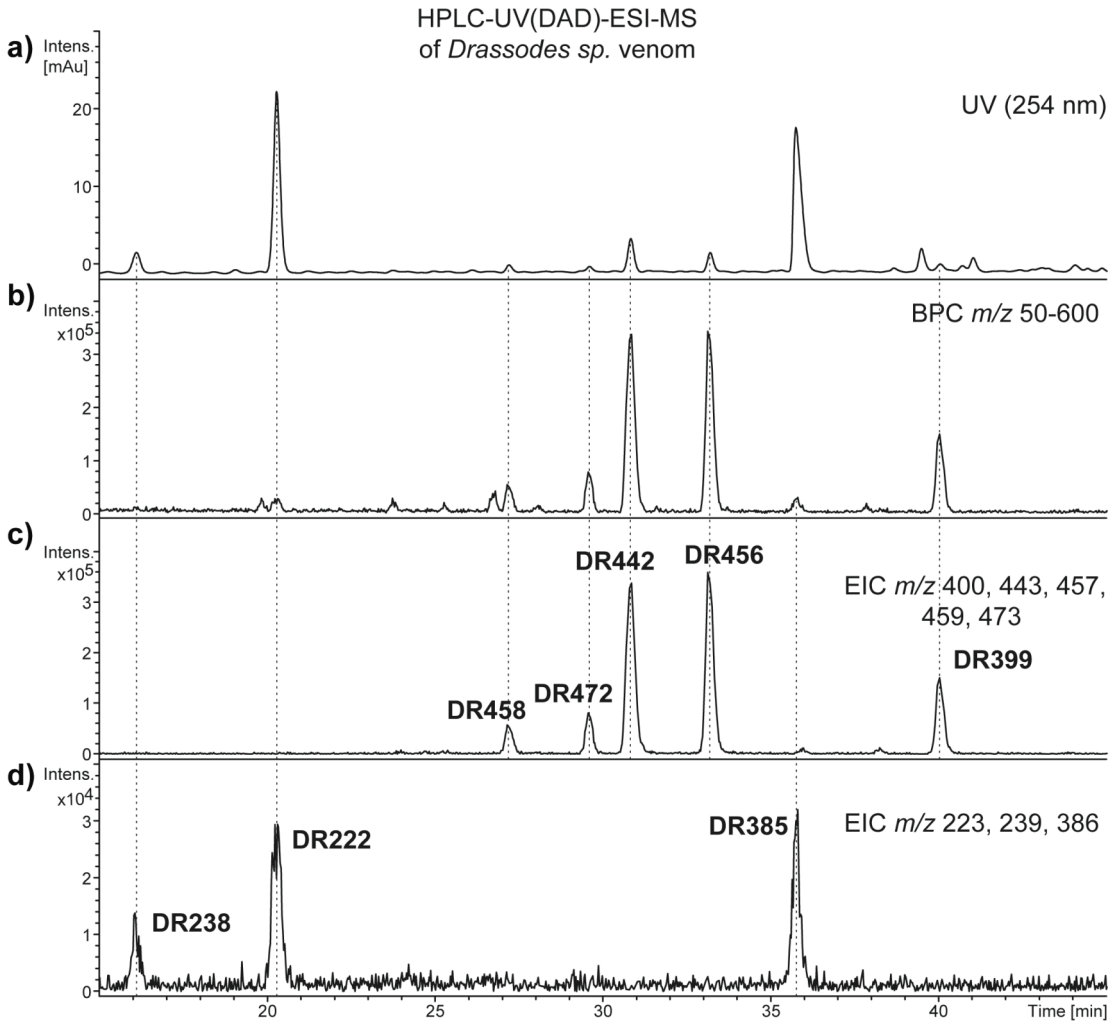

***Figure 5**. Relevant UV-trace and ion response chromatograms of an HPLC-UV(DAD)-ESI-MS run of* D. sp. *venom: (**a**) UV-chromatogram at 254 nm, (**b**) BPC at m/z 50 – 600 and EIC of (**c**) ions at m/z 400, 443, 457, 459 and 473 and (**d**) ions at m/z 223, 239 and 386.*

***Table 5**. Structures, retention times (rt), relative amounts, number of exchangeable protons and high-resolution ESI-MS data of acylpolyamines found in* Drassodes sp. *venom.*

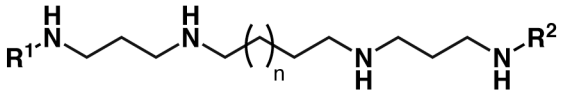

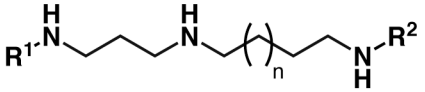

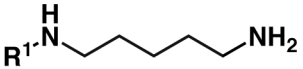

R^1	R^2	name	backbone[a]	rt [min]	r. a.[b] [%]	exch. protons	elem. comp. $[M+H]^+$	$[M+H]^+_{theo}$ m/z	$[M+H]^+_{exp.}$ m/z	Δm [ppm]
4-OH-Bz	4-OH-Bz	**DR442**	PA343	30.8	100	6	$C_{24}H_{35}O_4N_4$	443.26528	443.26565	0.8
		DR456	PA353	33.1	91	6	$C_{25}H_{37}O_4N_4$	457.28093	457.28050	–0.9
		DR385	PA34	35.8	8	5	$C_{21}H_{28}O_4N_3$	386.20743	386.20733	–0.3
		DR399	PA35	40.0	40	5	$C_{22}H_{30}O_4N_3$	400.22308	400.22287	–0.5
$(OH)_2$-Bz	4-OH-Bz	**DR458**	PA343	27.1	14	7	$C_{24}H_{35}O_5N_4$	459.26020	459.25995	–0.5
		DR472	PA353	29.6	19	7	$C_{25}H_{37}O_5N_4$	473.27585	473.27579	–0.1
4-OH-Bz	—	**DR222**	PA5	20.2	—	4	$C_{12}H_{19}O_2N_2$	223.14410	223.14376	–1.5
$(OH)_2$-Bz	—	**DR238**	PA5	16.0	—	5	$C_{12}H_{19}O_3N_2$	239.13902	239.13867	–1.4

[a] PA stands for polyamine, the figures designate the number of methylene units in-between the N-atoms.
[b] The values given represent the concentration in % relative to the most abundant acylpolyamine contained in the venom and were estimated on the basis of the peak integrals in their EIC obtained by HPLC-ESI-MS. For compounds **DR222** and **DR238**, this estimation was inappropriate due to different gas-phase basicites and therefore ion efficiencies compared to the other compounds.

4-OH-Bz = 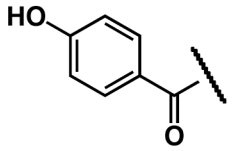

$(OH)_2$-Bz = 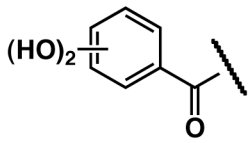

***Table 6**. Types, nominal masses and relative intensities of relevant HCD-MS/MS signals of acylpolyamines contained in* D. sp.

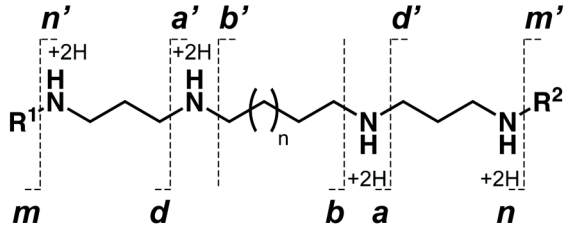

backbone[a]	name R^1 R^2	*m/z* (relative abundance) $[M+H]^+$ $[M+H-H_2O]^+$	***n*** ***n'***	***a*** ***a'***	***b*** ***b'***	***d*** ***d'***	***m*** ***m'***
PA343	**DR442** 4-OH-Bz 4-OH-Bz	443 (1) —	— —	— —	249 (73) = ***b***	178 (100) = ***d***	121 (5) = ***m***
	DR458 $(OH)_2$-Bz 4-OH-Bz	— —	— —	— —	265 (68) 249 (69)	194 (100) 178 (97)	137 (3) 121 (4)
PA353	**DR456** 4-OH-Bz 4-OH-Bz	457 (8) 439 (1)	337 (6) = ***n***	280 (3) = ***a***	263 (39) = ***b***	178 (100) = ***d***	121 (7) = ***m***
	DR472 $(OH)_2$-Bz 4-OH-Bz	473 (15) 455 (2)	353 (5) 337 (11)	296 (3) 280 (2)	279 (36) 263 (38)	194 (98) 178 (100)	137 (5) 121 (5)

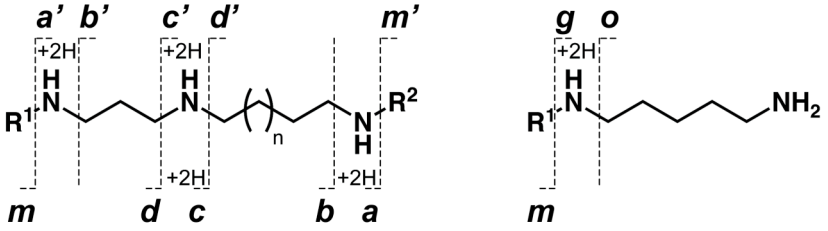

backbone[a]	name R^1 R^2	*m/z* (relative abundance) $[M+H]^+$ $[M+H-NH_3]^+$ $[M+H-H_2O]^+$	***a*** = ***a'*** ***a***–H_2O ***b*** = ***b'***	***c*** ***c'***	***d*** ***d'***	***m*** = ***m'***	***g*** ***o***
PA34	**DR385** 4-OH-Bz 4-OH-Bz	386 (26) 369 (1) 368 (2)	266 (16) 248 (1) 249 (5)	195 (1) —	178 (100) 192 (11)	121 (12)	
PA35	**DR399** 4-OH-Bz 4-OH-Bz	400 (22) 383 (2) 382 (2)	280 (20) 262 (2) 263 (4)	— 223 (1)	178 (100) 206 (1)	121 (11)	
PA5	**DR222** 4-OH-Bz	223 (1)[b] 206 (100)[b] —				121 (9)[b]	103 (1)[b] 86 (12)[b]
PA5	**DR238** $(OH)_2$-Bz	— 222 (100)[b] —				137 (4)[b]	103 (11)[b] 86 (28)[b]

[a] PA stands for polyamine, the figures designate the numbers of methylene units in-between the N-atoms.

[b] fragment ions obtained by CID-MS/MS performed in the ion trap of an LTQ Orbitrap instead of HCD-MS/MS performed in the octopole collision cell of an LTQ Orbitrap XL

3.3 Conclusions

By application of the extended method elaborated for the investigations of the venom of the spider *L.folium*, we were able to elucidate efficiently and with high confidence most of the acylpolyamines contained in the venoms of *O. lugubris, L. sp.* and *D. sp.*

The acylpolyamines found in these spiders, even though they are similar in structure to other spider toxins and contain structural units that have been found as components of other spider toxins as well [5,6], represent new natural products that have not been described previously. The toxins of *D. sp.* are of particular interest since they are members of the rather rare case of bis-acylated polyamines.

3.4 Experimental Part

3.4.1 Material

HPLC supra grade MeCN was purchased from Scharlau (Barcelona, Spain), trifluoroacetic acid (TFA) from Fluka (Buchs, Switzerland), and D_2O 99.9% and d_1-TFA 99.5% from Cambridge Isotope Laboratories, Inc. (Andover, Ma, USA). HPLC grade H_2O (< 5 ppm) was obtained by purification of deionized water with a MilliQ gradient apparatus (Millipore, Milford, MA, USA).

3.4.2 Venom Preparation

Lyophilized *O. lugubris*, *L. sp.* and *D. sp.* venom was purchased from Fauna Laboratories, Ltd (Almaty, Kazakhstan) and dissolved (~ 100 μg) in MeCN/H_2O + 0.1% TFA (1:3, 50 μl) or MeCN/D_2O + 0.1% d_1-TFA (1:3, 50 μl) for the LC-MS experiments in deuterated solvent. The venom and the stock solution was stored at -20 °C prior to use.

3.4.3 HPLC-UV(DAD)-ESI-MS and -MS/MS

LC-MS analyses were performed on a Hewlett-Packard 1100 HPLC system (Hewlett-Packard Co., Palo Alto, CA, U.S.A.) fitted with a HTS PAL autosampler (CTC Analytics, Zwingen, Switzerland), a Hewlett-Packard 1100 binary pump, and a Hewlett-Packard 1100 photodiode-array detector (DAD). The reversed-phase column used was an Interchim Uptisphere RP C18 column (UP3HDO-20QS, 3 μm, 2.3 × 200 mm, Interchim, Montluçon, France). After 5 μl injection, a step gradient from 5 to 20% B (solvent A: H_2O + 0.1% TFA, solvent B: MeCN + 0.1% TFA) over 40 min, then from 20 to 33% B over 15 min at a flow rate of 150 μl min^{-1} was applied. UV/VIS spectra of the eluent were acquired between 190 and 600 nm every 1 second directly after the column. The LC system was connected to an Esquire-LC quadrupole ion trap mass spectrometer (Bruker Daltonik GmbH, Bremen, Germany), equipped with an ESI Hewlett-Packard Atmospheric Pressure Ion (API) source. The MS-parameters were optimized to get the highest response with a minimum of in-source fragmentation. The parameters are: Nebulizer gas (N_2): 40 psi, dry gas (N_2): 9.5 l/min, dry temperature: 300 °C, HV capillary: 4500 V, HV EndPlate offset: –600 V, target mass: 400, compound stability: 80%, trap drive: 120%. The MS acquisitions were performed in positive ion mode at normal resolution (0.6 u at half peak height), and under conditions of ion charge control (ICC, target: 10'000). Full scan MS were recorded in the mass range from *m/z* 50 to 600 and averaged over 6 single spectra. MS/MS acquisitions were obtained in the mass range from *m/z* 50 – 600. The isolation width was 4 u, the fragmentation cut-off set by "fast calc", and the fragmentation amplitude set at 1V in the "SmartFrag" mode.

3.4.4 On-Column H/D Exchange HPLC-ESI-MS

The H/D exchange experiments were performed using identical conditions than for the HPLC-UV-ESI-MS and MS/MS experiments replacing water and TFA with deuterium oxide and d-TFA, respectively.

3.4.5 High Resolution Fourier Transform (FT) nLC-MS and -MS/MS

FT-MS measurements were performed using a Eksigent nano LC system (Eksigent Technologies, Dublin. CA, USA) online coupled to an hybrid linear ion trap – orbitrap mass spectrometer (LTQ-Orbitrap XL™, Thermo, Bremen, Germany) equipped with a nanoelectrospray ion source (nESI). Chromatographic separation was obtained with a 11 cm fused silica emitter, 75 μm inner diameter (BGB Analytik, Böckten, Switzerland), packed in-house with Uptisphere RP C_{18} resin (UP120-3HDO, 3 μm, Interchim, Montluçon, France).

1 μl sample (0.04 mg/ml lyophilized venom in MeCN/H_2O 1:99 + 0.05% TFA) was loaded onto the column. After loading, isocratic conditions (3% B over 5 min) followed by a linear gradient (3 to 22% B in 35 min) at a flow rate of 200 nl min^{-1} were applied (solvent A: H_2O/MeCN 99:1 + 0.05% TFA, solvent B: H_2O/MeCN 2:8 + 0.05% TFA).

The following settings were used: capillary temperature 200 °C, source voltage 1.7 kV, capillary voltage 49 V, tube lens 125 V.

Masses were calibrated immediately before the measurements externally according to manufacturers instructions. Furthermore, masses were calibrated internally during measurement using lock masses (429.088735 and 445.120025), resulting in a relative mass error of the measured masses lower then 2 ppm for MS and 5 ppm for MS/MS data.

The LTQ Orbitrap XL was operated in parallel mode, allowing the acquisition of an FT-MS spectrum in the orbitrap concurrent with the acquisition of two low resolution MS/MS spectra in the ion trap, followed by the acquisition of two FT-MS/MS spectra in the orbitrap. FT-MS spectra were acquired with a resolving power of 60000 full-width at half maximum (FWHM) at *m/z* 400 in a mass range from *m/z* 120 to 1000. Data dependent™ MS/MS spectra of the two most intense ions of the FT-MS spectrum were acquired by CID and detection in the linear ion trap (IT-MS/MS, low resolution) as well as by "higher-

energy" CID (HCD) in the HCD collision cell and subsequent analysis in the orbitrap (FT-MS/MS, high resolution). For the IT-CID-MS/MS, the isolation width was set to 2 *m/z* and the normalized collision energy to 30. FT-HCD-MS/MS data were acquired with a resolving power of 7500 FWHM at *m/z* 400, with an isolation width of 2 *m/z,* and a normalized collision energy of 35. The AGC target settings for the allowed number of ions in the mass analyzers were set to 5e5 for FT-MS, 1e4 for IT-MS/MS and 2e5 for FT-MS/MS experiments.

3.4.6 Amino Acid Analysis

The venom of *L. sp.* was fractionated using the same chromatographic conditions as applied for the HPLC-MS analysis and 20 µl of the venom sample was injected. The fraction between 27.4 and 28.2 min was collected. For the hydrolysis, half of the fraction (60 µl from 120 µl) was lyophilized and hydrolyzed in vapor with 6M HCl for 24 hours at 110 °C. The hydrolyzed sample was dissolved in 20 µl of 50 mM HCl containing the internal standards norvaline and sarcosine. The solutions were centrifuged, and 1 µl was injected for derivatization (with OPA/FMOC chemistry) and amino acid analysis (performed on a Amino Quant amino acid analyzer, Agilent).

3.5 References

[1] S. Bienz, P. Bisegger, A. Guggisberg, M. Hesse, *Nat. Prod. Rep.* **2005**, *22*, 647.

[2] S. Bienz, R. Detterbeck, C. Ensch, A. Guggisberg, U. Häusermann, C. Meisterhans, B. Wendt, C. Werner, M. Hesse, in *The Alkaloids, Vol. 58* (Ed.: G. A. Cordell), Academic Press, New York, **2002**, pp. 83.

[3] G. Karigiannis, D. Papaioannou, *Eur. J. Org. Chem.* **2000**, 1841.

[4] A. L. Mueller, R. Roeloffs, H. Jackson, in *The Alkaloids, Vol. 46* (Ed.: G. A. Cordell), Academic Press, New York, **1995**, pp. 63.

[5] M. S. Palma, T. Nakajima, *Toxin Rev.* **2005**, *24*, 209.

[6] A. Schäfer, H. Benz, W. Fiedler, A. Guggisberg, S. Bienz, M. Hesse, in *The Alkaloids, Vol. 45* (Ed.: G. A. Cordell), Academic Press, New York, **1994**, pp. 1.

[7] Y. Itagaki, T. Fujita, H. Naoki, T. Yasuhara, M. Andriantsiferana, T. Nakajima, *Nat. Toxins* **1997**, *5*, 1.

[8] S. Chesnov, L. Bigler, M. Hesse, *Eur. J. Mass Spectrom.* **2002**, *8*, 1.

[9] S. Chesnov, L. Bigler, M. Hesse, *Helv. Chim. Acta* **2001**, *84*, 2178.

[10] S. Chesnov, L. Bigler, M. Hesse, *Helv. Chim. Acta* **2000**, *83*, 3295.

[11] Q. Hu, R. J. Noll, H. Li, A. Makarov, M. Hardman, R. G. Cooks, *J. Mass Spectrom.* **2005**, *40*, 430.

[12] A. Makarov, E. Denisov, A. Kholomeev, W. Balschun, O. Lange, K. Strupat, S. Horning, *Anal. Chem.* **2006**, *78*, 2113.

[13] N. Manov, M. Tzouros, S. Chesnov, L. Bigler, S. Bienz, *Helv. Chim. Acta* **2002**, *85*, 2827.

[14] M. Tzouros, S. Chesnov, S. Bienz, M. Hesse, L. Bigler, *Toxicon* **2005**, *46*, 350.

[15] J.-M. El Hage Chahine, A.-M. Bauer, K. Baraldo, C. Lion, F. Ramiandrasoa, G. Kunesch, *Eur. J. Inorg. Chem.* **2001**, 2287.

[16] F. Trennheuser, G. Burkhard, H. Becker, *Phytochemistry* **1994**, *37*, 899.

CHAPTER 4

On the Benefits of Acquiring Mass Spectral Data with an LTQ Orbitrap XL

4.1 Introduction

In the last decades, mass spectrometry has become an indispensable tool for structural elucidation of unknown trace compounds from complex mixtures. In particular high-performance liquid chromatography (HPLC) and nanoLC (nLC) on-line coupled with mass spectrometry (MS) and tandem mass spectrometry (MS/MS) has been established as well-suited methods for the investigations of complex samples. This setup allows acquiring high quality analytical data of minute sample amounts due to its high sensitivity and selectivity.

HPLC-MS was also successfully used in our investigations, the structural elucidation of acylpolyamines from spider venoms. Thereby, the analytical procedure was successively optimized during our investigations. Initially, HPLC equipped with a UV diode array detector (DAD), and on-line coupled to atmospheric pressure chemical ionization (APCI) MS was used [1]. With this analytical setup, a total of 41 acylpolyamines were characterized from the venoms of the spiders *Agelenopsis aperta* [2,3] and *Paracoelotes birulai* [4].

Later, APCI was found to be inappropriate for the analysis of certain compounds, since it turned out that during APCI, artifacts were formed that could be misinterpreted as real sample constituents. Because electrospray ionization (ESI) did not lead to formation of artifacts, ESI proved to be more suitable for the analysis of unknown compounds (*Chapter 1*).

Together with the ionization source, also the type of mass analyzer was changed. A quadrupole ion trap instead of a triple quadrupole was used, which increased the sensitivity of the method. Thanks to the higher sensitivity of the quadrupole ion trap, even more acylpolyamines became amenable for detection and characterization.

A drawback of quadrupole ion traps is, however, the fact that low *m*/*z* fragment ions are discriminated in MS/MS experiments. This is called the "low-mass cutoff". As a consequence, structure-relevant fragment ions with low *m*/*z* generated by collision-induced dissociation (CID) were not detected. Hence, the advantage of the higher sensitivity of quadrupole ion traps was compensated by the potential loss of structure-relevant information.

Recently, nLC coupled to a LTQ Orbitrap XL instrument, a hybrid linear ion trap orbitrap mass spectrometer, was introduced and applied for the structure elucidation of acylpolyamines from the venom of the spiders *Larinioides folium* (*Chapter* 2), *Ozyptila lugubris*, *Lachesana sp.*, and *Drassodes sp.* (*Chapter 3*). It was shown that only thanks to this analytical setup, most of the acylpolyamines contained in these venoms became amenable for structural elucidation. The sensitivity of the method was increased by a factor of 500 due to the use of nLC resulting in less venom consumption compared with HPLC applications. Furthermore, an additionally installed octapole collision cell allowed to overcome the problems related to the "low-mass cutoff" observed with ion traps. The most important advantage, however, is that the LTQ Orbitrap XL instruments provide high-resolution MS and MS/MS data at high mass accuracy.

The benefits of measuring masses at high accuracy lies on the fact, that the exact mass of a molecular/fragment ion gives evidence of his elemental composition. For example, CO, CH_2CH_2, and N_2 have the same nominal mass of 28 amu but they differ in their theoretical exact mass (27.99492 for CO, 28.03130 for CH_2CH_2, and 28.0061 for N_2, respectively). To distinguish for instance the two isolated moieties $CO^{+\bullet}$ and $CH_2CH_2^{+\bullet}$ (absolute mass error: 0.03638 amu), the mass accuracy of the MS instrument does not need to be

very high and approximately 1300 ppm would be sufficient. Since the absolute mass difference for two molecules with higher masses, differing, *e.g.*, only in a CO and C_2H_4 moiety, remains the same but the overall mass increases, the relative mass deviation decreases dramatically. Therefore, a higher mass accuracy is demanded. For instance, already a mass accuracy of 72.7 ppm is needed to distinguish between two compounds with a nominal mass of 500 amu and differing in their exact mass by again 0.03638 amu (CO *versus* C_2H_4). Since the number of possible elemental combinations for a given nominal mass increases with the size of a molecule, also more theoretical chemical formula have to be compared for larger molecules. Even with the mass accuracy of the LTQ Orbitrap instrument (2 ppm with internal calibration), it is often not possible to assign a single elemental composition to a measured exact mass. In practice, constraints for the search of elemental compositions have to be defined such as the restriction to certain elements only, and the limitation of their appearance number.

Thus, structure-relevant information obtained from HPLC- and nLC-MS/MS analyses depends strongly on the type of mass analyzer used. The three mass analyzers used provide quite distinct analytical data related on their sensitivity, mode of MS/MS fragmentation, resolving power and precision.

As an overview, this chapter shortly describes the three different mass analyzers used and demonstrates the benefits of acquiring mass spectral data with an LTQ Orbitrap XL. Thereby, we focus mainly on two topics relevant for structural elucidation: (1) The loss of information due to the “low-mass cutoff” of ion trap instruments as well as (2) the impact of high-resolution and high mass accurate data.

4.2 Mass Analyzers

4.2.1 Triple Quadrupole (QqQ) Mass Spectrometer

Quadrupole devices are constructed of four rods with circular, or ideally, hyperbolic sections (*Figure 1*). A triple quadrupole instrument is composed of three quadrupole devices coupled serial, whereas the first and the third quadrupole (Q1 and Q3) are real mass analyzers and the center quadrupole q2 is a radio frequency (RF)-only quadrupole (*Figure 2*).

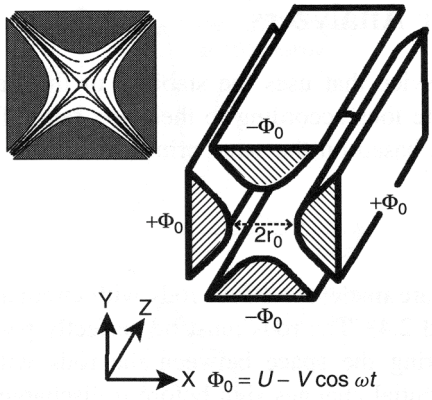

***Figure 1**. Quadrupole with hyperbolic rods and applied potentials. The equipotential lines are represented on the left [5].*

Quadrupole mass analyzers (Q1 and Q3) use the stability of the trajectories in oscillating electric fields (the quadrupole field) created by RF and direct current (DC) voltages to separate ions according to their *m*/*z* ratio. For given amplitude of a fixed ratio of RF to DC voltage, only ions of a single *m*/*z* value will pass the quadrupole, whereas all others are filtered off the beam. A mass spectrum is obtained by continuously increasing the amplitude of the RF and DC voltages while holding their ratio constant. Ions with different *m*/*z* are then successively detected. A quadrupole mass analyzer can also act as a simple transmission quadrupole. In this case, no DC voltage is applied, all charged particles with a *m*/*z* higher than a certain value have stable trajectories, causing all of them to be brought back systematically to the center of the rods.

No DC voltage is applied in an RF-only device (q2). It can be used as a collision cell. Ions emerging from Q1 are accelerated and fragmented by collision-induced dissociation (CID) with collision gas (N_2, Ar) at a pressure of 0.1 – 0.3 Pa. When no collision gas pressure is applied, q2 acts as a simple transmission quadrupole.

Various MS experiments can be performed with triple quadrupole instruments. The two scan modes used in our investigations are displayed in *Figure 2*.

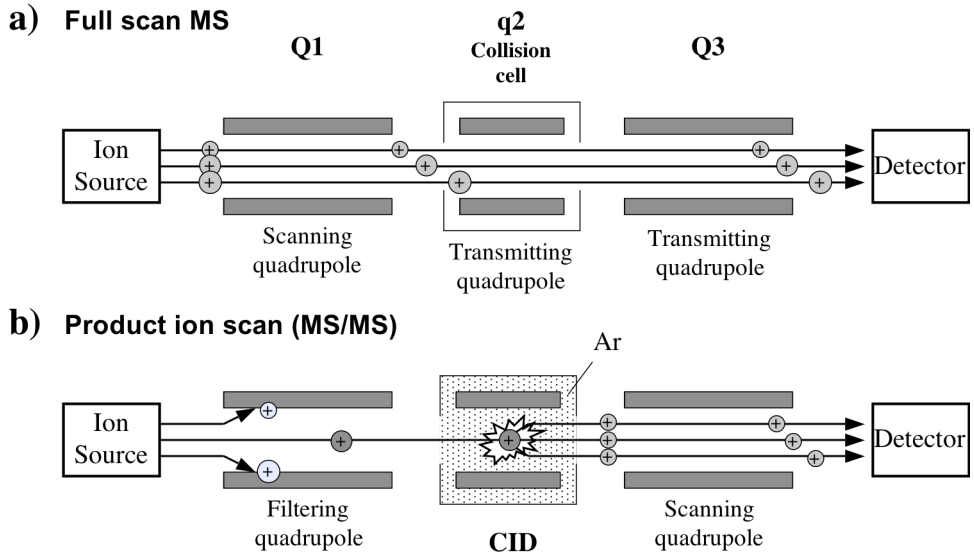

***Figure 2**. Diagram of a triple quadrupole instrument operating in (**a**) full scan (MS) and (**b**) product ion scan (MS/MS) modes.*

In the full scan mode (*Figure 2a*), Q1 is scanning over ions with different *m*/*z*, whereas q2 and Q3 act as transmission quadrupoles. In this mode, the triple quadrupole works like a single quadrupole by simply analyzing the ions generated in the ion source according to their *m*/*z*.

In the product ion scan (MS/MS) mode (*Figure 2b*), ions with a specific *m*/*z* are selected in the first quadrupole Q1 by holding the ratio of DC to RF constant. These ions undergo fragmentation upon collision-induced dissociation (CID) in the center RF-only quadrupole q2 by the use of argon as a collision gas. The fragment ions are then analyzed by quadrupole Q3. This experimental setup

allows acquiring individual MS/MS spectra of ions with different *m*/*z* arising at the same time in the ion source.

Usually, quadrupole mass spectrometers are operated at "unit resolution" (0.6 amu), *i.e.* they are low-resolution instruments. And since high-resolution is a prerequisite for acquiring mass spectrometric data with high mass accuracy, triple quadrupole mass spectrometers deliver MS and MS/MS data of low accuracy.

4.2.2 Quadrupole Ion Trap (QIT) Mass Spectrometer

There are two types of commercial QITs available, 3-dimensional (3D-QIT or Quistor) and linear quadrupole ion traps (LIT).

A 3D-QIT is constructed of a circular electrode, also called ring electrode, and two hyperbolic electrodes serving as endcaps (*Figure 3*). Holes at the center of the endcaps allow ions to pass in and out of the trap. This type of mass spectrometer uses a three-dimensional RF quadrupole field to store ions within defined boundaries. Ions of a defined *m*/*z* range can be trapped in a field that is created by applying a RF voltage to the ring electrode, while the endcaps are held at ground. An auxiliary voltage can be set to the exit endcap of the ion trap. This additional voltage is used for various purposes during the precursor ion isolation, fragmentation, and mass analysis phases of the scan sequence. Scans are performed by employing the effects of resonant ejection to remove ions of successively increasing *m*/*z* from the storage volume. The oscillation of ions in a QIT can be described by a radial and an axial secular frequency, each of them being a function of the *m*/*z* of the ions. If a auxiliary RF voltage, which matches the axial secular frequency of certain ions, is applied to the end caps, resonant ejection of the respective ions occurs. By scanning the auxiliary RF voltage upwards, ions of increasing *m*/*z* ration are successive ejected and detected.

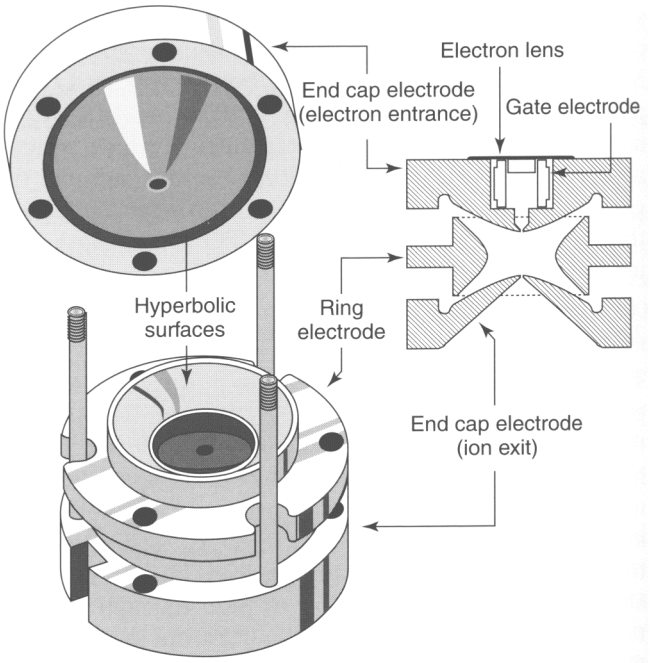

***Figure 3**: Schematic representation of a quadrupole ion trap mass spectrometer [6].*

Ion traps are also capable to perform MS/MS and even multiple stage MS/MS (MS^n) experiments. The general sequence of operation is illustrated in *Figure 4*. After accumulation of ions in the ion trap, ions with a specific *m*/*z* are isolated by expelling all the others at their axial secular frequency applied to the caps. To induce fragmentation, the energy of the ions of interest is increased by resonance excitation. The amplitude of the excitation is less then that used for resonance ejection but high enough to take up sufficient energy for CID with the helium gas present at 0.1 Pa in the trap. Then, the fragment ions are either accumulated and analyzed by successive resonant ejection (MS/MS), or alternatively, a fragment ion with a specific *m*/*z* is isolated and fragmented again. The isolation/fragmentation sequence can be repeated up to 10 times to provide MS^n spectra at the respective state.

Quadrupole ion traps are, like triple quadrupoles, instruments working at low-resolution and low mass accuracy. They have, however, a higher sensitivity as compared to triple quadrupole devices. A drawback of these instruments is the fact that low *m*/*z* fragment ions are lost during the fragmentation process of MS^n experiments, called "low-mass cutoff". It is principally possible to partially overcome the problem of the "low-mass

cutoff" in ion trap MS/MS experiments. The cutoff parameter, set by default to a third of the *m/z* of the precursor ion, can be decreased manually. This is, however, always accompanied by loss of sensitivity.

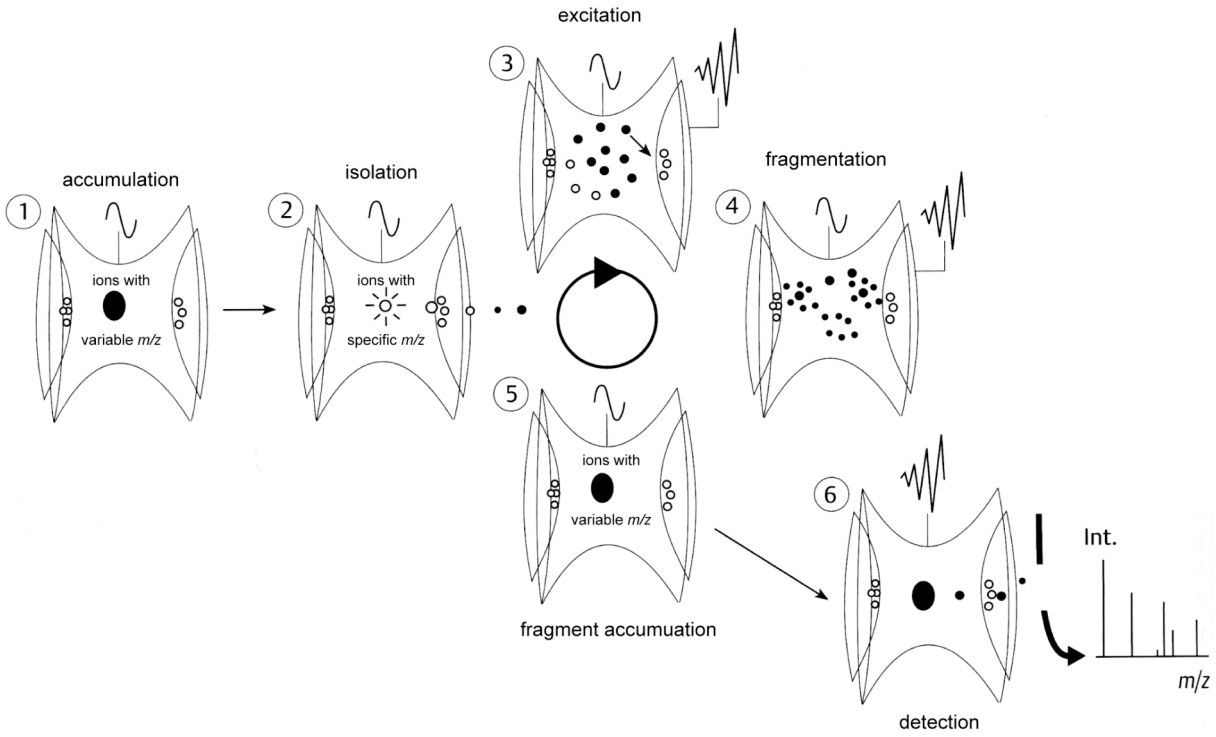

***Figure 4**. Schematic representation of an MS^n experiment performed in a quadrupole ion trap (extracted from the Bruker-HP-Esquire-LC operation manual).*

4.2.3 Hybrid Linear Ion Trap Orbitrap Mass Spectrometer

The orbitrap is a revolutionary Fourier transform mass spectrometer (FT-MS) developed by Makarov *et al.* [7] and it was commercialized in 2006 as a hybrid linear ion trap orbitrap mass spectrometer (LTQ Orbitrap) [8]. This instrument consists of a linear quadrupole ion trap, a RF-only "C-trap", and an orbitrap mass analyzer (*Figure 5*).

The front part of the instrument is a standard linear quadrupole ion trap mass spectrometer (LTQ®) capable of detecting MS or MS^n ions similar to the 3D-quadrupole ion trap (see above). Instead of detecting the accumulated ion populations in the ion trap, the whole ion package can also be sent through the C-trap, a curved RF-only quadrupole, to the orbitrap. The C-trap is used for trapping and cooling ions through collisions with nitrogen gas. The charged

particles are then injected in a short pulse into the orbitrap mass analyzer and begin to circle the inner electrode.

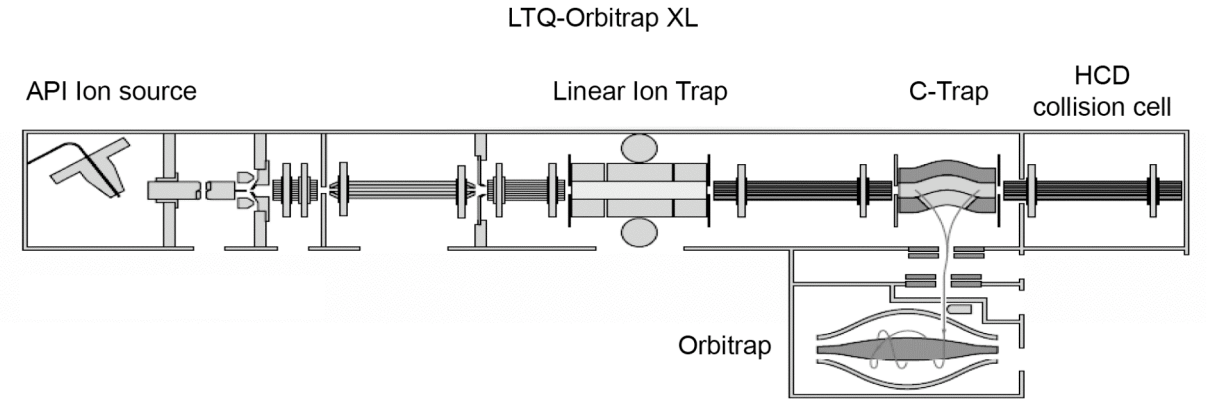

***Figure 5**. Schematic diagram of the second generation LTQ Orbitrap with the additional HCD collision cell.*

The orbitrap is composed of a central spindle-like and an outer barrel-like electrode (*Figure 6*). It operates by radially trapping ions around the central electrode. All ions have exactly the same amplitude but different frequencies according to their *m*/*z*. The frequencies are measured from the ion-image current that is induced in the outer electrode. Mass spectra are then obtained by subsequent Fourier transformations of the recorded ion frequencies.

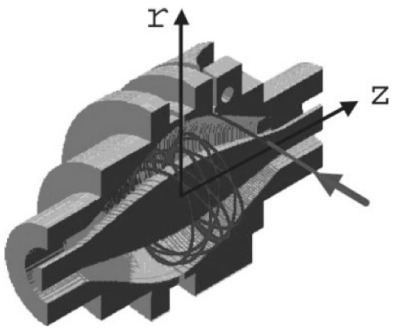

***Figure 6**. Cutaway view of the Orbitrap mass analyzer [7].*

With the arrangement LTQ, C-trap, and orbitrap, the user can choose to analyze ion populations either in the LTQ or in the orbitrap. MS and MS^n spectra with low-resolution and mass accuracy can be acquired in the LTQ. In contrast, the orbitrap analyzer provides high-resolution spectra at a maximum resolving power of 120’000 at full-with at half maximum (FWHM), and with

high accurate masses within 3 ppm with external calibration. Mass accuracy can be even increased to 2 ppm, when lock masses, *e.g.*, ionized polydimethylcyclosiloxanes from ambient air formed during the electrospray process [9], were used for internal recalibration [10]. In our case protonated $(Si(CH_3)_2O)_6$ is first accumulated in the LTQ and transferred to the C-trap. Additional ions from MS or MS^n experiments performed in the LTQ are then added to this lock masses, and the whole ion package is transferred to the orbitrap and analyzed. Internal recalibration can thus be used not only in full scan MS but also in MS^n experiments of any generation performed in the LTQ.

In the LTQ Orbitrap of second generation (LTQ Orbitrap XL) an additional octapole collision cell was added at the far end of the C-trap, allowing fragmentation at "higher-energy" collisional dissociation (HCD, *Figure 5*). Precursor ions are isolated in the linear ion trap and sent to the octapole collision cell for fragmentation. Thus, two different MS/MS experiments, either CID in the ion trap or HCD in the octapole collision cell, can be performed in such an instrumental setup.

In the following, the benefits and drawbacks of the several mass analyzers for the structural elucidation is discussed in a more general context and exemplified with **Agel489** and **LH446**, two naturally occurring acylpolyamines from spider venoms.

4.3 Drawback of the "Low-Mass Cutoff" in Ion Traps

The "low-mass cutoff" of a mass analyzer is the partial or complete suppression of ion detection in the low mass region. This is an effect inherently connected to quadrupole ion traps. The "low-mass cutoff" represents by nature a problem in cases, where MS/MS fragmentation leads to the loss of small structure-relevant ions from larger parent moieties. Such cases are rather frequent, particularly when polyfunctionalized compounds are investigated. It was thus not surprising that the "low-mass cutoff" became also an issue in the course of our investigations, the structural elucidation of polyamine derivatives from spider venom.

Figure 7 illustrates the differences of MS/MS spectra of **Agel489**, an acylpolyamine from the venom of *A. aperta*, obtained with the three mass analyzers that have been described above. It is readily recognized that two different types of MS/MS spectra were recorded. The MS/MS spectra obtained by CID in the quadrupole of the TSQ700 (*Figure 7a*) and HCD in the octapole collision cell of the LTQ-Orbitrap XL (*Figure 7d)* show fragment ions distributed all over the mass range from *m*/*z* 84 to 490. However, no or only a few fragment ions with low intensities were recorded below *m*/*z* 215, when CID was performed in the ion trap devices of the Esquire-LC or the LTQ-Orbitrap spectrometers (*Figure 7b* and *c*, respectively). Thus, the change from the triple quadrupole, used in the early investigations, to the QIT and hybrid LIT Orbitrap systems for the benefit of higher sensitivity, resolution and mass accuracy resulted in loss of structural information due to lacking low-*m*/*z*-signals. *Figure 7* clearly shows, for instance, that the signal cascade at *m*/*z* 129, 112, and 84 is missing. These signals, however, are of high relevance for the structural elucidation of **Agel489**, because they directly point to the terminal PA43 portion of the polyamine backbone.

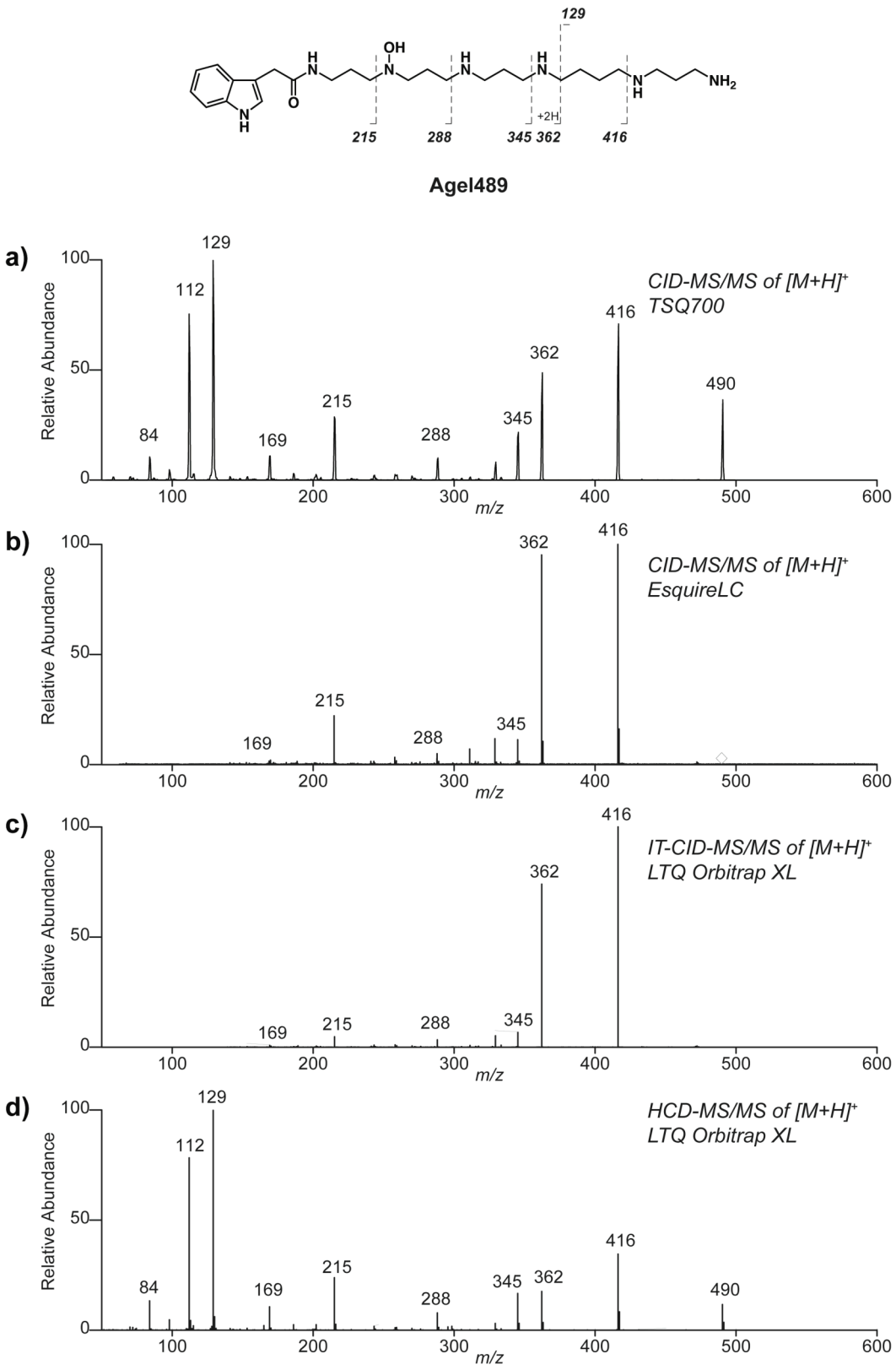

***Figure 7**. Structure of Agel489 with assignment of relevant fragment ions and MS/MS experiments of $[M+H]^+$ ions performed with different mass analyzers. CID-MS/MS performed (**a**) with a TSQ700 triple quadrupole, (**b**) with an EsquireLC QIT, and (**c**) in the ion trap of a LTQ Orbitrap XL. (**d**) HCD-MS/MS performed in the octopole collision cell of a LTQ Orbitrap XL.*

In the case of **Agel489**, it could be argued, though, that the loss of low-*m*/*z*-signals is not too vital since complementary ions, such as those recorded at *m*/*z* 362 and 416 can compensate for the missing responses. Undeniably, the spectra shown in *Figure 7a* and *d* do contain redundant information, and these indeed could be — though wrongly — regarded as useless. Access to such information, however, is in fact valuable since the significance of analytical deductions increases with the amount of supportive data. In addition, "complementary" signals that can compensate for "missing low-*m*/*z*-signals" are not always found in ion trap MS/MS. This is nicely illustrated with the two nLC-ESI-MS/MS spectra of **LH446** shown in *Figure 8*. The HCD-MS/MS signals at *m*/*z* 112, 146, 174, 183, 191, and 245 (*Figure 8b*), which are missing in the ion trap CID-MS/MS (*Figure 8a*), are crucial for the characterization of the polyamine portion and the chromophoric head moiety.

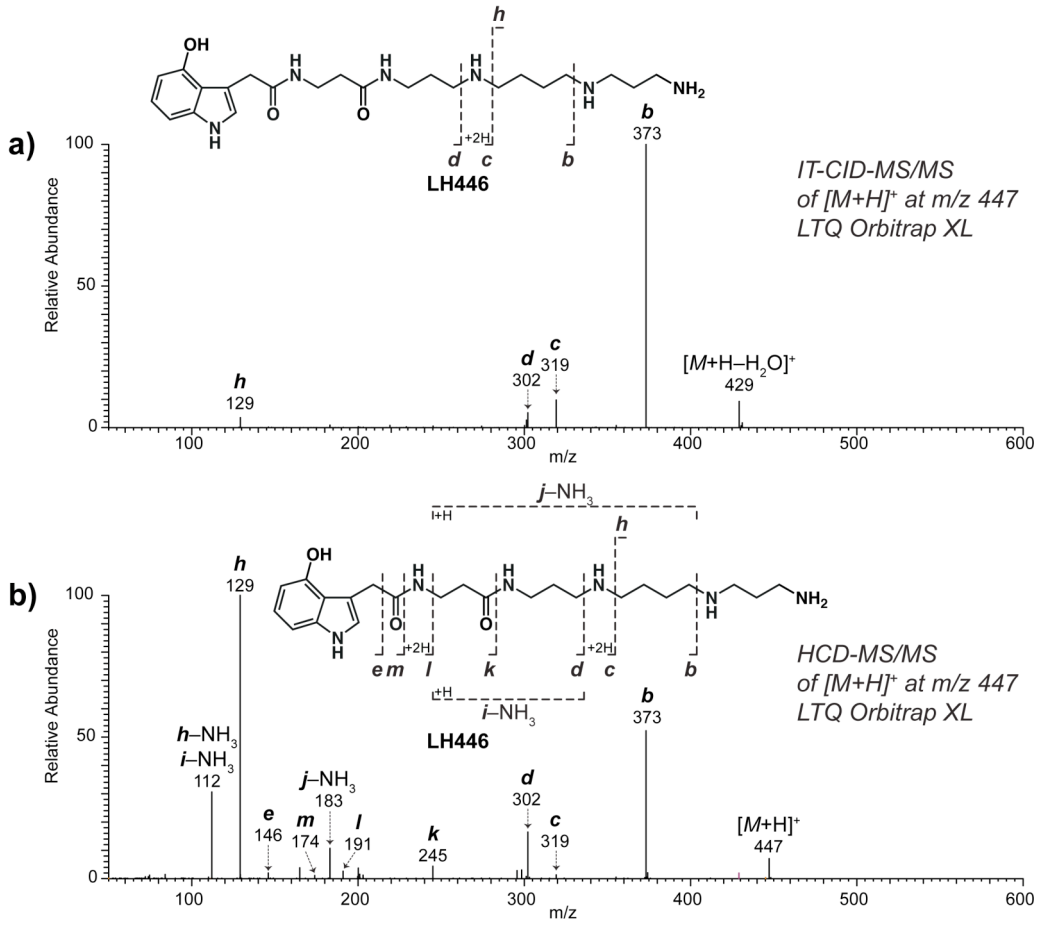

***Figure 8**. Structure of **LH446** with assignment of relevant fragment ions and nLC-ESI-MS/MS experiments of [M+H]⁺ ions. (**a**) CID-MS/MS performed in the ion trap and (**b**) HCD-MS/MS performed in the octopole collision cell of a LTQ Orbitrap XL.*

With these examples, we have shown that the extension of the LTQ-Orbitrap instrument with, *e.g.*, an HCD device represents a real solution. This setup maintains the high sensitivity of the instrument and allows acquisition of HR and high mass accuracy MS/MS data without "low-mass cutoff" (*Figure 7d*). Such a combination seems to be the instrumentation of choice for the sensitive analysis of molecules that lose (or might lose) small charged particles of structural significance upon CID.

4.4 Benefits of High-Resolution and High Mass Accuracy

High-resolution MS with high mass accuracy is not generally needed for all types of investigations. If already some knowledge about the analytes is available, *e.g.*, structural moieties are known from synthesis or fragmentation behavior from analogous compounds, low-resolution MS and MS/MS data are usually sufficient. If such knowledge is missing, however, MS and MS/MS data at high-resolution and high mass accuracy are rather beneficial.

The characterization of **LH446** exemplifies how the access to elemental compositions of ions simplifies the structural elucidation of unknown compounds.

Two structures **A** and **B** were proposed for **LH446** on the basis of UV(DAD)-ESI-MS and -MS/MS data acquired with a quadruple ion trap instrument (*Figure 9*)[1]. The structures differ obviously only in CO *versus* C_2H_4, located in the polyamine backbone, and a similar MS/MS pattern is expected. High accuracy MS, however, allowed the direct differentiation of the two compounds.

[1] Additional isomeric structures with the carboxyl group located at different places within the polyamine backbone could also be proposed.

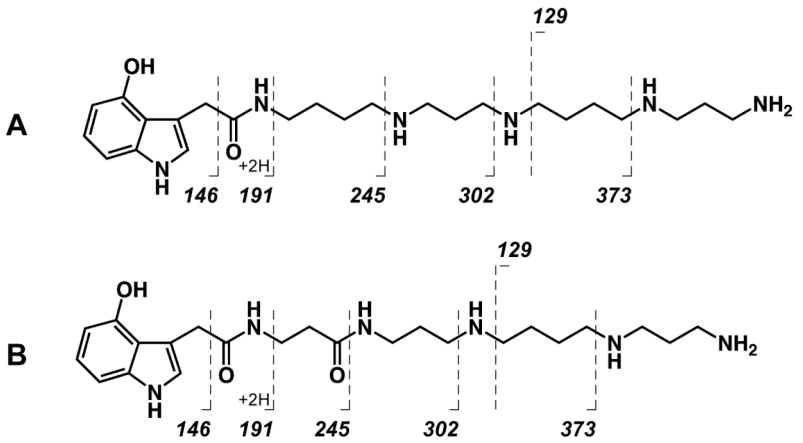

***Figure 9**. Structures proposed for **LH446** according to UV-absorption and low-resolution MS and MS/MS data.*

Figure 10 shows the ESI-MS of **LH446** acquired with a quadrupole ion trap at low- and with a LIT Orbitrap at high-resolution. Whereas the isotopes in spectrum *10a* are just baseline separated, *Figure 10b* shows sharp and well-separated signals with a resolution of 60'000 (FWHM). Such a high-resolution allows accurate mass measurements, because mass accuracy depends on sufficiently resolved peaks. With the mass accuracy of the LTQ Orbitrap XL (2 ppm at *m*/*z* 500 with internal calibration), two elemental compositions are possible for the ions detected at *m*/*z* 447.30734: $C_{23}H_{39}O_3N_6$ (theoretical exact mass 447.30782, relative mass error –1.1 ppm) and $C_{22}H_{43}O_7N_2$ (theoretical exact mass 447.30648, relative mass error 1.9 ppm). The following restrictions were defined: $C_{0–50}$, $H_{0–100}$, $N_{0–15}$, $O_{0–15}$; double bond equivalents –0.5 to 100; only even electron ions allowed.

The chemical formula for the quasi-molecular ion of structure **B** was not proposed. Its theoretical exact mass 447.34420 corresponding to $C_{24}H_{43}O_2N_6$ has a deviation of 81 ppm to the measured exact mass. This difference is largely above the error range of the instrument.

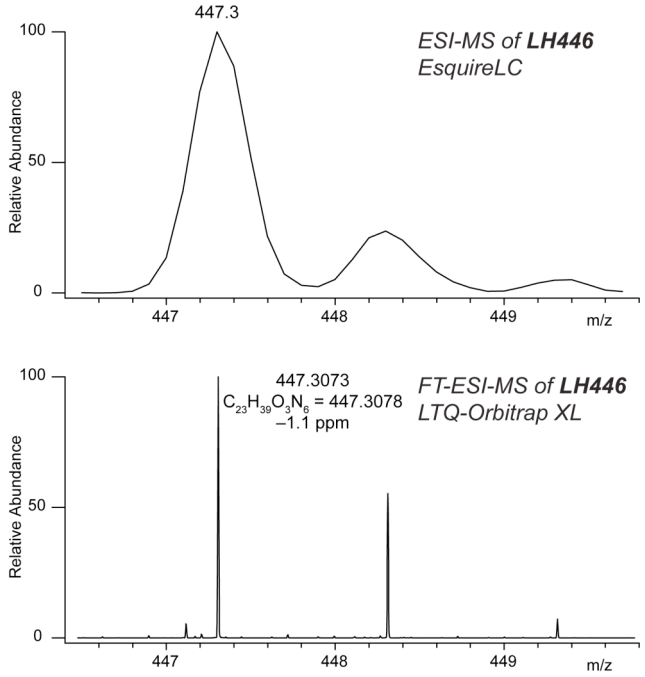

***Figure 10**. ESI-MS of **LH446** obtained (**a**) with an EsquireLC quadrupole ion trap and (**b**) with Fourier transform (FT) acquisition of a LTQ Orbitrap XL.*

Even though the assignment of the chemical formula of **LH446** was not directly feasible on the basis of the measured exact mass of $[M + H]^+$, the combination of this data with the fragmentation behavior and the UV spectrum of the compound allowed already the coarse structural elucidation of **LH446**.

The crucial information necessary to locate the carboxyl group within the polyamine backbone of **LH446** was obtained from high accuracy MS/MS data (*Figure 11*). The exact masses of the fragment ions registered at *m*/*z* 245 (fragment ***k***) and *m*/*z* 191 (fragment ***l***) prove the location of the CO group in-between the first two N-atoms of the polyamine backbone: The mass difference between these ions is consistent with C_3H_2O but not with C_4H_6. The position of the carbonyl group, however, could not be localized within this structural part by mass spectrometry. Hydrolysis and amino acid analysis confirmed finally that β-alanine is the structural component of **LH446**.

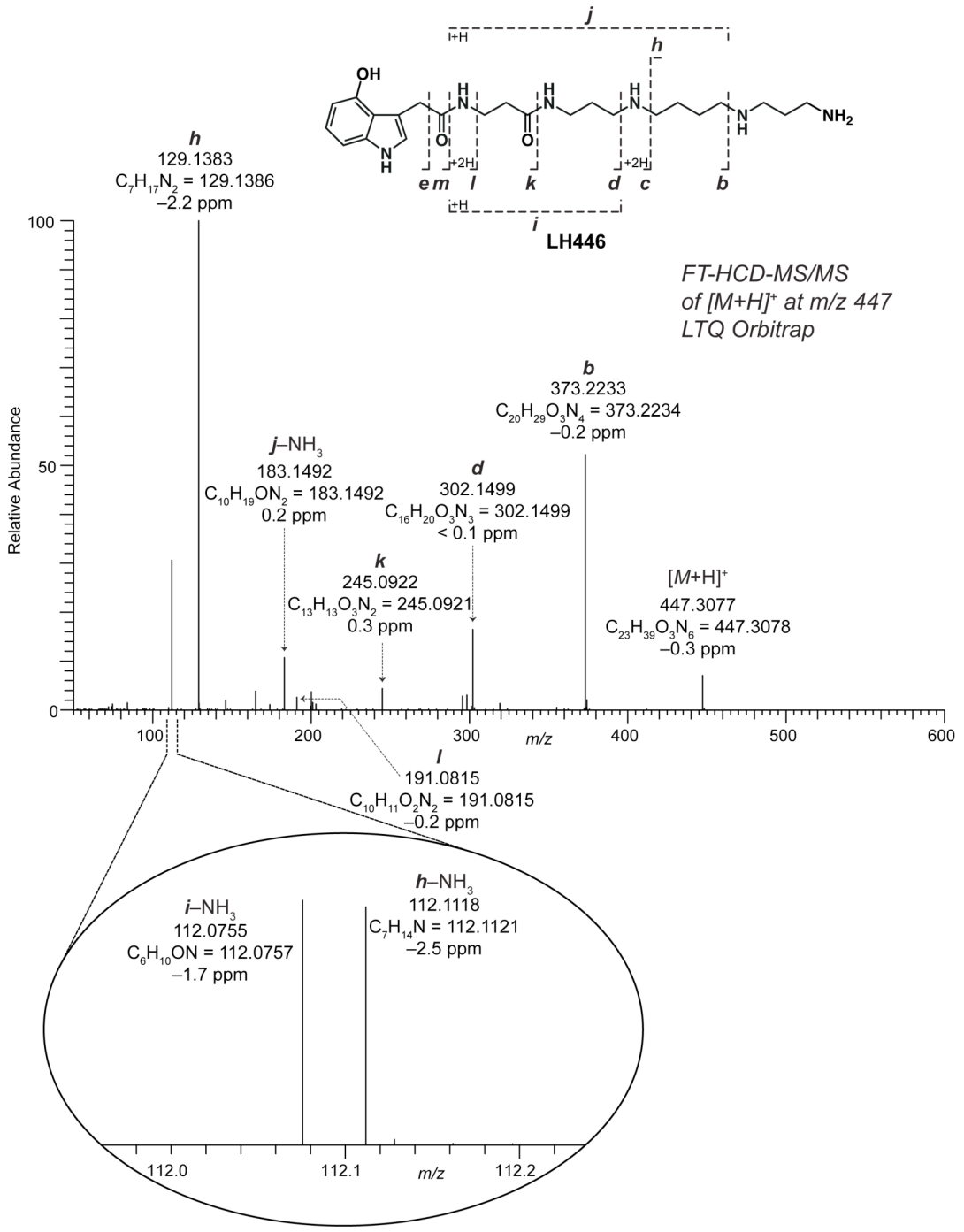

***Figure 11**. Structure of **LH446** with assignment of relevant fragment ions and nLC-ESI-MS/MS spectrum of [M+H]⁺ ions. HCD-MS/MS was performed in the octopole collision cell of a LTQ Orbitrap XL. FT acquisition in the orbitrap provided accurate masses of fragment ions.*

It is shown with the spectra of **LH446**, too, that even more and rather subtle information can be gathered from analytical data obtained by HR-MS/MS. For instance, the ion response detected at *m/z* 112 reveals that it does not originate from a single type of fragments. The insert of *Figure 11* clearly shows that two different signals with the same nominal but with different exact masses were

registered at *m*/*z* 112. The elemental compositions of these ions were unambiguously determined as $C_6H_{10}ON$ and $C_7H_{14}N$, respectively. Hence, acquiring MS data at high mass accuracy has a high significance not only for structural elucidations of unknown analytes but also for the study of fragmentation reactions. While fragments of the type ***h*** and ***h*** – NH_3 are readily proposed to explain the signals at *m*/*z* 129 and 112, fragments of type ***i*** and ***i*** – NH_3 are not that trivially recognized.

This example of the structural elucidation of **LH446** demonstrates that high mass accuracy and high-resolution mass spectral data as they can be acquired with a LTQ Orbitrap XL is of immense value for the analysis of unknown analytes. Chemical formula are readily obtained for not only molecular but also fragment ions, which leads to an immediate entry to structural information.

4.5 References

[1] S. Chesnov, L. Bigler, M. Hesse, *Eur. J. Mass Spectrom.* **2002**, *8*, 1.

[2] S. Chesnov, L. Bigler, M. Hesse, *Helv. Chim. Acta* **2001**, *84*, 2178.

[3] N. Manov, M. Tzouros, S. Chesnov, L. Bigler, S. Bienz, *Helv. Chim. Acta* **2002**, *85*, 2827.

[4] S. Chesnov, L. Bigler, M. Hesse, *Helv. Chim. Acta* **2000**, *83*, 3295.

[5] E. de Hoffmann, V. Stroobant, *Mass Spectrometry, Principles and Applications*, Second Edition ed., John Wiley & Sons, LTD, **2001**.

[6] R. E. March, *Int. J. Mass Spectrom.* **2000**, *200*, 285.

[7] Q. Hu, R. J. Noll, H. Li, A. Makarov, M. Hardman, R. G. Cooks, *J. Mass Spectrom.* **2005**, *40*, 430.

[8] A. Makarov, E. Denisov, A. Kholomeev, W. Balschun, O. Lange, K. Strupat, S. Horning, *Anal. Chem.* **2006**, *78*, 2113.

[9] A. Schlosser, R. Volkmer-Engert, *J. Mass Spectrom.* **2003**, *38*, 523.

[10] J. V. Olsen, L. M. F. de Godoy, G. Li, B. Macek, P. Mortensen, R. Pesch, A. Makarov, O. Lange, S. Horning, M. Mann, *Mol. Cell. Proteomics* **2005**, *4*, 2010.

SUMMARY — ZUSAMMENFASSUNG

1. English Version

Polyamines and their derivatives are widely found throughout the animal and plant kingdom. Since they exhibit a wide variety of important biological activities, new and efficient methods for their synthesis as well as more sensitive and selective methods for the identification and characterization of new compounds from natural sources are being sought.

Particularly polyamine-containing toxins of spider venoms have attracted the attention of the scientific community in the past decades. Since spider venom is a complex mixture of different types of compounds and the polyamine toxins contained therein are mostly available in trace amounts, sophisticated and sensitive analytical methods are required to detect and analyze these compounds. A meanwhile well-established methodology for the direct analysis of acylpolyamines in spider venoms — without prior isolation of the sample compounds — is high-performance liquid chromatography (HPLC), on-line coupled with mass spectrometry (MS) and tandem mass spectrometry (MS/MS). The performance of such an analytical setup has been demonstrated by the successful identification of most of the toxins from the venom of the spiders *Agelenopsis aperta* and *Paracoelotes birulai*.

The method proved insufficient, however, for the structural elucidation of the structurally more complex toxins from the venom of other spider species such as those from *Larinioides folium*. In addition, further investigations of *A. aperta* venom pointed out that this method is also inappropriate for the analysis of *N*-hydroxylated compounds because such analytes are prone to undergo decomposition during ionization. Thus, we were encouraged to develop a new analytical setup that (1) provides sufficient analytical data for the unambiguous characterization of polyamine derivatives of higher complexity

and (2) allows for the analysis of *N*-hydroxylated compounds without decomposition.

In *Chapter 1* the decomposition of *N*-hydroxylated compounds during atmospheric pressure chemical ionization (APCI) is discussed. This decomposition was studied with a synthetic *N*-hydroxylated tetraamine derivative. It was found that reduction, oxidation, and H_2O-elimination of the N-OH functionality occurred, forming the corresponding amines, *N*-oxides, and imines (*Figure 1*). The research further revealed that the APCI decomposition of hydroxylamines is dependent on the concentration of the analytes and on the acidity of the solution introduced into the ionization source. The pH-dependence was utilized for the development of an MS method that allows for the identification of N-OH functionalities within sample compounds, *i.e.* APCI-decomposition can likewise be enforced or inhibited by the addition of acid or base, respectively. The method was applied for the study of polyamine toxins from the venom of the spider *A. aperta* and also for mayfoline, a cyclic polyamine derivative of the shrub *Maytenus buxifolia*. It was demonstrated that the method can be employed in two ways. Firstly, it can be used to distinguish unavoidable artifacts from native compounds — as shown with the investigation of the spider venom of *A. aperta* — and secondly for the conclusive identification of N-OH functionalities within a compound.

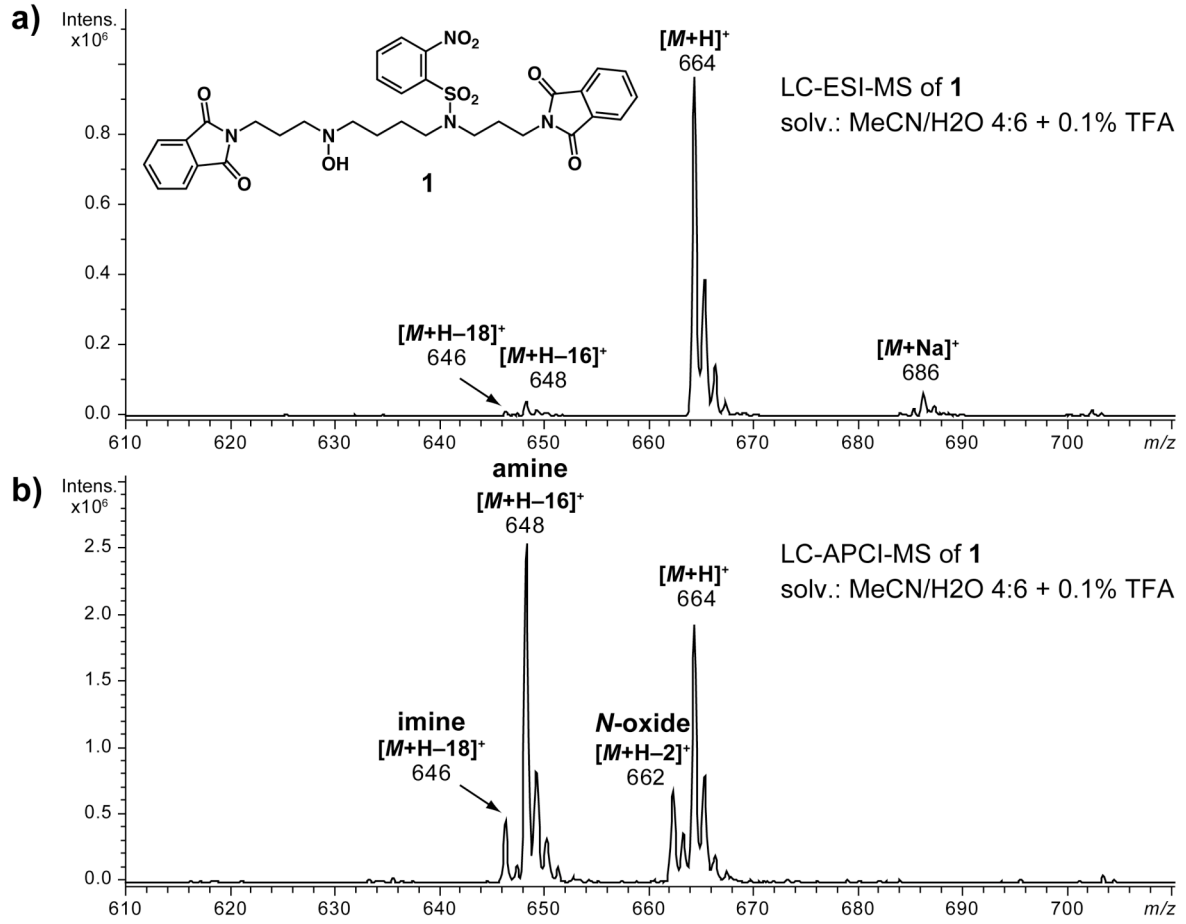

***Figure 1**. (**a**) HPLC-ESI-MS and (**b**) HPLC-APCI-MS of N-hydroxylated tetraamine derivative **1** in MeCN/H_2O (4:6) + 0.1% TFA.*

Chapter 2 describes the development and first application of a new extended analytical procedure allowing unequivocal characterization of polyamine toxins from the venom of the spider *L. folium*. The higher structural complexity of the polyamine compounds contained in this venom led to analytical challenges that could no longer be solved with the classical experimental setup. To obtain sufficient analytical data for the unambiguous structural assignment of the various compounds, the analytical setup had to be supplemented with on-column H/D-exchange HPLC-MS, nanoLC (nLC) connected to high-resolution *Fourier* transform mass spectrometry (FTMS), and amino acid analysis of venom fractions. This extended analytical procedure finally allowed for the detection and structural elucidation of 40 acylpolyamine derivatives, whereas most of them were found for the first time in natural sources. It was found that these toxins contain, in addition to the α,ω-aminopolyazaalkane backbones and the chromophoric acyl head groups,

which are common for all spider toxins, also asparagine as a linker unit between these two moieties and methylated N-atoms (*Figure 2*). Overall, nine different chromophoric head groups — more than have been found so far in any other spider species — and six different polyamine backbones were identified.

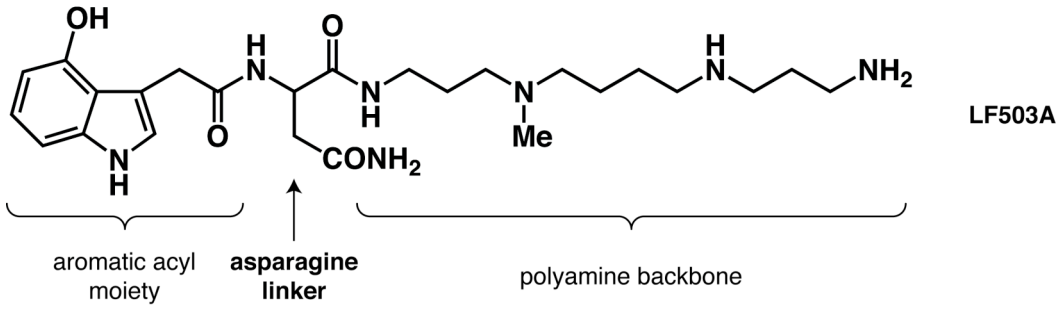

***Figure 2**. General structure of acylpolyamines contained in* L. folium *exemplified by **LF503A**.*

Chapter 3 deals with the implementation of the methods developed in the previous chapter to the study of new venoms. In *Chapter 3*, the structural elucidation of the polyamine derivatives contained in the venom of the spiders *Ozyptila lugubris*, *Lachesana sp.*, and *Drassodes sp* is described. In total, 20 different acylpolyamines were structurally elucidated. The several structures show a scheme of constitution, exemplarily shown with **OZ375**, **LH446**, and **DR442**, which are common for the respective spider species (*Figure 3*).

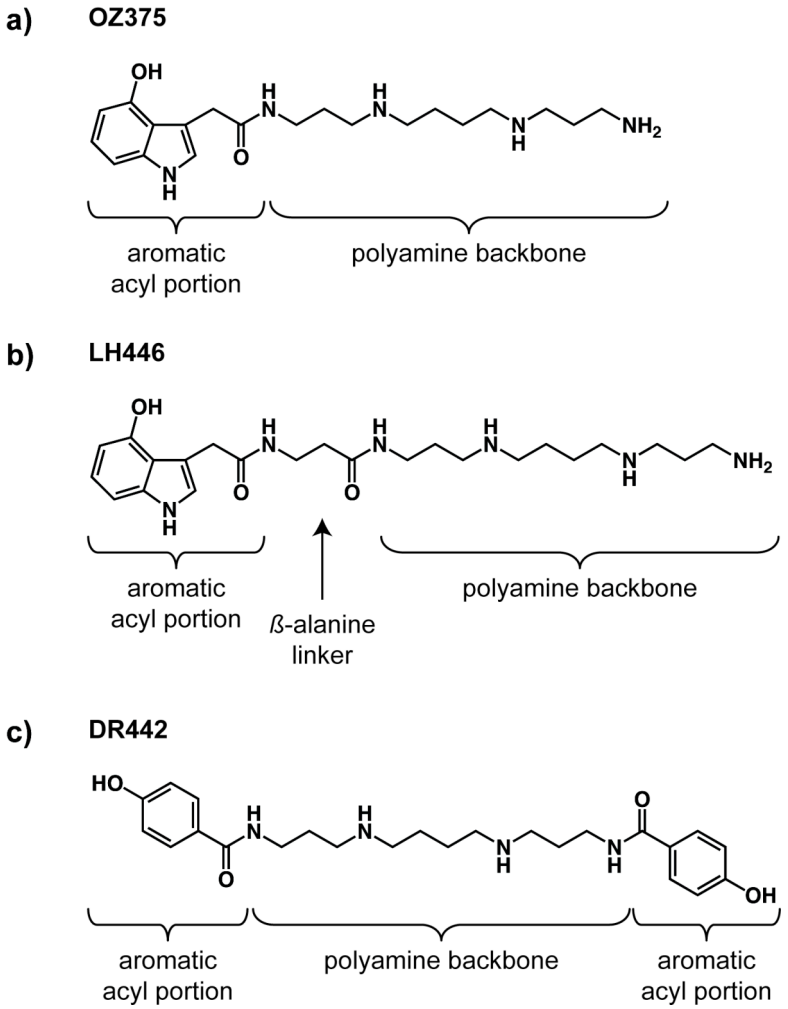

***Figure 3**. Spider specific general structures of the acylpolyamines exemplified with (a) **OZ389**, (b) **LH446** and (c) **DR442** found in the venom of* O. lugubris, L. sp., *and* D. sp., *respectively.*

Chapter 4 is meant to serve as a reference for chemists that are no MS specialists but are interested in the detailed mass spectrometric aspects of the investigations presented in the *Chapters 2* and *3*. *Chapter 4* shortly describes the principles of the mass analyzers used for the experiments in this dissertation. In addition, the influence of the selection of the type of mass analyzer for structural elucidation of unknown compounds is discussed in a more general context and illustrated with the structural elucidation of **Agel489** and **LH446**, two natural products from the venom of the spiders *A. aperta* and *L. sp.*

It was shown that quadrupole ion trap mass spectrometers are less suitable for the structural elucidation of unknown acylpolyamines, because relevant indicative fragment ions can be lost during MS/MS experiments due to the

"low-mass cutoff". Further, it was demonstrated that hybrid linear ion trap orbitrap instruments like the LTQ Orbitrap XL provided most structure-relevant data. These instruments retain the high sensitivity of ion traps and, due to the additionally installed octopole collision cell, fragment ions over the full *m*/*z* range are acquired. In addition, mass spectral data with high-resolution and high mass accuracy are provided. Hence, among the used mass spectrometers, the LTQ Orbitrap XL has been established as the most suitable instrument for structural elucidation of unknown compounds.

2. Deutsche Version

Polyamine und Polyaminderivate werden bei zahlreichen Tier- und Pflanzenarten gefunden. Da diese Verbindungen wichtige biologische Aktivitäten aufzeigen, verwundert es nicht, dass sowohl neue und effiziente Methoden für ihre Synthese als auch sensitivere und selektivere analytische Methoden für ihre Bestimmung und Strukturaufklärung von neuen Naturstoffen gesucht werden.

Dabei wurden vor allem Polyamin-Toxine aus Spinnengift untersucht. Da sich das Spinnengift aus einem komplexen Gemisch verschiedenster Verbindungsklassen zusammensetzt und die darin enthaltenen Polyamin-Toxine meist nur in kleinsten Mengen vorkommen, werden hoch entwickelte und sensitive analytische Methoden benötigt, um diese Verbindungen zu detektieren und zu identifizieren. Eine sensitive und mittlerweile etablierte Methode, die es erlaubt, Acylpoylamine im Spinnengift direkt und ohne vorgängige Reinigung der Probemoleküle zu analysieren, ist Hochleistungs-Flüssigkeitschromatographie gekoppelt mit Tandem-Massenspektrometrie (HPLC-MS/MS). Die Leistungsfähigkeit dieser gekoppelten Methode wurde im Rahmen der Strukturaufklärung der Acylpolyamine im Spinnengift von *A. aperta* und *P. birulai* eindrücklich dargestellt.

Bei Untersuchungen von strukturell komplizierteren Acylpolyaminen, wie sie zum Beispiel im Spinnengift von *L. folium* gefunden werden, zeigte sich jedoch, dass diese Methode für deren Strukturaufklärung ungenügend ist. Des Weiteren hat sich die Unzulänglichkeit der beschriebenen Methode bei zusätzlichen Untersuchungen am Spinnengift von *A. aperta* herausgestellt. Darin enthaltene *N*-hydroxylierte Verbindungen werden anscheinend während des Ionisationsprozesses zersetzt. Deshalb war es das Ziel der vorliegenden Arbeit, ein neues analytisches Setup zu entwickeln, das (1) genügend analytische Daten erzielt, um auch die strukturell komplizierteren Verbindungen zu identifizieren und (2) es auch erlaubt, *N*-hydroxylierte Verbindungen zersetzungsfrei zu analysieren.

In *Kapitel 1* wird die Zersetzung von *N*-hydroxylierten Verbindungen während Atmospheric Pressure Chemical Ionization (APCI) beschrieben. Die zugrunde liegenden Zersetzungssreaktionen wurden mit Hilfe von synthetischen *N*-hydroxylierten Modelverbindungen untersucht. Dabei stellte sich heraus, dass während des Ionisationsprozesses Reduktion, Oxidation und Wasserelimination des Analyten unter Bildung des entsprechenden Amins, N-Oxids und Imins stattgefunden hatten (*Figur 1*). Weitere Untersuchungen zeigten, dass die Zersetzungsrate sowohl von der Konzentration der Probe als auch vom pH-Wert der Probelösung abhängig ist. Basierend auf dieser Tatsache konnte eine Methode zur Identifikation der N-OH Funktionalität von Probemolekülen entwickelt werden, mit deren Hilfe die APCI-Zersetzung wahlweise durch Zugabe von Säure oder Base beschleunigt bzw. unterdrückt werden kann. Diese Methode wurde anschliessend zur Strukturanalyse zweier verschiedener Naturstofftypen angewendet: den Polyamin-Toxinen des Spinnengifts von *A. aperta* sowie Mayfoline, einem zyklischen Polyamin des *Maytenus buxifolia* Strauches. Dabei stellte sich heraus, dass die entwickelte Methode sowohl zur Unterscheidung von Artefakten und tatsächlichen Naturstoffen als auch zur direkten Bestimmung der N-OH Funktionalitäten von Probemolekülen gebraucht werden kann.

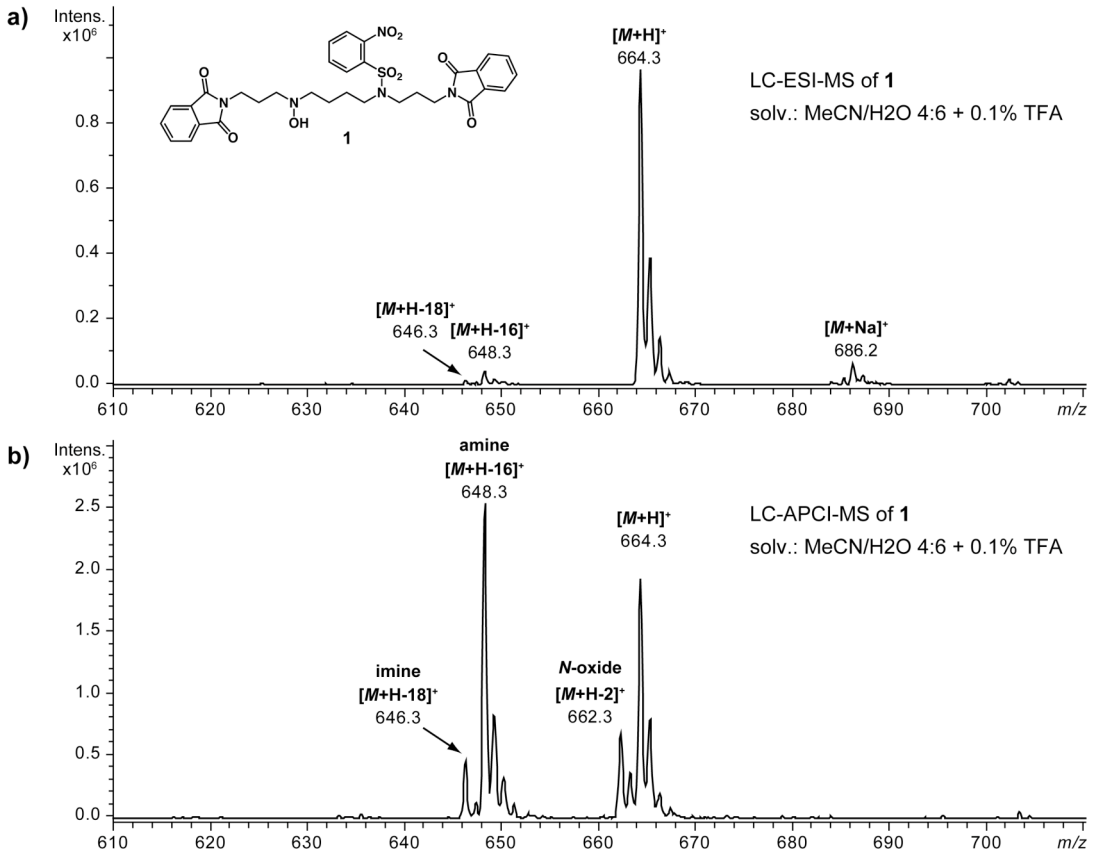

***Figur 1**. (a) HPLC-ESI-MS und (b) HPLC-APCI-MS des* N-*hydroxylierten Tetraamins **1** in MeCN/H_2O (4:6) + 0.1% TFA*

Kapitel 2 zeigt die Strukturaufklärung der Polyamin-Toxine im Spinnengift von *L. folium*. Die höhere Komplexität der Toxin-Strukturen dieses Giftes hat zu einer analytischen Problemstellung geführt, die nicht mehr mit dem bestehenden experimentellen Setup gelöst werden konnte. Um ausreichende analytische Daten zur eindeutigen Bestimmung der jeweiligen Polyamin-Toxinen zu erhalten, wurde die bestehende HPLC-UV(DAD)-MS/MS Methode mit (1) on-column H/D Austausch HPLC-MS (2) nano LC gekoppelt mit hochauflösender *Fourier* Transform Massenspektrometrie (FT-MS) und (3) Aminosäureanalyse von Spinnengiftfraktionen ergänzt. Mit diesem erweiterten analytischen Setup konnte die Struktur von insgesamt 40 Acylpolyaminen bestimmt werden. Dabei besitzen alle charakterisierten Verbindungen den gleichen modularen Aufbau. Sie sind aus einer α,ω-Aminopolyazaalkankette, die über die Aminosäure Asparagin mit einer aromatischen Kopfgruppe verbunden ist, zusammengesetzt (*Figur 2*). Im

Gesamten sind neun verschiedene aromatische Kopfgruppen und sechs unterschiedliche Polyaminketten gefunden worden.

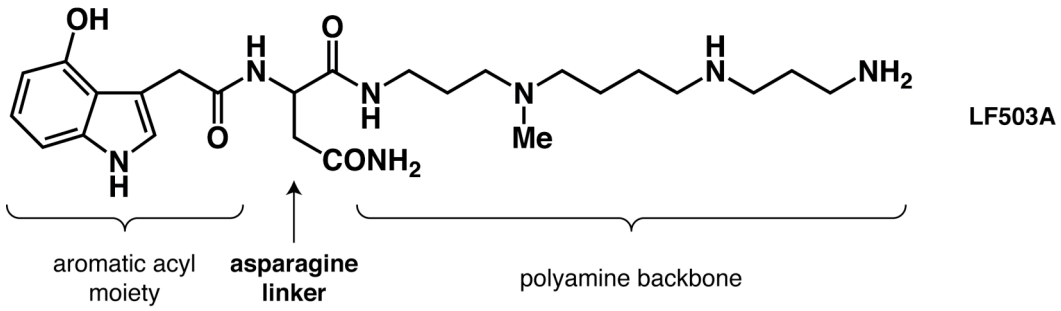

***Figur 2**. Allgemeine Struktur von den Acylpolyaminen von* L. folium *dargestellt mit **LF503A**.*

Kapitel 3 beschreibt die Strukturaufklärung der Polyaminverbindungen der Spinnengifte von *O. lugubris*, *L. sp.* und *D. sp.* Analog zu *Kapitel 2* wurde das erweiterte analytische Setup mit on-column H/D-Austausch HPLC-MS, nanoLC gekoppelt mit FTMS, und, falls notwendig, Aminosäureanalyse der Spinnengiftfraktionen angewendet. Im Gesamten wurden die Strukturen von 20 Acylpolyaminen aufgeklärt. Analog zu Kapitel 2 konnte dabei den Verbindungen der unterschiedlichen Spinnengifte je nach Spinnenart ein gemeinsames allgemeines Aufbauschema zugeordnet werden (*Figur 3*).

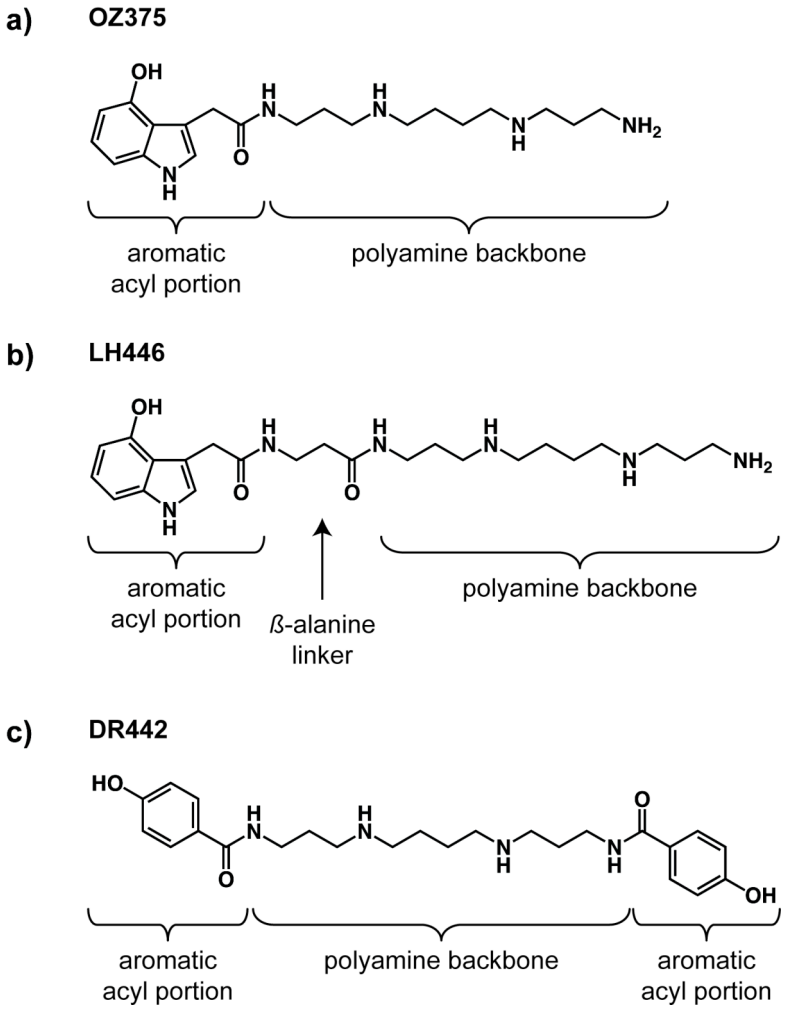

***Figur 3**. Allgemeine Struktur der Acylpolyamine von (a)* O. lugubris, *(b)* L. sp. *und (c)* D. sp. *veranschaulicht mit den Verbindungen **OZ389**, **LH446** und **DR442**.*

Kapitel 4 stellt eine Übersicht der für die zur Strukturaufklärung von Acylpolyaminen benutzten Massenanalysatoren dar. Es wurden insgesamt drei verschiedene Typen von Massenanalysatoren benutzt, ein Triple Quadrupole, eine Ionenfalle und ein Hybrid-Massenspektrometer bestehend aus einer Ionenfalle gekoppelt mit einer Orbitrap. Die drei Typen von Massenspektrometern werden kurz vorgestellt und die typspezifischen analytischen Daten miteinander verglichen. Dabei stellte sich heraus, dass Ionenfallen aufgrund des "low-mass cutoffs" für die Strukturaufklärung von unbekannten Verbindungen ungeeignet sind, da für die Strukturaufklärung wichtige Fragment-Ionen mit kleinem *m/z Wert* während des MS/MS Experiments verloren gehen. Des Weiteren wird der Einfluss von hochaufgelösten und massengenauen MS und MS/MS Daten zur Strukturaufklärung von unbekannten Verbindungen besprochen. Es hat sich

gezeigt, dass hochaufgelöste MS und MS/MS Daten mit hoher Massengenauigkeit die Bestimmung der Elementzusammensetzung der detektierten Ionen erlauben und dadurch die Strukturaufklärung von unbekannten Verbindungen stark vereinfachen.

Appendix A: HCD-MS/MS Data of Chapter 2

Type A compounds

	ion type	*m/z measured*	*m/z theor.*	*rel. error (ppm)*	*Composition*	*rel. Int.*	*Int.*
LF487A	h-NH3-C2H4	84.0803	84.0808	-5.93	C5 H10 N	1.14	1593
	h-NH3	112.1115	112.1121	-4.79	C7 H14 N	30.23	42258
	h	129.1381	129.1386	-4.43	C7 H17 N2	100	139787
	e	130.0648	130.0651	-2.52	C9 H8 N	1.39	1949
	j-NH3-NH3	138.0542	138.055	-5.12	C7 H8 O2 N	2.2	3082
	j	172.1069	172.1081	-6.96	C7 H14 O2 N3	0.79	1110
	d-NH3	312.1342	312.1343	-0.09	C17 H18 O3 N3	25.59	35769
	d	329.1605	329.1608	-0.85	C17 H21 O3 N4	12.43	17375
	c-H2O	342.1929	342.1925	1.32	C18 H24 O2 N5	0.43	596
	c-NH3	343.1773	343.1765	2.55	C18 H23 O3 N4	1.98	2767
	c	360.2025	360.203	-1.45	C18 H26 O3 N5	4.53	6331
	b	414.2504	414.25	1.17	C22 H32 O3 N5	6.84	9564
	M+H	488.3323	488.3344	-4.22	C25 H42 O3 N7	0.39	551
LF503A	int.	72.0804	72.0808	-4.91	C4 H10 N	1.35	42788
	h-NH3-C2H4	84.0805	84.0808	-2.72	C5 H10 N	1.62	51280
	h-NH3	112.1119	112.1121	-1.48	C7 H14 N	30.46	967036
	h	129.1385	129.1386	-1.33	C7 H17 N2	100	3175086
	j-NH3-NH3	138.0548	138.055	-0.9	C7 H8 O2 N	3.13	99522
	e	146.0601	146.06	0.34	C9 H8 O N	2.14	68051
	j-NH3	155.0815	155.0815	-0.15	C7 H11 O2 N2	1.78	56463
	j	172.1082	172.1081	0.78	C7 H14 O2 N3	3.86	122683
	d-H2O	327.1463	327.1452	3.43	C17 H19 O3 N4	0.55	17459
	d-NH3	328.1295	328.1292	1.11	C17 H18 O4 N3	22.88	726408
	d	345.1561	345.1557	1.07	C17 H21 O4 N4	11.89	377552
	c-H2O	358.1884	358.1874	2.8	C18 H24 O3 N5	1.41	44812
	c-NH3	359.1709	359.1714	-1.41	C18 H23 O4 N4	2.47	78565
	c	376.1981	376.1979	0.56	C18 H26 O4 N5	5.09	161493
	b	430.245	430.2449	0.31	C22 H32 O4 N5	6.65	211031
	M+H	504.3299	504.3293	1.19	C25 H42 O4 N7	0.95	30039
LF448A	int.	72.0805	72.0808	-4.39	C4 H10 N	1.2	10954
	h-NH3-C2H4	84.0806	84.0808	-2.4	C5 H10 N	1.92	17518
	asn imm. Ion	87.0551	87.0553	-2	C3 H7 O N2	1.46	13268
	h-NH3	112.1119	112.1121	-1.23	C7 H14 N	35.67	324633
	h	129.1385	129.1386	-1.13	C7 H17 N2	100	910186
	j-NH3-NH3	138.0549	138.055	-0.62	C7 H8 O2 N	1.84	16756
	j-NH3	155.0815	155.0815	-0.27	C7 H11 O2 N2	1.03	9330
	j	172.1082	172.1081	0.95	C7 H14 O2 N3	0.6	5478
	d-NH3	273.1237	273.1234	1.12	C15 H17 O3 N2	29.15	265283
	d	290.15	290.1499	0.43	C15 H20 O3 N3	14.59	132751
	c-H2O	303.1821	303.1816	1.73	C16 H23 O2 N4	0.92	8410
	c-NH3	304.1665	304.1656	3.21	C16 H22 O3 N3	1.66	15103
	c	321.1925	321.1921	1.26	C16 H25 O3 N4	4.49	40822
	b	375.2381	375.2391	-2.57	C20 H31 O3 N4	9.83	89451
	M+H	449.3242	449.3235	1.72	C23 H41 O3 N6	0.94	8597
LF464A	h-NH3-C2H4	84.08	84.0808	-9.48	C5 H10 N	1.06	679
	asn imm. Ion	87.0552	87.0553	-1.04	C3 H7 O N2	0.68	433
	h-NH3	112.1116	112.1121	-4.04	C7 H14 N	33.34	21336
	h	129.1381	129.1386	-4.05	C7 H17 N2	100	63989
	d-NH3	289.1175	289.1183	-2.68	C15 H17 O4 N2	28.36	18150
	d	306.1437	306.1448	-3.84	C15 H20 O4 N3	12.61	8066
	c	337.1873	337.187	0.76	C16 H25 O4 N4	2.6	1661
	b	391.2321	391.234	-4.77	C20 H31 O4 N4	8.26	5286

	ion type	*m/z measured*	*m/z theor.*	*rel. error (ppm)*	*Composition*	*rel. Int.*	*Int.*
LF480A	int.	72.0801	72.0808	-9.26	C4 H10 N	0.86	1767
	h-NH3-C2H4	84.0801	84.0808	-8.15	C5 H10 N	1.59	3274
	asn imm. Ion	87.0544	87.0553	-10.08	C3 H7 O N2	1.27	2617
	h-NH3	112.1113	112.1121	-6.62	C7 H14 N	31.24	64230
	h	129.1378	129.1386	-6.74	C7 H17 N2	100	205622
	j-NH3-NH3	138.0542	138.055	-5.26	C7 H8 O2 N	1.48	3052
	j-NH3	155.0806	155.0815	-6.02	C7 H11 O2 N2	3.26	6701
	j	172.1074	172.1081	-3.94	C7 H14 O2 N3	7.83	16109
	d-H2O	304.128	304.1292	-3.82	C15 H18 O4 N3	1.99	4088
	d-NH3	305.1124	305.1132	-2.65	C15 H17 O5 N2	19.05	39178
	d	322.139	322.1397	-2.25	C15 H20 O5 N3	8.89	18289
	c-H2O	335.1696	335.1714	-5.27	C16 H23 O4 N4	0.56	1149
	c-NH3	336.1557	336.1554	0.95	C16 H22 O5 N3	1.1	2268
	c	353.1806	353.1819	-3.69	C16 H25 O5 N4	3.82	7853
	b	407.2278	407.2289	-2.59	C20 H31 O5 N4	9.27	19070
	M+H	481.3107	481.3133	-5.49	C23 H41 O5 N6	1.37	2811
LF516A	int.	72.0805	72.0808	-4.18	C4 H10 N	1.15	25407
	h-NH3-C2H4	84.0806	84.0808	-1.78	C5 H10 N	1.7	37673
	h-NH3	112.1119	112.1121	-1.21	C7 H14 N	30.77	679986
	h	129.1385	129.1386	-1.1	C7 H17 N2	100	2210167
	e-CH3N	130.0649	130.0651	-1.35	C9 H8 N	0.54	11837
	j-NH3-NH3	138.055	138.055	0.22	C7 H8 O2 N	1.36	30166
	j-NH3	155.0814	155.0815	-0.36	C7 H11 O2 N2	1.92	42339
	e	159.0918	159.0917	0.7	C10 H11 N2	1.94	42904
	j	172.1082	172.1081	0.9	C7 H14 O2 N3	6.71	148284
	d-NH3-NH3	324.1348	324.1343	1.69	C18 H18 O3 N3	2	44180
	d-NH3	341.1613	341.1608	1.45	C18 H21 O3 N4	14.44	319080
	d	358.1879	358.1874	1.46	C18 H24 O3 N5	9.29	205381
	c-H2O	371.2197	371.219	1.91	C19 H27 O2 N6	0.71	15592
	c-NH3	372.2026	372.203	-1.21	C19 H26 O3 N5	1.47	32387
	c	389.23	389.2296	1.16	C19 H29 O3 N6	3.63	80283
	b	443.2771	443.2765	1.33	C23 H35 O3 N6	5.41	119573
LF517A	int.	72.0803	72.0808	-6.96	C4 H10 N	0.95	6182
	h-NH3-C2H4	84.0804	84.0808	-5.02	C5 H10 N	1.74	11375
	h-NH3	112.1117	112.1121	-3.79	C7 H14 N	31.48	205287
	h	129.1381	129.1386	-3.89	C7 H17 N2	100	652058
	j-NH3-NH3	138.0545	138.055	-3.49	C7 H8 O2 N	1.91	12459
	j-NH3	155.0813	155.0815	-1.25	C7 H11 O2 N2	1.23	8007
	j	172.1079	172.1081	-1.15	C7 H14 O2 N3	1.13	7357
	d-NH3-H2O	324.1342	324.1343	-0.16	C18 H18 O3 N3	2.35	15293
	d-H2O	341.1612	341.1608	1.05	C18 H21 O3 N4	0.38	2473
	d-NH3	342.1451	342.1448	0.72	C18 H20 O4 N3	21.99	143417
	d	359.1717	359.1714	0.96	C18 H23 O4 N4	11.57	75466
	c-H2O	372.2034	372.203	0.96	C19 H26 O3 N5	0.61	3951
	c-NH3	373.1873	373.187	0.75	C19 H25 O4 N4	2.4	15617
	c	390.2134	390.2136	-0.37	C19 H28 O4 N5	3.75	24467
	b	444.261	444.2605	1.05	C23 H34 O4 N5	5.75	37463
	M+H	518.3438	518.3449	-2.17	C26 H44 O4 N7	0.7	4536
LF477A	h-NH3	112.112	112.1121	-1.06	C7 H14 N	28.32	13136
	h	129.1385	129.1386	-1.27	C7 H17 N2	100	46383
	j	172.1062	172.1081	-10.58	C7 H14 O2 N3	1.44	667
	d-NH3	302.1498	302.1499	-0.32	C16 H20 O3 N3	18.19	8438
	d	319.1769	319.1765	1.46	C16 H23 O3 N4	11.43	5302
	c	350.2195	350.2187	2.28	C17 H28 O3 N5	2.58	1195
	b	404.2658	404.2656	0.44	C21 H34 O3 N5	6.79	3148

	ion type	*m/z measured*	*m/z theor.*	*rel. error (ppm)*	*Composition*	*rel. Int.*	*Int.*
LF478A	int.	72.0803	72.0808	-7.03	C4 H10 N	1.13	7811
	h-NH3-C2H4	84.0804	84.0808	-4.31	C5 H10 N	3.06	21120
	asn imm. Ion	87.0549	87.0553	-4.9	C3 H7 O N2	1.28	8809
	h-NH3	112.1117	112.1121	-3.2	C7 H14 N	34.03	234544
	h	129.1382	129.1386	-2.95	C7 H17 N2	100	689203
	j-NH3-NH3	138.0548	138.055	-0.94	C7 H8 O2 N	1.63	11226
	j-NH3	155.0813	155.0815	-1.42	C7 H11 O2 N2	1.07	7408
	j	172.1081	172.1081	0.32	C7 H14 O2 N3	0.61	4206
	d-NH3	303.1342	303.1339	0.73	C16 H19 O4 N2	26.73	184243
	d	320.1607	320.1605	0.79	C16 H22 O4 N3	13.55	93412
	c-NH3	334.1767	334.1761	1.78	C17 H24 O4 N3	1.66	11417
	c	351.2025	351.2027	-0.39	C17 H27 O4 N4	3.44	23727
	b	405.2501	405.2496	1.13	C21 H33 O4 N4	7.67	52856
	M+H	479.3357	479.334	3.41	C24 H43 O4 N6	0.81	5578

Type B compounds

	ion type	*m/z measured*	*m/z theor.*	*rel. error (ppm)*	*Composition*	*rel. Int.*	*Int.*
LF487B	int	86.0959	86.0964	-6.22	C5 H12 N	1.94	4994
	h-NH3-C2H4	98.0959	98.0964	-5.02	C6 H12 N	4.97	12782
	h-NH3	126.1272	126.1277	-4.35	C8 H16 N	57.05	146749
	e	130.0647	130.0651	-3.56	C9 H8 N	9.06	23295
	j-NH3-H2O	137.0705	137.0709	-3.35	C7 H9 O N2	1.42	3648
	j-2*NH3	138.0545	138.055	-3.48	C7 H8 O2 N	5.62	14460
	h	143.1538	143.1543	-3.13	C8 H19 N2	100	257247
	j-NH3	155.0809	155.0815	-3.99	C7 H11 O2 N2	2.44	6276
	j	172.1078	172.1081	-1.73	C7 H14 O2 N3	2.85	7322
	g	217.2384	217.2387	-1.28	C11 H29 N4	10.2	26248
	i-NH3-H2O	222.1602	222.1601	0.41	C12 H20 O N3	1.45	3741
	i-2*NH3	223.1439	223.1441	-1.07	C12 H19 O2 N2	3.84	9873
	i-NH3	240.1698	240.1707	-3.42	C12 H22 O2 N3	1.89	4868
	i	257.1968	257.1972	-1.5	C12 H25 O2 N4	3.88	9994
	f-2*NH3-H2O	279.2176	279.2179	-1.12	C15 H27 O N4	2.54	6525
	f-2*NH3	297.2291	297.2285	1.99	C15 H29 O2 N4	1.21	3115
	d-H2O	311.1505	311.1503	0.81	C17 H19 O2 N4	1.85	4747
	d-NH3	312.1342	312.1343	-0.34	C17 H18 O3 N3	37.62	96788
	f-H2O	313.1377	313.1408	-9.84	C15 H17 O2 N6	3.72	9560
	f-NH3	314.2557	314.2551	1.94	C15 H32 O2 N5	1.9	4883
	d	329.1605	329.1608	-0.84	C17 H21 O3 N4	16.45	42330
	f	331.282	331.2816	1.13	C15 H35 O2 N6	2.7	6955
	b-H2O	396.2391	396.2394	-0.76	C22 H30 O2 N5	5.24	13480
	b-NH3	397.2221	397.2234	-3.43	C22 H29 O3 N4	7.25	18661
	b	414.2497	414.25	-0.61	C22 H32 O3 N5	32.42	83397
	a	431.2743	431.2765	-5.09	C22 H35 O3 N6	1.07	2760
	M+H-H2O-NH3	453.2971	453.2973	-0.35	C25 H37 O2 N6	1.05	2691
	M+H-H20	470.3247	470.3238	1.98	C25 H40 O2 N7	1.47	3793
	M+H-NH3	471.3076	471.3078	-0.48	C25 H39 O3 N6	5.33	13706
	M+H	488.3341	488.3344	-0.46	C25 H42 O3 N7	26.17	67312

	ion type	*m/z measured*	*m/z theor.*	*rel. error (ppm)*	*Composition*	*rel. Int.*	*Int.*
LF503B	int.	86.0964	86.0964	-0.71	C5 H12 N	1.77	21900
	asn imm. Ion	87.0553	87.0553	-0.44	C3 H7 O N2	2.15	26665
	h-NH3-C2H4	98.0964	98.0964	0.11	C6 H12 N	4.77	58994
	h-NH3	126.1278	126.1277	0.21	C8 H16 N	50.59	626245
	j-2*NH3	138.0551	138.055	1.06	C7 H8 O2 N	5.41	66915
	h	143.1545	143.1543	1.35	C8 H19 N2	100	1237849
	e	146.0602	146.06	0.85	C9 H8 O N	11.6	143609
	j-NH3	155.0818	155.0815	1.93	C7 H11 O2 N2	4	49573
	j	172.1084	172.1081	2.24	C7 H14 O2 N3	6.49	80368
	g	217.2392	217.2387	2.54	C11 H29 N4	14.82	183499
	i-NH3-H2O	222.1607	222.1601	2.87	C12 H20 O N3	1.51	18699
	i-2*NH3	223.1445	223.1441	1.96	C12 H19 O2 N2	4.05	50194
	i-NH3	240.1717	240.1707	4.32	C12 H22 O2 N3	2.52	31213
	i	257.1978	257.1972	2.19	C12 H25 O2 N4	7.18	88910
	f-2*NH3-H2O	279.2188	279.2179	3.11	C15 H27 O N4	3.23	39997
	f-2*NH3	297.2293	297.2285	2.73	C15 H29 O2 N4	1.98	24449
	f-NH3	314.2558	314.2551	2.4	C15 H32 O2 N5	2.95	36540
	d-H2O	327.1462	327.1452	3.05	C17 H19 O3 N4	2.11	26075
	d-NH3	328.1301	328.1292	2.77	C17 H18 O4 N3	24.47	302956
	f	331.2824	331.2816	2.35	C15 H35 O2 N6	5.92	73327
	d	345.1566	345.1557	2.66	C17 H21 O4 N4	12.62	156218
	b-H2O	412.2353	412.2343	2.47	C22 H30 O3 N5	4.24	52463
	b-NH3	413.2171	413.2183	-3.04	C22 H29 O4 N4	5.92	73304
	b	430.2457	430.2449	1.98	C22 H32 O4 N5	23.76	294065
	M+H-H20	486.3195	486.3187	1.67	C25 H40 O3 N7	1.91	23656
	M+H-NH3	487.3024	487.3027	-0.78	C25 H39 O4 N6	5.64	69825
	M+H	504.3298	504.3293	0.99	C25 H42 O4 N7	25.84	319857
LF448B	int.	86.0962	86.0964	-2.52	C5 H12 N	2.7	22326
	asn imm. Ion	87.055	87.0553	-3.13	C3 H7 O N2	5.86	48575
	h-NH3-C2H4	98.0962	98.0964	-1.97	C6 H12 N	6.56	54330
	h-NH3	126.1275	126.1277	-1.71	C8 H16 N	64.98	538293
	j-NH3-H2O	137.0708	137.0709	-0.79	C7 H9 O N2	1.99	16496
	j-2*NH3	138.0549	138.055	-0.53	C7 H8 O2 N	4.49	37195
	h	143.1542	143.1543	-0.41	C8 H19 N2	100	828334
	j-NH3	155.0813	155.0815	-1.33	C7 H11 O2 N2	2.76	22892
	j	172.1082	172.1081	1.07	C7 H14 O2 N3	1.85	15318
	g	217.2388	217.2387	0.39	C11 H29 N4	8.19	67806
	i-NH3-H2O	222.16	222.1601	-0.24	C12 H20 O N3	1.3	10786
	i-2*NH3	223.1441	223.1441	-0.18	C12 H19 O2 N2	3.19	26456
	i-NH3	240.171	240.1707	1.46	C12 H22 O2 N3	2.19	18140
	i	257.1975	257.1972	1.18	C12 H25 O2 N4	1.71	14164
	d-H2O	272.1395	272.1394	0.52	C15 H18 O2 N3	2.31	19126
	d-NH3	273.1236	273.1234	0.89	C15 H17 O3 N2	45.77	379130
	f-2*NH3-H2O	279.218	279.2179	0.1	C15 H27 O N4	2.23	18508
	d	290.1499	290.1499	-0.02	C15 H20 O3 N3	17.68	146452
	f-2*NH3	297.2292	297.2285	2.33	C15 H29 O2 N4	1.05	8685
	f-NH3	314.2552	314.2551	0.61	C15 H32 O2 N5	1.58	13124
	b-H2O	357.2287	357.2285	0.67	C20 H29 O2 N4	7.31	60576
	b-NH3	358.2115	358.2125	-2.86	C20 H28 O3 N3	7.44	61639
	b	375.2389	375.2391	-0.41	C20 H31 O3 N4	43.8	362776
	a	392.2655	392.2656	-0.3	C20 H34 O3 N5	1.53	12662
	M+H-H2O-NH3	414.2871	414.2864	1.84	C23 H36 O2 N5	1.34	11083
	M+H-H2O	431.3128	431.3129	-0.25	C23 H39 O2 N6	1.37	11357
	M+H-NH3	432.2959	432.2969	-2.33	C23 H38 O3 N5	4.75	39381
	M+H	449.323	449.3235	-1.07	C23 H41 O3 N6	30.43	252039

	ion type	*m/z measured*	*m/z theor.*	*rel. error (ppm)*	*Composition*	*rel. Int.*	*Int.*
LF464B	int.	86.0961	86.0964	-4	C5 H12 N	2.5	10530
	asn imm. Ion	87.0549	87.0553	-4.14	C3 H7 O N2	5.85	24646
	h-NH3-C2H4	98.0961	98.0964	-3.64	C6 H12 N	6.26	26380
	e	107.0491	107.0491	-0.24	C7 H7 O	2.14	9005
	h-NH3	126.1274	126.1277	-2.81	C8 H16 N	63.64	268196
	j-NH3-H2O	137.0707	137.0709	-1.46	C7 H9 O N2	1.69	7103
	j-2*NH3	138.0546	138.055	-2.85	C7 H8 O2 N	4.94	20823
	h	143.154	143.1543	-1.7	C8 H19 N2	100	421397
	j-NH3	155.0814	155.0815	-0.9	C7 H11 O2 N2	2.64	11137
	j	172.1079	172.1081	-0.81	C7 H14 O2 N3	2.17	9131
	g	217.2388	217.2387	0.56	C11 H29 N4	7.49	31579
	i-NH3-H2O	222.1609	222.1601	3.54	C12 H20 O N3	0.9	3798
	i-2*NH3	223.1438	223.1441	-1.45	C12 H19 O2 N2	3.27	13796
	i-NH3	240.1699	240.1707	-3.13	C12 H22 O2 N3	2.22	9370
	i	257.1975	257.1972	0.99	C12 H25 O2 N4	2.2	9273
	d-H2O	288.1342	288.1343	-0.18	C15 H18 O3 N3	2.3	9676
	d-NH3	289.1181	289.1183	-0.64	C15 H17 O4 N2	45.7	192563
	f-2*NH3	297.2285	297.2285	-0.12	C15 H29 O2 N4	0.99	4178
	d	306.1445	306.1448	-1.16	C15 H20 O4 N3	17.66	74410
	f-NH3	314.255	314.2551	-0.02	C15 H32 O2 N5	1.18	4965
	f	331.2819	331.2816	0.86	C15 H35 O2 N6	0.62	2631
	b-H2O	373.223	373.2234	-1.04	C20 H29 O3 N4	7.46	31432
	b-NH3	374.207	374.2074	-1.28	C20 H28 O4 N3	8.26	34825
	b	391.2335	391.234	-1.14	C20 H31 O4 N4	43.66	183977
	a	408.2602	408.2605	-0.89	C20 H34 O4 N5	1.32	5552
	M+H-H2O-NH3	430.2795	430.2813	-4.06	C23 H36 O3 N5	1.22	5146
	M+H-H2O	447.3087	447.3078	1.94	C23 H39 O3 N6	1.04	4389
	M+H-NH3	448.2914	448.2918	-1.04	C23 H38 O4 N5	5.58	23527
	M+H	465.3179	465.3184	-0.93	C23 H41 O4 N6	31.38	132213
LF480B	asn imm. Ion	87.055	87.0553	-3.17	C3 H7 O N2	5.44	2784
	h-NH3-C2H4	98.0963	98.0964	-1.02	C6 H12 N	4.04	2071
	h-NH3	126.1273	126.1277	-3.38	C8 H16 N	56.6	28991
	j-2*NH3	138.0545	138.055	-3.56	C7 H8 O2 N	3.94	2019
	h	143.1539	143.1543	-2.53	C8 H19 N2	100	51222
	j-NH3	155.0815	155.0815	0.02	C7 H11 O2 N2	6.94	3553
	j	172.1079	172.1081	-0.62	C7 H14 O2 N3	10.43	5343
	g	217.2389	217.2387	0.86	C11 H29 N4	8.89	4551
	i-2*NH3	223.1412	223.1441	-13.02	C12 H19 O2 N2	1.07	547
	i-NH3	240.1671	240.1707	-14.88	C12 H22 O2 N3	1.61	822
	i	257.1968	257.1972	-1.56	C12 H25 O2 N4	7.04	3606
	f-2*NH3-H2O	279.2198	279.2179	6.67	C15 H27 O N4	2.85	1462
	d-H2O	304.129	304.1292	-0.58	C15 H18 O4 N3	2.52	1289
	d-NH3	305.1134	305.1132	0.74	C15 H17 O5 N2	23.78	12178
	f-NH3	314.2543	314.2551	-2.29	C15 H32 O2 N5	2.67	1368
	d	322.1387	322.1397	-3.24	C15 H20 O5 N3	9.73	4983
	f	331.2824	331.2816	2.27	C15 H35 O2 N6	6.28	3216
	b-H2O	389.218	389.2183	-0.75	C20 H29 O4 N4	5.53	2831
	b-NH3	390.203	390.2023	1.67	C20 H28 O5 N3	5.51	2822
	b	407.2288	407.2289	-0.18	C20 H31 O5 N4	34.26	17550
	M+H-H2O-NH3	446.27	446.2762	-13.94	C23 H36 O4 N5	1.04	533
	M+H-NH3	464.2874	464.2867	1.38	C23 H38 O5 N5	3.4	1743
	M+H	481.3142	481.3133	1.8	C23 H41 O5 N6	31.51	16138

	ion type	*m/z measured*	*m/z theor.*	*rel. error (ppm)*	*Composition*	*rel. Int.*	*Int.*
LF516B	int.	86.0962	86.0964	-2.94	C5 H12 N	2.21	33752
	h-NH3-C2H4	98.0962	98.0964	-2.41	C6 H12 N	6.69	102409
	h-NH3	126.1275	126.1277	-1.71	C8 H16 N	46.3	708422
	e-CH3N	130.0649	130.0651	-1.73	C9 H8 N	2.93	44773
	j-2*NH3	138.0549	138.055	-0.66	C7 H8 O2 N	2.52	38543
	h	143.1542	143.1543	-0.57	C8 H19 N2	100	1529983
	j-NH3	155.0815	155.0815	0.04	C7 H11 O2 N2	4.11	62867
	e	159.0917	159.0917	0.06	C10 H11 N2	13.05	199637
	j	172.1081	172.1081	0.21	C7 H14 O2 N3	11.22	171597
	g	217.2387	217.2387	0.28	C11 H29 N4	12.58	192525
	i-2*NH3	223.144	223.1441	-0.25	C12 H19 O2 N2	2.35	35884
	i-NH3	240.1709	240.1707	0.97	C12 H22 O2 N3	2.76	42274
	i	257.1972	257.1972	0.04	C12 H25 O2 N4	14.84	227006
	f-2*NH3-H2O	279.2182	279.2179	1.05	C15 H27 O N4	3.34	51081
	f-2*NH3	297.2292	297.2285	2.29	C15 H29 O2 N4	1.46	22399
	f-NH3	314.2553	314.2551	0.67	C15 H32 O2 N5	3.97	60777
	d-2*NH3	324.1344	324.1343	0.39	C18 H18 O3 N3	2.1	32167
	f	331.2817	331.2816	0.29	C15 H35 O2 N6	13.41	205112
	d-NH3	341.1611	341.1608	0.7	C18 H21 O3 N4	14.46	221268
	d	358.1874	358.1874	0.21	C18 H24 O3 N5	7.73	118283
	b-H2O-NH3	408.2392	408.2394	-0.47	C23 H30 O2 N5	3.96	60620
	b-H2O	425.2661	425.266	0.3	C23 H33 O2 N6	2.11	32293
	b-NH3	426.2481	426.25	-4.27	C23 H32 O3 N5	4.77	73029
	b	443.2765	443.2765	-0.01	C23 H35 O3 N6	21.5	328977
	M+H-NH3	500.3338	500.3344	-1.06	C26 H42 O3 N7	4.18	63899
	M+H	517.3607	517.3609	-0.41	C26 H45 O3 N8	23.84	364728
LF517B	int.	86.096	86.0964	-4.75	C5 H12 N	2.32	61898
	asn imm. Ion	87.0548	87.0553	-5.59	C3 H7 O N2	1.28	34073
	h-NH3-C2H4	98.096	98.0964	-4.43	C6 H12 N	6.01	160263
	h-NH3	126.1273	126.1277	-3.35	C8 H16 N	57.36	1530579
	e-CH2O	130.0646	130.0651	-4.03	C9 H8 N	1.31	34822
	j-2*NH3	138.0547	138.055	-1.86	C7 H8 O2 N	4.86	129561
	h	143.154	143.1543	-2.02	C8 H19 N2	100	2668243
	j-NH3	155.0812	155.0815	-2.08	C7 H11 O2 N2	3.25	86849
	e	160.0756	160.0757	-0.68	C10 H10 O N	1.55	41411
	j	172.1081	172.1081	0.1	C7 H14 O2 N3	2.93	78258
	g	217.2387	217.2387	-0.05	C11 H29 N4	8.47	225973
	i-NH3-H2O	222.1603	222.1601	0.94	C12 H20 O N3	1.29	34545
	i-2*NH3	223.1439	223.1441	-0.74	C12 H19 O2 N2	4.27	113963
	i-NH3	240.1709	240.1707	1.01	C12 H22 O2 N3	2.11	56250
	i	257.1974	257.1972	0.58	C12 H25 O2 N4	3.23	86100
	f-2*NH3-H2O	279.2181	279.2179	0.43	C15 H27 O N4	2.43	64880
	f-2*NH3	297.2289	297.2285	1.32	C15 H29 O2 N4	1.56	41643
	f-NH3	314.255	314.2551	-0.16	C15 H32 O2 N5	1.74	46342
	d-NH3-H2O	324.1347	324.1343	1.37	C18 H18 O3 N3	3.99	106508
	f	331.2821	331.2816	1.49	C15 H35 O2 N6	1.61	42894
	d-H2O	341.1619	341.1608	3.23	C18 H21 O3 N4	1.69	45094
	d-NH3	342.1452	342.1448	1.06	C18 H20 O4 N3	28.49	760284
	d	359.1719	359.1714	1.39	C18 H23 O4 N4	13.57	361960
	b-H2O	426.2501	426.25	0.31	C23 H32 O3 N5	3.16	84287
	b-NH3	427.2322	427.234	-4.15	C23 H31 O4 N4	6.68	178150
	b	444.2607	444.2605	0.43	C23 H34 O4 N5	29.12	776861
	M+H-NH3	501.3186	501.3184	0.43	C26 H41 O4 N6	4.77	127265
	M+H	518.3456	518.3449	1.32	C26 H44 O4 N7	21.12	563489

	ion type	*m/z measured*	*m/z theor.*	*rel. error (ppm)*	*Composition*	*rel. Int.*	*Int.*
LF477B	H-NH3-C2H4	98.0962	98.0964	-2.5	C6 H12 N	4.42	2705
	e	120.0805	120.0808	-2.44	C8 H10 N	9.17	5614
	h-NH3	126.1274	126.1277	-2.76	C8 H16 N	47.33	28960
	j-2*NH3	138.055	138.055	0.27	C7 H8 O2 N	0.97	592
	h	143.154	143.1543	-1.99	C8 H19 N2	100	61193
	j-NH3	155.0818	155.0815	1.81	C7 H11 O2 N2	4.31	2637
	j	172.1077	172.1081	-2.18	C7 H14 O2 N3	9.09	5562
	g	217.2388	217.2387	0.77	C11 H29 N4	7.72	4721
	i-2*NH3	223.1452	223.1441	5.04	C12 H19 O2 N2	1.82	1114
	i-NH3	240.1705	240.1707	-0.74	C12 H22 O2 N3	2.19	1337
	i	257.1969	257.1972	-1.26	C12 H25 O2 N4	10.24	6265
	f-2*NH3-H2O	279.2179	279.2179	-0.09	C15 H27 O N4	2.86	1748
	d-NH3	302.1498	302.1499	-0.47	C16 H20 O3 N3	26.49	16210
	f-NH3	314.2569	314.2551	5.77	C15 H32 O2 N5	0.95	583
	d	319.1761	319.1765	-1.13	C16 H23 O3 N4	13.53	8280
	f	331.2801	331.2816	-4.51	C15 H35 O2 N6	8.31	5086
	b-NH3-H2O	369.2279	369.2285	-1.66	C21 H29 O2 N4	6.63	4060
	b-H2O	386.2538	386.2551	-3.33	C21 H32 O2 N5	3.1	1896
	b-NH3	387.2394	387.2391	0.83	C21 H31 O3 N4	4.74	2899
	b	404.2649	404.2656	-1.81	C21 H34 O3 N5	35.62	21794
	M+H-H2O-NH3	443.3143	443.3129	3.23	C24 H39 O2 N6	0.95	582
	M+H-NH3	461.325	461.3235	3.34	C24 H41 O3 N6	4.96	3035
	M+H	478.3487	478.35	-2.66	C24 H44 O3 N7	34.7	21236
LF478B	int.	86.0959	86.0964	-6.67	C5 H12 N	2.6	8628
	asn imm. Ion	87.0546	87.0553	-8.17	C3 H7 O N2	3.12	10373
	h-NH3-C2H4	98.0958	98.0964	-6.83	C6 H12 N	6.01	19960
	h-NH3	126.127	126.1277	-5.4	C8 H16 N	60.9	202334
	i-2*NH3	138.0543	138.055	-4.46	C7 H8 O2 N	4.85	16102
	h	143.1537	143.1543	-3.95	C8 H19 N2	100	332214
	i-NH3	155.0808	155.0815	-4.37	C7 H11 O2 N2	3.14	10443
	i	172.1074	172.1081	-4.02	C7 H14 O2 N3	1.6	5299
	g	217.238	217.2387	-2.87	C11 H29 N4	7.03	23351
	i-NH3-H2O	222.1589	222.1601	-5.15	C12 H20 O N3	1.11	3685
	i-2*NH3	223.1437	223.1441	-1.75	C12 H19 O2 N2	3.6	11949
	i-NH3	240.1701	240.1707	-2.25	C12 H22 O2 N3	2.07	6878
	i	257.1964	257.1972	-3.12	C12 H25 O2 N4	2.85	9480
	f-2*NH3-H2O	279.2173	279.2179	-2.44	C15 H27 O N4	2.16	7167
	f-2*NH3	297.2278	297.2285	-2.32	C15 H29 O2 N4	1.06	3512
	d-H2O	302.1486	302.1499	-4.38	C16 H20 O3 N3	1.61	5347
	d-NH3	303.1335	303.1339	-1.45	C16 H19 O4 N2	46.81	155502
	f-NH3	314.2547	314.2551	-1.05	C15 H32 O2 N5	1.23	4083
	d	320.1601	320.1605	-1.26	C16 H22 O4 N3	19.75	65602
	b-H2O	387.239	387.2391	-0.09	C21 H31 O3 N4	4.71	15635
	b-NH3	388.2221	388.2231	-2.48	C21 H30 O4 N3	8.11	26930
	b	405.249	405.2496	-1.51	C21 H33 O4 N4	44.06	146372
	M+H-H2O-NH3	444.2963	444.2969	-1.36	C24 H38 O3 N5	1.24	4103
	M+H-NH3	462.3061	462.3075	-3	C24 H40 O4 N5	5.38	17873
	M+H	479.3331	479.334	-1.97	C24 H43 O4 N6	30.35	100838

Type C compounds

	ion type	*m/z measured*	*m/z theor.*	*rel. error (ppm)*	*Composition*	*rel. Int.*	*Int.*
LF487C	int. ion	86.0962	86.0964	-2.96	C5 H12 N	2.89	63502
	h-NH3	98.0962	98.0964	-2.37	C6 H12 N	35.14	773020
	h	115.1227	115.123	-1.96	C6 H15 N2	100	2199881
	int ion	126.1275	126.1277	-1.57	C8 H16 N	7.36	161912
	e	130.065	130.0651	-1.1	C9 H8 N	13.37	294154
	int ion	143.1542	143.1543	-0.76	C8 H19 N2	9.69	213082
	g-NH3	200.2121	200.2121	-0.18	C11 H26 N3	2.38	52359
	g	217.2388	217.2387	0.69	C11 H29 N4	23.58	518738
	i-NH3-H2O	222.1598	222.1601	-1.43	C12 H20 O N3	1.24	27278
	i-2*NH3	223.144	223.1441	-0.34	C12 H19 O2 N2	4.23	93123
	i-NH3	240.1709	240.1707	1.06	C12 H22 O2 N3	4.67	102806
	i	257.1973	257.1972	0.39	C12 H25 O2 N4	4.77	105027
	f-2*NH3	297.2287	297.2285	0.83	C15 H29 O2 N4	6.49	142693
	f-NH3	314.2551	314.2551	0.1	C15 H32 O2 N5	7.56	166292
	f	331.2817	331.2816	0.25	C15 H35 O2 N6	7.49	164768
	d	357.1913	357.1921	-2.24	C19 H25 O3 N4	2.1	46174
	c	374.2184	374.2187	-0.65	C19 H28 O3 N5	2.66	58525
	b-H2O	396.2402	396.2394	2.1	C22 H30 O2 N5	2.79	61444
	b-NH3	397.2216	397.2234	-4.52	C22 H29 O3 N4	4.75	104514
	b	414.2497	414.25	-0.74	C22 H32 O3 N5	64.14	1411049
	a	431.2763	431.2765	-0.43	C22 H35 O3 N6	4.82	105950
	M+H-H2O	470.3241	470.3238	0.7	C25 H40 O2 N7	2.8	61531
	M+H-NH3	471.3073	471.3078	-1.15	C25 H39 O3 N6	14.24	313189
	M+H	488.3336	488.3344	-1.65	C25 H42 O3 N7	90.34	1987466
LF503C	int. ion	86.0963	86.0964	-1.79	C5 H12 N	2.69	32110
	asn imm. Ion	87.055	87.0553	-3.26	C3 H7 O N2	2.98	35569
	h-NH3	98.0962	98.0964	-2.08	C6 H12 N	30.22	361212
	h	115.1228	115.123	-1.53	C6 H15 N2	97.39	1164186
	int ion	126.1276	126.1277	-1.05	C8 H16 N	8.32	99493
	int ion	143.1543	143.1543	-0.16	C8 H19 N2	11.47	137123
	e	146.06	146.06	0.02	C9 H8 O N	20.25	242047
	g-NH3	200.2119	200.2121	-1.11	C11 H26 N3	2.78	33216
	g	217.2389	217.2387	1.04	C11 H29 N4	37.8	451845
	i-2*NH3	223.1442	223.1441	0.22	C12 H19 O2 N2	4.37	52208
	i-NH3	240.171	240.1707	1.32	C12 H22 O2 N3	5.11	61125
	i	257.1974	257.1972	0.87	C12 H25 O2 N4	9.5	113537
	f-2*NH3	297.2288	297.2285	0.85	C15 H29 O2 N4	8.79	105032
	f-NH3	314.2553	314.2551	0.81	C15 H32 O2 N5	11.03	131796
	f	331.2818	331.2816	0.65	C15 H35 O2 N6	19.73	235848
	d	373.1875	373.187	1.25	C19 H25 O4 N4	2.1	25118
	c	390.2138	390.2136	0.65	C19 H28 O4 N5	2.59	30911
	b-H2O	412.2343	412.2343	0.02	C22 H30 O3 N5	2.58	30874
	b-NH3	413.2171	413.2183	-2.98	C22 H29 O4 N4	5.08	60713
	b	430.2451	430.2449	0.41	C22 H32 O4 N5	51.97	621187
	a	447.2713	447.2714	-0.25	C22 H35 O4 N6	4.32	51629
	M+H-H2O	486.3187	486.3187	-0.12	C25 H40 O3 N7	3.24	38741
	M+H-NH3	487.3021	487.3027	-1.34	C25 H39 O4 N6	15.09	180375
	M+H	504.329	504.3293	-0.58	C25 H42 O4 N7	100	1195369
LF448C	int. ion	86.0963	86.0964	-1.4	C5 H12 N	1.28	1645
	asn imm. Ion	87.0547	87.0553	-6.74	C3 H7 O N2	3.58	4595
	h-NH3	98.0959	98.0964	-5.81	C6 H12 N	26	33326
	h	115.1224	115.123	-4.88	C6 H15 N2	74.27	95209
	int. ion	126.1275	126.1277	-2.08	C8 H16 N	4.56	5840
	int. ion	143.1541	143.1543	-1.55	C8 H19 N2	5.69	7295
	g	217.2382	217.2387	-2.23	C11 H29 N4	11.54	14791
	i-2*NH3	223.1442	223.1441	0.34	C12 H19 O2 N2	2.77	3549
	i-NH3	240.1692	240.1707	-6.1	C12 H22 O2 N3	3.31	4244
	i	257.1977	257.1972	2.03	C12 H25 O2 N4	1.85	2373

	ion type	*m/z measured*	*m/z theor.*	*rel. error (ppm)*	*Composition*	*rel. Int.*	*Int.*
LF448C (cont.)	f-2*NH3	297.2287	297.2285	0.76	C15 H29 O2 N4	2.95	3779
	f-H2O	313.2711	313.271	0.36	C15 H33 O N6	1.37	1752
	f-NH3	314.2553	314.2551	0.82	C15 H32 O2 N5	4.35	5580
	d	318.1784	318.1812	-8.74	C17 H24 O3 N3	1.42	1818
	f	331.2771	331.2744	8.18	C21 H35 O N2	1.51	1934
	c	335.205	335.2078	-8.11	C17 H27 O3 N4	1.92	2462
	b-H2O	357.2291	357.2285	1.57	C20 H29 O2 N4	2.89	3710
	b-NH3	358.2136	358.2125	3.08	C20 H28 O3 N3	3.35	4300
	b	375.2387	375.2391	-0.96	C20 H31 O3 N4	75.55	96853
	a	392.2663	392.2656	1.81	C20 H34 O3 N5	4.78	6130
	M+H-H2O	431.3126	431.3129	-0.65	C23 H39 O2 N6	2.48	3174
	N+H-NH3	432.2968	432.2969	-0.31	C23 H38 O3 N5	14.67	18803
	M+H	449.3232	449.3235	-0.7	C23 H41 O3 N6	100	128190
LF464C	int. ion	86.0965	86.0964	1	C5 H12 N	0.72	566
	asn imm. Ion	87.0551	87.0553	-1.75	C3 H7 O N2	5.21	4108
	h-NH3	98.0962	98.0964	-2.2	C6 H12 N	30.77	24262
	e	107.0493	107.0491	1.67	C7 H7 O	1.31	1034
	h	115.1228	115.123	-1.61	C6 H15 N2	85.32	67264
	int ion	126.1275	126.1277	-1.83	C8 H16 N	11.26	8878
	int ion	143.1542	143.1543	-0.34	C8 H19 N2	15.48	12206
	g	217.2389	217.2387	0.87	C11 H29 N4	13.84	10914
	i-2*NH3	223.1453	223.1441	5.29	C12 H19 O2 N2	1.94	1533
	i-NH3	240.171	240.1707	1.3	C12 H22 O2 N3	4.36	3438
	i	257.1977	257.1972	1.92	C12 H25 O2 N4	3.17	2499
	f-2*NH3	297.2275	297.2285	-3.27	C15 H29 O2 N4	3.14	2473
	f-NH3	314.2563	314.2551	3.86	C15 H32 O2 N5	4.44	3498
	f	331.2818	331.2816	0.45	C15 H35 O2 N6	2.59	2041
	b-H2O	373.2231	373.2234	-0.88	C20 H29 O3 N4	3.87	3048
	b-NH3	374.2081	374.2074	1.76	C20 H28 O4 N3	3.93	3097
	b	391.2341	391.234	0.29	C20 H31 O4 N4	77.93	61442
	a	408.2617	408.2605	2.87	C20 H34 O4 N5	5.44	4289
	M+H-H2O	447.3067	447.3078	-2.57	C23 H39 O3 N6	1.65	1301
	M+H-NH3	448.291	448.2918	-1.9	C23 H38 O4 N5	14.75	11628
	M+H	465.3184	465.3184	0.1	C23 H41 O4 N6	100	78838
LF480C	int. ion	86.0963	86.0964	-0.93	C5 H12 N	2.47	6274
	asn imm. Ion	87.0552	87.0553	-0.93	C3 H7 O N2	7.66	19453
	h-NH3	98.0964	98.0964	-0.4	C6 H12 N	34.78	88325
	h	115.123	115.123	0.19	C6 H15 N2	100	253986
	int.ion	126.1278	126.1277	0.22	C8 H16 N	15.22	38669
	int. ion	143.1544	143.1543	1.21	C8 H19 N2	19.88	50494
	g-NH3	200.2127	200.2121	2.84	C11 H26 N3	2.53	6418
	g	217.2393	217.2387	2.73	C11 H29 N4	25.44	64614
	i-NH3-H2O	222.1609	222.1601	3.72	C12 H20 O N3	1.5	3813
	i-2*NH3	223.1447	223.1441	2.49	C12 H19 O2 N2	2.52	6409
	i-NH3	240.1713	240.1707	2.66	C12 H22 O2 N3	7.37	18707
	i	257.1977	257.1972	2.03	C12 H25 O2 N4	19.47	49451
	f-2*NH3	297.2293	297.2285	2.57	C15 H29 O2 N4	3.8	9639
	f-NH3	314.2559	314.2551	2.54	C15 H32 O2 N5	11.37	28890
	f	331.2823	331.2816	2.25	C15 H35 O2 N6	28.25	71754
	b-H2O	389.2199	389.2183	3.95	C20 H29 O4 N4	4.16	10573
	b-NH3	390.2012	390.2023	-2.94	C20 H28 O5 N3	4.47	11358
	b	407.2296	407.2289	1.65	C20 H31 O5 N4	63.8	162042
	a	424.2559	424.2554	1.15	C20 H34 O5 N5	4.54	11529
	M+H-H2O	463.3038	463.3027	2.2	C23 H39 O4 N6	3.82	9691
	M+H-NH3	464.2863	464.2867	-0.99	C23 H38 O5 N5	12.66	32149
	M+H	481.3138	481.3133	1.15	C23 H41 O5 N6	93.31	236999

Type D compounds

	ion type	*m/z measured*	*m/z theor.*	*rel. error (ppm)*	*Composition*	*rel. Int.*	*Int.*
LF473D	int. ion	72.0804	72.0808	-5.63	C4 H10 N	0.94	3546
	H-NH3-C2H4	84.0806	84.0808	-1.84	C5 H10 N	2.44	9230
	h-NH3	112.1119	112.1121	-1.3	C7 H14 N	38.37	145334
	h	129.1385	129.1386	-1.33	C7 H17 N2	100	378802
	e	130.0649	130.0651	-1.44	C9 H8 N	3.77	14296
	J-NH3-H2O	137.0708	137.0709	-1.2	C7 H9 O N2	1	3771
	j-2*NH3	138.0549	138.055	-0.72	C7 H8 O2 N	2.71	10249
	j-NH3	155.0818	155.0815	1.64	C7 H11 O2 N2	1.05	3985
	j	172.1082	172.1081	0.65	C7 H14 O2 N3	1.44	5465
	g	203.223	203.223	0.04	C10 H27 N4	0.38	1431
	i-NH3-H2O	208.1448	208.1444	1.91	C11 H18 O N3	1.29	4890
	i-2*NH3	209.1286	209.1285	0.57	C11 H17 O2 N2	3.03	11484
	i-NH3	226.1555	226.155	2.18	C11 H20 O2 N3	2.02	7649
	i	243.1817	243.1816	0.4	C11 H23 O2 N4	3.66	13873
	d-H2O	311.1501	311.1503	-0.62	C17 H19 O2 N4	1.22	4606
	d-NH3	312.1347	312.1343	1.33	C17 H18 O3 N3	19.58	74184
	f	317.2668	317.266	2.69	C14 H33 O2 N6	0.89	3372
	d	329.1609	329.1608	0.37	C17 H21 O3 N4	8.64	32720
	b-H2O	382.224	382.2238	0.77	C21 H28 O2 N5	6.69	25342
	b-NH3	383.208	383.2078	0.5	C21 H27 O3 N4	6.84	25900
	b	400.2344	400.2343	0.12	C21 H30 O3 N5	38.83	147082
	M+H	474.3248	474.3187	12.88	C24 H40 O3 N7	2.36	8936
LF489D	int. ion	72.0806	72.0808	-2.85	C4 H10 N	0.63	4744
	h-NH3-C2H4	84.0806	84.0808	-2.08	C5 H10 N	1.89	14149
	asn imm. Ion	87.0551	87.0553	-1.78	C3 H7 O N2	0.71	5347
	h-NH3	112.1119	112.1121	-1.4	C7 H14 N	33.88	253458
	h	129.1385	129.1386	-1.3	C7 H17 N2	100	748032
	j-2*NH3	138.0549	138.055	-0.64	C7 H8 O2 N	2.3	17173
	e	146.0601	146.06	0.18	C9 H8 O N	5.15	38526
	j-NH3	155.0814	155.0815	-0.74	C7 H11 O2 N2	1.51	11308
	j	172.1082	172.1081	0.91	C7 H14 O2 N3	2.97	22188
	g	203.223	203.223	0.02	C10 H27 N4	0.82	6152
	i-NH3-H2O	208.1445	208.1444	0.35	C11 H18 O N3	1.63	12214
	i-2*NH3	209.1284	209.1285	-0.12	C11 H17 O2 N2	2.97	22251
	i-NH3	226.1553	226.155	1.24	C11 H20 O2 N3	2.14	16007
	i	243.1818	243.1816	1.05	C11 H23 O2 N4	5.77	43182
	d-H2O	327.1456	327.1452	1.35	C17 H19 O3 N4	1.43	10669
	d-NH3	328.1295	328.1292	1.02	C17 H18 O4 N3	12.32	92148
	d	345.1561	345.1557	1.08	C17 H21 O4 N4	6.69	50076
	b-H2O	398.219	398.2187	0.75	C21 H28 O3 N5	5.88	43953
	b-NH3	399.2012	399.2027	-3.81	C21 H27 O4 N4	5.23	39105
	b	416.2291	416.2292	-0.35	C21 H30 O4 N5	31.79	237804
	M+H	490.3119	490.3136	-3.54	C24 H40 O4 N7	2.96	22178
LF434D	h-NH3-C2H4	84.0805	84.0808	-3.11	C5 H10 N	1.89	1424
	asn imm. Ion	87.0557	87.0553	4.57	C3 H7 O N2	0.62	470
	h-NH3	112.1117	112.1121	-3.27	C7 H14 N	38.23	28794
	h	129.1383	129.1386	-2.83	C7 H17 N2	100	75325
	j-2*NH3	138.0547	138.055	-2.01	C7 H8 O2 N	3.01	2264
	d-NH3	273.1235	273.1234	0.37	C15 H17 O3 N2	18.23	13732
	d	290.1501	290.1499	0.51	C15 H20 O3 N3	7.02	5286
	b-H2O	343.2124	343.2129	-1.26	C19 H27 O2 N4	6.47	4874
	b-NH3	344.197	344.1969	0.33	C19 H26 O3 N3	4.83	3638
	b	361.2226	361.2234	-2.31	C19 H29 O3 N4	41.9	31558

	ion type	*m/z measured*	*m/z theor.*	*rel. error (ppm)*	*Composition*	*rel. Int.*	*Int.*
LF450D	int. ion	72.0804	72.0808	-4.64	C4 H10 N	1.12	3252
	h-NH3-C2H4	84.0805	84.0808	-3.34	C5 H10 N	1.98	5771
	asn imm. Ion	87.055	87.0553	-3.19	C3 H7 O N2	1.4	4095
	e	107.0495	107.0491	3.67	C7 H7 O	0.39	1149
	h-NH3	112.1118	112.1121	-2.6	C7 H14 N	38.92	113469
	h	129.1383	129.1386	-2.62	C7 H17 N2	100	291556
	j-NH3-H2O	137.0711	137.0709	0.95	C7 H9 O N2	0.77	2234
	j-2*NH3	138.0545	138.055	-3.14	C7 H8 O2 N	1.79	5216
	j-NH3	155.0816	155.0815	0.62	C7 H11 O2 N2	1.07	3106
	j	172.1079	172.1081	-0.62	C7 H14 O2 N3	2.16	6290
	i-NH3-H2O	208.144	208.1444	-2.2	C11 H18 O N3	0.62	1798
	i-2*NH3	209.1281	209.1285	-1.91	C11 H17 O2 N2	1.46	4258
	i-NH3	226.1549	226.155	-0.25	C11 H20 O2 N3	1.02	2978
	i	243.1808	243.1816	-3.06	C11 H23 O2 N4	0.99	2883
	d-H2O	288.1339	288.1343	-1.45	C15 H18 O3 N3	0.9	2619
	d-NH3	289.1182	289.1183	-0.13	C15 H17 O4 N2	13.46	39232
	c-H2O	305.1624	305.1608	5.29	C15 H21 O3 N4	0.38	1120
	d	306.1446	306.1448	-0.88	C15 H20 O4 N3	5.78	16846
	c	323.1704	323.1714	-2.89	C15 H23 O4 N4	1.37	3998
	b-H2O	359.2077	359.2078	-0.21	C19 H27 O3 N4	4.79	13976
	b-NH3	360.1915	360.1918	-0.89	C19 H26 O4 N3	3.88	11327
	b	377.2183	377.2183	-0.22	C19 H29 O4 N4	31.27	91166
	M+H	451.3012	451.3027	-3.43	C22 H39 O4 N6	1.99	5811
LF466D	h-NH3-C2H4	84.0814	84.0808	7.85	C5 H10 N	1.52	543
	h-NH3	112.112	112.1121	-0.23	C7 H14 N	34.38	12306
	h	129.1386	129.1386	-0.55	C7 H17 N2	100	35797
	j-2*NH3	138.055	138.055	0.49	C7 H8 O2 N	1.44	514
	j	172.1082	172.1081	0.56	C7 H14 O2 N3	3.49	1250
	i	243.1816	243.1816	0.34	C11 H23 O2 N4	3.83	1370
	d-NH3	305.1146	305.1145	0.12	C16 H13 O N6	11	3937
	b-H2O	375.202	375.2027	-1.88	C19 H27 O4 N4	6.14	2198
	b-NH3	376.1855	376.1867	-3.22	C19 H26 O5 N3	1.46	524
	b	393.2134	393.2132	0.28	C19 H29 O5 N4	41.47	14847
	M+H	467.2972	467.2976	-0.86	C22 H39 O5 N6	2.72	973
LF502D	h-NH3-C2H4	84.0808	84.0808	0.46	C5 H10 N	2.43	4871
	h-NH3	112.1122	112.1121	0.68	C7 H14 N	33.44	67103
	h	129.1387	129.1386	0.67	C7 H17 N2	100	200676
	e-CH3N	130.0655	130.0651	2.61	C9 H8 N	0.93	1863
	j-2*NH3	138.0548	138.055	-0.88	C7 H8 O2 N	0.77	1543
	j-NH3	155.0813	155.0815	-1.36	C7 H11 O2 N2	1.49	2984
	e	159.0919	159.0917	1.67	C10 H11 N2	5.77	11572
	j	172.1087	172.1081	3.55	C7 H14 O2 N3	5.1	10240
	g	203.2232	203.223	0.7	C10 H27 N4	0.5	1001
	i-NH3-H2O	208.1446	208.1444	0.89	C11 H18 O N3	1.8	3621
	i-2*NH3	209.1285	209.1285	0.37	C11 H17 O2 N2	1.95	3905
	i-NH3	226.1558	226.155	3.45	C11 H20 O2 N3	2.12	4246
	i	243.1822	243.1816	2.68	C11 H23 O2 N4	13.59	27273
	d-2*NH3	324.1358	324.1343	4.81	C18 H18 O3 N3	0.85	1699
	d-NH3	341.1618	341.1608	2.9	C18 H21 O3 N4	7.91	15878
	d	358.1885	358.1874	3.2	C18 H24 O3 N5	5.21	10465
	b-NH3-H2O	394.225	394.2238	3.29	C22 H28 O2 N5	5.35	10739
	b-H2O	411.2526	411.2503	5.64	C22 H31 O2 N6	3.31	6635
	b-NH3	412.2355	412.2343	2.75	C22 H30 O3 N5	5.46	10966
	b	429.2619	429.2609	2.37	C22 H33 O3 N6	30.23	60671

	ion type	*m/z measured*	*m/z theor.*	*rel. error (ppm)*	*Composition*	*rel. Int.*	*Int.*
LF503D	h	129.138	129.1386	-5.19	C7 H17 N2	100	226070
	j-2*NH3	138.0544	138.055	-4.26	C7 H8 O2 N	2.22	5026
	j-NH3	155.0814	155.0815	-0.54	C7 H11 O2 N2	1.62	3657
	e	160.0759	160.0757	1.2	C10 H10 O N	0.65	1470
	j	172.1073	172.1081	-4.47	C7 H14 O2 N3	1.38	3122
	i-NH3-H2O	208.1442	208.1444	-1.1	C11 H18 O N3	1.27	2874
	i-2*NH3	209.1281	209.1285	-1.63	C11 H17 O2 N2	3.35	7564
	i-NH3	226.1543	226.155	-3.33	C11 H20 O2 N3	2.09	4723
	i	243.1807	243.1816	-3.4	C11 H23 O2 N4	2.5	5645
	d-H2O-NH3	324.1361	324.1343	5.77	C18 H18 O3 N3	1.43	3239
	d-H2O	341.1606	341.1608	-0.6	C18 H21 O3 N4	1.32	2978
	d-NH3	342.1447	342.1448	-0.43	C18 H20 O4 N3	16.25	36741
	d	359.1712	359.1714	-0.58	C18 H23 O4 N4	8	18081
	b-H2O	412.2335	412.2343	-1.93	C22 H30 O3 N5	4.86	10991
	b-NH3	413.2179	413.2183	-1.13	C22 H29 O4 N4	6.8	15374
	b	430.2447	430.2449	-0.44	C22 H32 O4 N5	39.88	90157
	M+H	504.3279	504.3293	-2.71	C25 H42 O4 N7	2.5	5653

Type E compounds

	ion type	*m/z measured*	*m/z theor.*	*rel. error (ppm)*	*Composition*	*rel. Int.*	*Int.*
LF473E	int. ion	72.0801	72.0808	-8.92	C4 H10 N	2.93	4944
	int. ion	84.0802	84.0808	-6.86	C5 H10 N	2.78	4683
	h-NH3	98.0959	98.0964	-5.7	C6 H12 N	26.44	44591
	int. ion	112.1116	112.1121	-4.69	C7 H14 N	20.2	34056
	h	115.1224	115.123	-4.99	C6 H15 N2	84.27	142101
	int ion	129.138	129.1386	-4.84	C7 H17 N2	5.62	9469
	e	130.0646	130.0651	-4.26	C9 H8 N	12.56	21186
	g-NH3	186.1961	186.1965	-2	C10 H24 N3	8.98	15149
	g	203.2227	203.223	-1.74	C10 H27 N4	20.68	34876
	i-NH3-H2O	208.1455	208.1444	5.26	C11 H18 O N3	0.74	1245
	i-2*NH3	209.1279	209.1285	-2.7	C11 H17 O2 N2	3.45	5819
	i-NH3	226.1542	226.155	-3.55	C11 H20 O2 N3	3.2	5396
	i	243.181	243.1816	-2.29	C11 H23 O2 N4	3.89	6551
	f-2*NH3	283.2127	283.2129	-0.69	C14 H27 O2 N4	4.72	7965
	f-NH3	300.2394	300.2394	-0.16	C14 H30 O2 N5	6.62	11159
	f	317.2658	317.266	-0.62	C14 H33 O2 N6	6.87	11591
	d-NH3	326.1508	326.1499	2.63	C18 H20 O3 N3	1.67	2813
	d	343.176	343.1765	-1.22	C18 H23 O3 N4	3.52	5928
	c	360.2025	360.203	-1.41	C18 H26 O3 N5	1.8	3032
	b-H2O	382.2228	382.2238	-2.61	C21 H28 O2 N5	3.23	5453
	b-NH3	383.2075	383.2078	-0.76	C21 H27 O3 N4	7.22	12182
	b	400.234	400.2343	-0.87	C21 H30 O3 N5	58.81	99170
	a	417.2612	417.2609	0.85	C21 H33 O3 N6	4.65	7848
	M+H-H2O-NH3	439.2825	439.2816	1.95	C24 H35 O2 N6	1.09	1832
	M+H-H2O	456.3085	456.3081	0.8	C24 H38 O2 N7	1.86	3139
	M+H-NH3	457.2922	457.2922	0	C24 H37 O3 N6	16.63	28040
	M+H	474.3186	474.3187	-0.18	C24 H40 O3 N7	100	168629
LF489E	int. ion	72.0803	72.0808	-5.99	C4 H10 N	3.18	7139
	asn imm ion	87.0551	87.0553	-1.98	C3 H7 O N2	2.96	6639
	h-NH3	98.0962	98.0964	-2.08	C6 H12 N	24.09	54071
	int. ion	112.1119	112.1121	-1.27	C7 H14 N	21.05	47252
	h	115.1228	115.123	-1.69	C6 H15 N2	88.22	198047
	int ion	129.1385	129.1386	-1.1	C7 H17 N2	8.08	18136
	e	146.06	146.06	-0.53	C9 H8 O N	19.5	43781
	g-NH3	186.1965	186.1965	0.12	C10 H24 N3	13.48	30259
	g	203.2231	203.223	0.43	C10 H27 N4	32.59	73163
	i-2*NH3	209.1284	209.1285	-0.36	C11 H17 O2 N2	3.31	7430
	i-NH3	226.1553	226.155	1.24	C11 H20 O2 N3	3.45	7753
	i	243.1817	243.1816	0.65	C11 H23 O2 N4	8.69	19515
	f-2*NH3	283.2132	283.2129	1.08	C14 H27 O2 N4	7.34	16486

	ion type	*m/z measured*	*m/z theor.*	*rel. error (ppm)*	*Composition*	*rel. Int.*	*Int.*
LF489E (cont.)	f-NH3	300.2397	300.2394	0.96	C14 H30 O2 N5	9.28	20843
	f	317.2661	317.266	0.57	C14 H33 O2 N6	18.79	42177
	d	359.1714	359.1714	0.15	C18 H23 O4 N4	3.7	8317
	c	376.1975	376.1979	-1.11	C18 H26 O4 N5	1.82	4096
	b-H2O	398.2213	398.2187	6.68	C21 H28 O3 N5	2.52	5649
	b-NH3	399.2021	399.2027	-1.5	C21 H27 O4 N4	6.45	14480
	b	416.2295	416.2292	0.58	C21 H30 O4 N5	44.54	99982
	a	433.2569	433.2558	2.59	C21 H33 O4 N6	4.35	9766
	M+H-H2O	472.3033	472.3031	0.55	C24 H38 O3 N7	2.57	5767
	M+H-NH3	473.2867	473.2871	-0.78	C24 H37 O4 N6	16.16	36275
	M+H	490.313	490.3136	-1.31	C24 H40 O4 N7	100	224490
LF434E	int. ion	72.0804	72.0808	-4.92	C4 H10 N	2.99	16691
	asn amm. Ion	87.055	87.0553	-3.15	C3 H7 O N2	6.42	35883
	h-NH3	98.0962	98.0964	-2.31	C6 H12 N	28.72	160589
	int. ion	112.1119	112.1121	-1.23	C7 H14 N	17.88	99960
	h	115.1228	115.123	-1.83	C6 H15 N2	84.45	472169
	int. ion	129.1384	129.1386	-2	C7 H17 N2	6.8	38035
	g-NH3	186.1964	186.1965	-0.18	C10 H24 N3	5.94	33219
	g	203.2231	203.223	0.45	C10 H27 N4	15.27	85367
	i-2*NH3	209.1283	209.1285	-0.9	C11 H17 O2 N2	2.35	13124
	i-NH3	226.1551	226.155	0.25	C11 H20 O2 N3	2.69	15025
	i	243.1815	243.1816	-0.08	C11 H23 O2 N4	1.87	10433
	f-2*NH3	283.2142	283.2129	4.66	C14 H27 O2 N4	3.41	19043
	d-NH3	287.1394	287.139	1.24	C16 H19 O3 N2	2.34	13068
	f-NH3	300.2396	300.2394	0.64	C14 H30 O2 N5	4.54	25363
	d	304.1661	304.1656	1.67	C16 H22 O3 N3	3.08	17202
	f	317.2663	317.266	1.09	C14 H33 O2 N6	2.51	14023
	c	321.1911	321.1921	-3.26	C16 H25 O3 N4	1.36	7616
	b-H2O	343.2127	343.2129	-0.42	C19 H27 O2 N4	3.99	22324
	b-NH3	344.1961	344.1969	-2.3	C19 H26 O3 N3	5.86	32738
	b	361.2235	361.2234	0.34	C19 H29 O3 N4	68.1	380801
	a	378.2506	378.25	1.78	C19 H32 O3 N5	4.98	27828
	M+H-NH3-H2O	400.2718	400.2707	2.72	C22 H34 O2 N5	1.5	8368
	M+H-H2O	417.2977	417.2973	1.15	C22 H37 O2 N6	2.05	11452
	M+H-NH3	418.2812	418.2813	-0.26	C22 H36 O3 N5	15.49	86622
	M+H	435.3076	435.3078	-0.39	C22 H39 O3 N6	100	559142
LF450E	int. ion	84.0805	84.0808	-3.13	C5 H10 N	1.02	592
	asn imm.i ion	87.0547	87.0553	-7.04	C3 H7 O N2	5.84	3404
	h-NH3	98.0957	98.0964	-7.59	C6 H12 N	27.44	16000
	int. ion	112.1113	112.1121	-6.94	C7 H14 N	18.86	10998
	h	115.1222	115.123	-6.89	C6 H15 N2	80.89	47171
	int. ion	129.1377	129.1386	-7.11	C7 H17 N2	6.76	3940
	g-NH3	186.1959	186.1965	-3.02	C10 H24 N3	5.28	3076
	g	203.2226	203.223	-2.3	C10 H27 N4	12.68	7396
	i-2*NH3	209.1279	209.1285	-2.69	C11 H17 O2 N2	1.85	1076
	i-NH3	226.1538	226.155	-5.32	C11 H20 O2 N3	2.5	1455
	i	243.1827	243.1816	4.73	C11 H23 O2 N4	1.82	1062
	f-2*NH3	283.2112	283.2129	-5.89	C14 H27 O2 N4	2.15	1255
	f-NH3	300.2383	300.2394	-3.69	C14 H30 O2 N5	3.72	2170
	d-NH3	303.1324	303.1339	-5.01	C16 H19 O4 N2	1	583
	f	317.2637	317.266	-7.18	C14 H33 O2 N6	1.66	970
	d	320.1636	320.1605	9.6	C16 H22 O4 N3	2.15	1255
	b-H2O	359.2074	359.2078	-0.97	C19 H27 O3 N4	2.95	1718
	b-NH3	360.1913	360.1918	-1.22	C19 H26 O4 N3	5.32	3105
	b	377.2177	377.2183	-1.6	C19 H29 O4 N4	67.02	39083
	a	394.2434	394.2449	-3.66	C19 H32 O4 N5	3.3	1925
	M+H-NH3	434.2761	434.2762	-0.08	C22 H36 O4 N5	14.96	8726
	M+H	451.3018	451.3027	-2.02	C22 H39 O4 N6	100	58316

	ion type	*m/z measured*	*m/z theor.*	*rel. error (ppm)*	*Composition*	*rel. Int.*	*Int.*
LF466E	int. ion	72.0804	72.0808	-5.02	C4 H10 N	2.74	16129
	asn imm. Ion	87.055	87.0553	-3.11	C3 H7 O N2	7.64	44949
	h-NH3	98.0962	98.0964	-2.78	C6 H12 N	27.53	162039
	int. ion	112.1119	112.1121	-2.01	C7 H14 N	23.27	136983
	h	115.1227	115.123	-2.24	C6 H15 N2	85.83	505251
	e	123.044	123.0441	-0.68	C7 H7 O2	1.38	8127
	int. ion	129.1384	129.1386	-1.83	C7 H17 N2	7.87	46299
	g-NH3	186.1964	186.1965	-0.6	C10 H24 N3	9.44	55554
	g	203.223	203.223	0.08	C10 H27 N4	21.51	126639
	i-NH3-H2O	208.1447	208.1444	1.03	C11 H18 O N3	1.44	8462
	i-2*NH3	209.1289	209.1285	1.99	C11 H17 O2 N2	1.93	11353
	i-NH3	226.1547	226.155	-1.51	C11 H20 O2 N3	3.81	22432
	i	243.1815	243.1816	-0.29	C11 H23 O2 N4	13.93	82020
	f-2*NH3	283.213	283.2129	0.38	C14 H27 O2 N4	3.63	21379
	f-NH3	300.2393	300.2394	-0.21	C14 H30 O2 N5	10.26	60379
	f	317.2659	317.266	-0.3	C14 H33 O2 N6	25.75	151583
	d-NH3	319.1291	319.1288	0.68	C16 H19 O5 N2	1.1	6472
	d	336.1555	336.1554	0.3	C16 H22 O5 N3	2.26	13329
	b-H2O	375.2026	375.2027	-0.11	C19 H27 O4 N4	3.63	21367
	b-NH3	376.1866	376.1867	-0.21	C19 H26 O5 N3	4.12	24240
	b	393.213	393.2132	-0.75	C19 H29 O5 N4	56.22	330933
	a	410.2394	410.2398	-0.9	C19 H32 O5 N5	4.08	24044
	M+H-NH3-H2O	432.2606	432.2605	0.21	C22 H34 O4 N5	1.01	5929
	M+H-H2O	449.2873	449.2871	0.53	C22 H37 O4 N6	3.13	18416
	M+H-NH3	450.2707	450.2711	-0.78	C22 H36 O5 N5	15.34	90317
	M+H	467.2972	467.2976	-0.91	C22 H39 O5 N6	100	588654

Type F compounds

	ion type	*m/z measured*	*m/z theor.*	*rel. error (ppm)*	*Composition*	*rel. Int.*	*Int.*
LF430F	int. ion	86.0959	86.0964	-6.06	C5 H12 N	8.36	19570
	g-2*NH3-C2H4	98.0958	98.0964	-6.03	C6 H12 N	1.75	4096
	g-2*NH3	126.1271	126.1277	-4.9	C8 H16 N	5.94	13894
	e	130.0646	130.0651	-4.27	C9 H8 N	20.4	47735
	g-NH3	143.1537	143.1543	-4.31	C8 H19 N2	10.62	24847
	g	160.1803	160.1808	-3.12	C8 H22 N3	30.91	72320
	j	200.1387	200.1394	-3.03	C9 H18 O2 N3	0.74	1738
	f-2*NH3-H2O	222.1595	222.1601	-2.73	C12 H20 O N3	2.47	5787
	f-3*NH3	223.1436	223.1441	-2.28	C12 H19 O2 N2	4.04	9447
	f-NH3-H2O	239.1863	239.1866	-1.57	C12 H23 O N4	5.23	12227
	f-2*NH3	240.1702	240.1707	-1.9	C12 H22 O2 N3	17.44	40800
	f-NH3	257.1967	257.1972	-2.09	C12 H25 O2 N4	14.8	34628
	f	274.2235	274.2238	-1.09	C12 H28 O2 N5	16.57	38768
	d	357.1918	357.1921	-0.92	C19 H25 O3 N4	4	9364
	c	374.2195	374.2187	2.33	C19 H28 O3 N5	3.43	8016
	M+H-NH3-H2O	396.2388	396.2394	-1.51	C22 H30 O2 N5	3.38	7912
	M+H-2*NH3	397.2238	397.2234	0.88	C22 H29 O3 N4	6.01	14075
	M+H-H2O	413.2656	413.266	-0.95	C22 H33 O2 N6	4.67	10927
	M+H-NH3	414.2495	414.25	-1.09	C22 H32 O3 N5	47.87	112008
	M+H	431.2762	431.2765	-0.79	C22 H35 O3 N6	100	233997
LF446F	int.ion	86.0959	86.0964	-5.82	C5 H12 N	9.07	23160
	asn imm. Ion	87.0547	87.0553	-6.64	C3 H7 O N2	4.27	10908
	g-2*NH3-C2H4	98.0957	98.0964	-6.98	C6 H12 N	1.6	4088
	g-2*NH3	126.1272	126.1277	-4.37	C8 H16 N	6.62	16895
	g-NH3	143.1537	143.1543	-3.76	C8 H19 N2	12.92	32993
	e	146.0596	146.06	-3.35	C9 H8 O N	35.24	89990
	g	160.1803	160.1808	-3.19	C8 H22 N3	49.52	126454
	j	200.1386	200.1394	-3.92	C9 H18 O2 N3	1.43	3661
	f-2*NH3-H2O	222.1598	222.1601	-1.11	C12 H20 O N3	2.55	6503
	f-3*NH3	223.1434	223.1441	-3.04	C12 H19 O2 N2	4.07	10383
	f-NH3-H2O	239.1859	239.1866	-2.89	C12 H23 O N4	6.02	15374

	ion type	*m/z measured*	*m/z theor.*	*rel. error (ppm)*	*Composition*	*rel. Int.*	*Int.*
LF446F (cont.)	f-2*NH3	240.1702	240.1707	-1.68	C12 H22 O2 N3	23.91	61055
	f-H2O	256.2125	256.2132	-2.52	C12 H26 O N5	1.44	3678
	f-NH3	257.1967	257.1972	-1.96	C12 H25 O2 N4	26.87	68613
	f	274.2234	274.2238	-1.4	C12 H28 O2 N5	37.45	95651
	d	373.1852	373.187	-4.79	C19 H25 O4 N4	3.33	8508
	c	390.2133	390.2136	-0.6	C19 H28 O4 N5	2.19	5597
	M+H-NH3-H2O	412.2337	412.2343	-1.57	C22 H30 O3 N5	2.54	6492
	M+H-2*NH3	413.2166	413.2183	-4.23	C22 H29 O4 N4	5.88	15011
	M+H-H2O	429.2612	429.2609	0.85	C22 H33 O3 N6	1.92	4902
	M+H-NH3	430.2442	430.2449	-1.54	C22 H32 O4 N5	39.97	102066
	M+H	447.2708	447.2714	-1.44	C22 H35 O4 N6	100	255383
LF391F	int. ion	86.0958	86.0964	-7.55	C5 H12 N	5.63	15318
	asn imm. Ion	87.0546	87.0553	-7.53	C3 H7 O N2	7.82	21277
	e	91.0537	91.0542	-5.73	C7 H7	1.22	3319
	g-2*NH3-C2H4	98.0956	98.0964	-8.47	C6 H12 N	1.72	4677
	g-2*NH3	126.1269	126.1277	-6.73	C8 H16 N	5.05	13731
	g-NH3	143.1536	143.1543	-4.57	C8 H19 N2	7.16	19475
	g	160.1801	160.1808	-4.29	C8 H22 N3	20.01	54432
	j-NH3	183.1113	183.1128	-8.28	C9 H15 O2 N2	0.52	1403
	f-2*NH3-H2O	222.1594	222.1601	-3.17	C12 H20 O N3	1.55	4204
	f-3*NH3	223.1435	223.1441	-2.69	C12 H19 O2 N2	3.04	8259
	f-NH3-H2O	239.1859	239.1866	-3.18	C12 H23 O N4	3.37	9169
	f-2*NH3	240.1699	240.1707	-2.94	C12 H22 O2 N3	11.31	30751
	f-H2O	256.2127	256.2132	-1.74	C12 H26 O N5	1.49	4059
	f-NH3	257.1965	257.1972	-2.9	C12 H25 O2 N4	8.41	22871
	f	274.2232	274.2238	-1.99	C12 H28 O2 N5	5.26	14314
	d	318.1809	318.1812	-0.99	C17 H24 O3 N3	3.94	10718
	c	335.2072	335.2078	-1.72	C17 H27 O3 N4	3.92	10674
	M+H-H2O-NH3	357.2276	357.2285	-2.62	C20 H29 O2 N4	3.06	8326
	M+H-2*NH3	358.2116	358.2125	-2.57	C20 H28 O3 N3	4.75	12917
	M+H-H2O	374.2549	374.2551	-0.36	C20 H32 O2 N5	4.15	11283
	M+H-NH3	375.2382	375.2391	-2.32	C20 H31 O3 N4	49.59	134889
	M+H	392.265	392.2656	-1.61	C20 H34 O3 N5	100	271988
LF407F	int. ion	86.0964	86.0964	-0.71	C5 H12 N	8.12	72678
	asn imm. ion	87.0552	87.0553	-0.65	C3 H7 O N2	11.34	101523
	g-2*NH3-C2H4	98.0964	98.0964	-0.29	C6 H12 N	2.36	21077
	e	107.0492	107.0491	0.19	C7 H7 O	4.87	43606
	g-2*NH3	126.1279	126.1277	1.2	C8 H16 N	6.56	58734
	g-NH3	143.1545	143.1543	1.34	C8 H19 N2	9.36	83757
	g	160.1812	160.1808	2.18	C8 H22 N3	24.99	223633
	j-NH3	183.1133	183.1128	2.62	C9 H15 O2 N2	0.95	8482
	j	200.1396	200.1394	1.39	C9 H18 O2 N3	0.82	7307
	f-2*NH3-H2O	222.1604	222.1601	1.25	C12 H20 O N3	2.34	20961
	f-3*NH3	223.1447	223.1441	2.48	C12 H19 O2 N2	3.94	35236
	f-NH3-H2O	239.1873	239.1866	2.74	C12 H23 O N4	4.63	41411
	f-2*NH3	240.1713	240.1707	2.8	C12 H22 O2 N3	14.99	134112
	f-H2O	256.2137	256.2132	2.13	C12 H26 O N5	1.78	15894
	f-NH3	257.1978	257.1972	2.45	C12 H25 O2 N4	11.4	101981
	f	274.2246	274.2238	3.23	C12 H28 O2 N5	8.68	77712
	d	334.177	334.1761	2.52	C17 H24 O4 N3	4.6	41134
	c	351.2035	351.2027	2.43	C17 H27 O4 N4	4.17	37282
	M+H-NH3-H2O	373.2242	373.2234	2.16	C20 H29 O3 N4	3.77	33745
	M+H-2*NH3	374.2081	374.2074	1.87	C20 H28 O4 N3	5.38	48190
	M+H-H2O	390.2504	390.25	1.11	C20 H32 O3 N5	4.82	43097
	M+H-NH3	391.2349	391.234	2.36	C20 H31 O4 N4	53.51	478867
	M+H	408.2612	408.2605	1.64	C20 H34 O4 N5	100	894939

	ion type	*m/z measured*	*m/z theor.*	*rel. error (ppm)*	*Composition*	*rel. Int.*	*Int.*
LF423F	int. ion	86.0964	86.0964	0.27	C5 H12 N	11.81	183302
	asn imm. Ion	87.0553	87.0553	-0.08	C3 H7 O N2	16.54	256679
	g-2*NH3-C2H4	98.0965	98.0964	0.25	C6 H12 N	3.18	49375
	e	123.0442	123.0441	1.32	C7 H7 O2	4.17	64708
	g-2*NH3	126.1279	126.1277	1.17	C8 H16 N	12.56	194910
	g-NH3	143.1546	143.1543	2.32	C8 H19 N2	18.34	284535
	g	160.1813	160.1808	2.67	C8 H22 N3	44.9	696720
	j	200.14	200.1394	3.34	C9 H18 O2 N3	2.44	37866
	f-2*NH3-H2O	222.1607	222.1601	2.95	C12 H20 O N3	3	46539
	f-3*NH3	223.1447	223.1441	2.71	C12 H19 O2 N2	3.45	53598
	f-NH3-H2O	239.1874	239.1866	3.32	C12 H23 O N4	6.52	101175
	f-2*NH3	240.1715	240.1707	3.63	C12 H22 O2 N3	21.04	326419
	f-NH3	257.198	257.1972	3.09	C12 H25 O2 N4	35.54	551551
	f	274.2246	274.2238	3.1	C12 H28 O2 N5	52.28	811272
	d	350.172	350.171	2.75	C17 H24 O5 N3	3.68	57164
	c	367.1985	367.1976	2.55	C17 H27 O5 N4	3.02	46909
	M+H-NH3-H2O	389.2199	389.2183	3.98	C20 H29 O4 N4	4.7	72892
	M+H-2*NH3	390.2016	390.2023	-1.95	C20 H28 O5 N3	5.03	78094
	M+H-H2O	406.2465	406.2449	4.02	C20 H32 O4 N5	7.65	118774
	M+H-NH3	407.2296	407.2289	1.63	C20 H31 O5 N4	43.96	682090
	M+H	424.2565	424.2554	2.56	C20 H34 O5 N5	100	1551717

Appendix B: HCD-MS/MS Data of Chapter 3

Ozyptila lugubris compounds

	ion type	*m/z measured*	*m/z theor.*	*rel. error (ppm)*	*Composition*	*rel. Int.*	*Int.*
OZ359	h-NH3-C2H4	84.08022	84.08078	-6.57	C5 H10 N	1.53	1629.2
	h-NH3	112.11152	112.11208	-4.94	C7 H14 N	38.99	41649.6
	h	129.13803	129.13863	-4.59	C7 H17 N2	100	106817.3
	e	130.06458	130.06513	-4.22	C9 H8 N	1.25	1340.3
	d	215.11743	215.11789	-2.12	C13 H15 O N2	82.04	87630.6
	b	286.19118	286.19139	-0.74	C17 H24 O N3	71.22	76074.3
	M+H	360.27559	360.27579	-0.55	C20 H34 O N5	8.87	9469.7
OZ375	int.	72.08043	72.08078	-4.8	C4 H10 N	0.66	1504.1
	h-NH3-C2H4	84.08074	84.08078	-0.47	C5 H10 N	1.35	3069.1
	h-NH3	112.11202	112.11208	-0.46	C7 H14 N	34.15	77848.2
	h	129.13855	129.13863	-0.61	C7 H17 N2	100	227990
	e	146.06007	146.06004	0.2	C9 H8 O N	1.5	3419.6
	m	174.05602	174.05496	6.09	C10 H8 O2 N	0.24	538.4
	g	203.2235	203.22302	2.36	C10 H27 N4	0.62	1414.4
	c-H2O	230.12962	230.12879	3.63	C13 H16 O N3	0.38	868.4
	d	231.11313	231.1128	1.4	C13 H15 O2 N2	80.48	183488.2
	b-H2O	284.17459	284.17574	-4.04	C17 H22 O N3	0.34	770.2
	b	302.1868	302.1863	1.65	C17 H24 O2 N3	62.93	143475.8
	M+H-H2O	358.26233	358.26014	6.13	C20 H32 O N5	1.15	2611.1
	M+H	376.27101	376.2707	0.81	C20 H34 O2 N5	10.17	23185.4
OZ373	H-NH3-C2H4	98.09615	98.09643	-2.79	C6 H12 N	2.71	1825.5
	h-NH3	126.12749	126.12773	-1.87	C8 H16 N	35.65	24022.3
	e	130.06486	130.06513	-2.02	C9 H8 N	2.44	1641.4
	h	143.15412	143.15428	-1.09	C8 H19 N2	58.92	39707.3
	h+NH3	160.18118	160.18082	2.24	C8 H22 N3	0.67	453.9
	d	215.11787	215.11789	-0.1	C13 H15 O N2	100	67389.1
	g	217.23915	217.23867	2.2	C11 H29 N4	3.67	2473.4
	b	300.20721	300.20704	0.58	C18 H26 O N3	42.9	28909.6
	a	317.23468	317.23359	3.44	C18 H29 O N4	0.83	556.6
	M+H-H2O	356.27985	356.28087	-2.88	C21 H34 N5	3.33	2244.5
	M+H-NH3	357.26364	357.26489	-3.49	C21 H33 O N4	3.09	2085.4
	M+H	374.29162	374.29144	0.48	C21 H36 O N5	43.02	28989.6
OZ389	int.	86.09611	86.09643	-3.69	C5 H12 N	1.1	4454.7
	h-NH3-C2H4	98.09621	98.09643	-2.22	C6 H12 N	2.82	11369.6
	h-NH3	126.12763	126.12773	-0.75	C8 H16 N	31.69	127888.4
	h	143.15431	143.15428	0.22	C8 H19 N2	61.87	249702.8
	e	146.06012	146.06004	0.52	C9 H8 O N	2.99	12080.7
	h+NH3	160.18107	160.18082	1.52	C8 H22 N3	0.44	1765.4
	m	174.05459	174.05496	-2.1	C10 H8 O2 N	0.86	3488.9
	d-C2H4	203.08154	203.0815	0.2	C11 H11 O2 N2	0.57	2318.3
	g	217.23902	217.23867	1.62	C11 H29 N4	10.56	42629.3
	d	231.11308	231.1128	1.21	C13 H15 O2 N2	100	403612.5
	b	316.20225	316.20195	0.92	C18 H26 O2 N3	33.34	134565.7
	a	333.22967	333.2285	3.5	C18 H29 O2 N4	1.34	5398.1
	M+H-H2O	372.27638	372.27579	1.59	C21 H34 O N5	6.19	24998.7
	M+H-NH3	373.25948	373.2598	-0.88	C21 H33 O2 N4	2.62	10582.5
	M+H	390.28657	390.28635	0.57	C21 H36 O2 N5	37.93	153075.6

	ion type	*m/z measured*	*m/z theor.*	*rel. error (ppm)*	*Composition*	*rel. Int.*	*Int.*
OZ318A	int	72.08016	72.08078	-8.58	C4 H10 N	10.27	17239.9
	h-NH3	112.11178	112.11208	-2.61	C7 H14 N	0.68	1133.4
	h	129.13811	129.13863	-3.96	C7 H17 N2	1.7	2860.9
	e	146.05949	146.06004	-3.76	C9 H8 O N	3.02	5065.1
	g	146.16525	146.16517	0.55	C7 H20 N3	1.66	2782.3
	m	174.05542	174.05496	2.64	C10 H8 O2 N	0.58	968.7
	d-C2H4	203.07976	203.0815	-8.6	C11 H11 O2 N2	0.59	997.9
	c-H2O	230.12883	230.12879	0.16	C13 H16 O N3	1.17	1960.1
	d	231.1124	231.1128	-1.75	C13 H15 O2 N2	100	167871.2
	c	248.13928	248.13935	-0.29	C13 H18 O2 N3	8.94	15007.9
	M+H-NH3	302.1861	302.1863	-0.66	C17 H24 O2 N3	25.61	42990.5
	M+H	319.21184	319.21285	-3.19	C17 H27 O2 N4	15.8	26516.7
OZ332A	int.	86.09596	86.09643	-5.47	C5 H12 N	6.97	20937.1
	h	143.15466	143.15428	2.65	C8 H19 N2	0.69	2057.8
	e	146.05981	146.06004	-1.58	C9 H8 O N	2.89	8669
	g	160.18059	160.18082	-1.44	C8 H22 N3	4.47	13423.2
	m	174.05515	174.05496	1.14	C10 H8 O2 N	1.1	3300.8
	d-C2H4	203.08179	203.0815	1.43	C11 H11 O2 N2	0.6	1799.6
	c-H2O	230.12787	230.12879	-4	C13 H16 O N3	0.15	456.6
	d	231.11252	231.1128	-1.22	C13 H15 O2 N2	100	300359.4
	c	248.13909	248.13935	-1.05	C13 H18 O2 N3	2.65	7950.5
	M+H-H2O	315.21813	315.21794	0.59	C18 H27 O N4	2.62	7869.2
	M+H-NH3	316.20219	316.20195	0.74	C18 H26 O2 N3	8.86	26612.2
	M+H	333.22869	333.2285	0.55	C18 H29 O2 N4	36.76	110421.8
OZ318B	int.	72.0804	72.08078	-5.17	C4 H10 N	4.71	5819.2
	h-NH3	112.11183	112.11208	-2.2	C7 H14 N	7.72	9526.5
	h	129.13831	129.13863	-2.43	C7 H17 N2	9.53	11768
	e	146.06008	146.06004	0.25	C9 H8 O N	7.72	9531.9
	g	146.16498	146.16517	-1.31	C7 H20 N3	7.76	9580.7
	m	174.05421	174.05496	-4.29	C10 H8 O2 N	2.13	2626.9
	d' (transa.)	231.11242	231.1128	-1.66	C13 H15 O2 N2	4.15	5128.8
	d	245.12847	245.12845	0.04	C14 H17 O2 N2	37.84	46715.2
	c	262.15501	262.155	0.03	C14 H20 O2 N3	4.84	5980.7
	M+H-H2O	301.2023	301.20229	0.05	C17 H25 O N4	2.74	3376.8
	M+H-NH3	302.18606	302.1863	-0.8	C17 H24 O2 N3	33.06	40820.3
	M+H	319.21274	319.21285	-0.36	C17 H27 O2 N4	100	123463.9
OZ332B	int	86.09627	86.09643	-1.84	C5 H12 N	5.82	26958.3
	H-NH3-C2H4	98.0965	98.09643	0.74	C6 H12 N	1.36	6297.8
	h-NH3	126.12759	126.12773	-1.05	C8 H16 N	3.99	18461.7
	h	143.15431	143.15428	0.23	C8 H19 N2	4.18	19340
	e	146.06019	146.06004	1	C9 H8 O N	6.44	29816.1
	g	160.18089	160.18082	0.43	C8 H22 N3	11.04	51146.3
	m	174.05519	174.05496	1.34	C10 H8 O2 N	2.42	11189.1
	d' (transa)	231.11273	231.1128	-0.32	C13 H15 O2 N2	2.3	10658.8
	d	259.14465	259.1441	2.1	C15 H19 O2 N2	5.6	25957.3
	c	276.17103	276.17065	1.38	C15 H22 O2 N3	8.93	41358.8
	M+H-NH3-H2O	298.19186	298.19139	1.58	C18 H24 O N3	0.62	2869.7
	M+H-H2O	315.21833	315.21794	1.24	C18 H27 O N4	3.47	16073.8
	M+H-NH3	316.20222	316.20195	0.84	C18 H26 O2 N3	44.96	208272.8
	M+H	333.22894	333.2285	1.32	C18 H29 O2 N4	100	463210.8

Lachesana sp. compounds

	ion type	*m/z measured*	*m/z theor.*	*rel. error (ppm)*	*Composition*	*rel. Int.*	*Int.*
LH430	H-NH3-C2H4	84.08052	84.08078	-3.03	C5 H10 N	1.83	2495.4
	i-NH3	112.07551	112.07569	-1.57	C6 H10 O N	38.78	52879.3
	h-NH3	112.1118	112.11208	-2.45	C7 H14 N	35.25	48065.4
	h	129.13833	129.13863	-2.25	C7 H17 N2	100	136372.2
	e	130.06436	130.06513	-5.92	C9 H8 N	0.81	1099.7
	m	158.06018	158.06004	0.89	C10 H8 O N	0.4	550
	j-NH3	183.14905	183.14919	-0.79	C10 H19 O N2	9.79	13347.8
	j	200.17504	200.17574	-3.51	C10 H22 O N3	1.04	1418.1
	k	229.09681	229.09715	-1.48	C13 H13 O2 N2	2.46	3360.1
	d	286.155	286.155	-0.03	C16 H20 O2 N3	21.53	29355
	b	357.22836	357.2285	-0.4	C20 H29 O2 N4	56.18	76616.3
	M+H-H2O	413.30179	413.30234	-1.33	C23 H37 O N6	0.35	482.7
	M+H	431.31321	431.3129	0.71	C23 H39 O2 N6	5.36	7304.6
LH446	int.	72.08065	72.08078	-1.73	C4 H10 N	0.65	1859.6
	h-NH3-C2H4	84.08055	84.08078	-2.66	C5 H10 N	1.45	4166.7
	i-NH3	112.0755	112.07569	-1.72	C6 H10 O N	30.59	88018
	h-NH3	112.1118	112.11208	-2.46	C7 H14 N	29.78	85683.8
	i	129.102	129.10224	-1.83	C6 H13 O N2	1.43	4118.2
	h	129.13834	129.13863	-2.18	C7 H17 N2	100	287731.3
	e	146.05975	146.06004	-1.98	C9 H8 O N	1.98	5700.2
	l-NH3	174.05532	174.05496	2.09	C10 H8 O2 N	1.08	3103.4
	j-NH3	183.14922	183.14919	0.17	C10 H19 O N2	10.69	30764.8
	l	191.08146	191.0815	-0.23	C10 H11 O2 N2	2.59	7444.5
	j	200.17581	200.17574	0.34	C10 H22 O N3	3.71	10666.7
	k	245.09215	245.09207	0.32	C13 H13 O3 N2	4.36	12542.9
	c-H2O	301.16549	301.1659	-1.36	C16 H21 O2 N4	0.75	2147.7
	d	302.14991	302.14992	-0.02	C16 H20 O3 N3	16.44	47301.8
	c	319.17675	319.17647	0.89	C16 H23 O3 N4	1.31	3772.7
	b-H2O	355.2118	355.21285	-2.97	C20 H27 O2 N4	0.49	1415.8
	b	373.22333	373.22342	-0.25	C20 H29 O3 N4	52.21	150211
	M+H	447.30766	447.30782	-0.34	C23 H39 O3 N6	7.03	20217.4
LH444	i-NH3	112.0755	112.07569	-1.69	C6 H10 O N	61.95	11376.7
	h-NH3	126.12756	126.12773	-1.34	C8 H16 N	39.09	7179.1
	h	143.15417	143.15428	-0.72	C8 H19 N2	71.83	13190.7
	j-NH3	197.16469	197.16484	-0.74	C11 H21 O N2	7.7	1414.5
	g	217.2408	217.23867	9.78	C11 H29 N4	3.45	632.8
	d	286.15485	286.155	-0.54	C16 H20 O2 N3	29.64	5442.9
	b	371.24396	371.24415	-0.52	C21 H31 O2 N4	38.11	6997.7
	M+H	445.3287	445.32855	0.34	C24 H41 O2 N6	55.73	10233.7
LH460	int.	86.09627	86.09643	-1.84	C5 H12 N	1.81	13728.5
	h-NH3-C2H4	98.0963	98.09643	-1.26	C6 H12 N	4.07	30808.6
	i-NH3	112.07559	112.07569	-0.89	C6 H10 O N	73.36	555492.1
	h-NH3	126.12759	126.12773	-1.07	C8 H16 N	49.63	375765.3
	i	129.10214	129.10224	-0.75	C6 H13 O N2	4.31	32611.2
	h	143.15431	143.15428	0.21	C8 H19 N2	100	757208.7
	e	146.06004	146.06004	-0.03	C9 H8 O N	5.47	41413.6
	l-NH3	174.05538	174.05496	2.43	C10 H8 O2 N	2.76	20912.7
	l	191.08165	191.0815	0.75	C10 H11 O2 N2	6.17	46749.1
	j-NH3	197.16507	197.16484	1.14	C11 H21 O N2	14.44	109320.8
	j	214.19159	214.19139	0.94	C11 H24 O N3	6.46	48895.7
	g	217.23896	217.23867	1.33	C11 H29 N4	7.17	54256.7
	k	245.09251	245.09207	1.79	C13 H13 O3 N2	9.22	69786.5
	d	302.15024	302.14992	1.08	C16 H20 O3 N3	29.4	222600.5
	c	319.17615	319.17647	-1	C16 H23 O3 N4	1.12	8492
	b	387.23919	387.23907	0.31	C21 H31 O3 N4	39.41	298421
	a	404.26584	404.26562	0.56	C21 H34 O3 N5	2.26	17094.9
	M+H-H2O	443.31337	443.3129	1.06	C24 H39 O2 N6	4.12	31197.2
	M+H	461.32354	461.32347	0.17	C24 H41 O3 N6	52.88	400413.7

Drassodes sp. compounds

	ion type	*m/z measured*	*m/z theor.*	*rel. error (ppm)*	*Composition*	*rel. Int.*	*Int.*
DR442	int.	112.11172	112.11208	-3.13	C7 H14 N	2.23	69841.9
	m	121.02817	121.02841	-1.91	C7 H5 O2	4.56	143027
	int.	129.13819	129.13863	-3.4	C7 H17 N2	1.41	44033.9
	c-H2O	177.10232	177.10224	0.46	C10 H13 O N2	0.41	12891.7
	d	178.08601	178.08626	-1.36	C10 H12 O2 N	100	3133404
	b	249.15952	249.15975	-0.93	C14 H21 O2 N2	73.25	2295073.5
	a	266.18498	266.1863	-4.98	C14 H24 O2 N3	0.3	9321.5
	n	323.24447	323.24415	0.98	C17 H31 O2 N4	0.2	6319.2
	M+H	443.2653	443.26528	0.05	C24 H35 O4 N4	1.05	32871.9
DR458	int	112.11163	112.11208	-4	C7 H14 N	3.36	3779.4
	m'	121.02818	121.02841	-1.88	C7 H5 O2	3.74	4206.4
	int.	129.13805	129.13863	-4.47	C7 H17 N2	3.48	3918.3
	m	137.02313	137.02332	-1.36	C7 H5 O3	3.21	3607.6
	d'	178.08605	178.08626	-1.17	C10 H12 O2 N	97.11	109181.7
	d	194.08094	194.08117	-1.17	C10 H12 O3 N	100	112434.3
	b'	249.15973	249.15975	-0.09	C14 H21 O2 N2	69	77575.9
	b	265.15458	265.15467	-0.35	C14 H21 O3 N2	67.59	75996.2
DR456	int	86.09591	86.09643	-6.05	C5 H12 N	0.64	4588.5
	m	121.02803	121.02841	-3.11	C7 H5 O2	7.32	52605.8
	int	126.12733	126.12773	-3.13	C8 H16 N	2.11	15149.2
	int	143.154	143.15428	-1.95	C8 H19 N2	2.85	20487.6
	c-H2O	177.103	177.10224	4.27	C10 H13 O N2	0.62	4435.8
	d	178.08595	178.08626	-1.74	C10 H12 O2 N	100	719073.5
	b	263.17532	263.1754	-0.32	C15 H23 O2 N2	39.37	283084.8
	a	280.2021	280.20195	0.52	C15 H26 O2 N3	3.18	22849.8
	n-H2O	319.24985	319.24924	1.91	C18 H31 O N4	0.39	2840
	n-NH3	320.23511	320.23325	5.79	C18 H30 O2 N3	0.22	1606
	n	337.26019	337.2598	1.16	C18 H33 O2 N4	6.29	45255.6
	M+H-H2O	439.2707	439.27037	0.76	C25 H35 O3 N4	1.32	9515
	M+H	457.28156	457.28093	1.37	C25 H37 O4 N4	7.98	57408.8
DR472	int.	86.09624	86.09643	-2.19	C5 H12 N	0.64	699.4
	m'	121.02824	121.02841	-1.33	C7 H5 O2	5.46	5989.1
	int.	126.12732	126.12773	-3.21	C8 H16 N	3.98	4359
	m	137.02315	137.02332	-1.27	C7 H5 O3	5.26	5760.5
	int.	143.15405	143.15428	-1.55	C8 H19 N2	6.58	7216.1
	d'	178.08621	178.08626	-0.24	C10 H12 O2 N	100	109618.1
	c-H2O	193.09654	193.09715	-3.17	C10 H13 O2 N2	0.52	568.1
	d	194.08113	194.08117	-0.2	C10 H12 O3 N	97.68	107072.9
	b'	263.17561	263.1754	0.78	C15 H23 O2 N2	37.56	41171.2
	b	279.17063	279.17032	1.12	C15 H23 O3 N2	35.95	39402.4
	a'	280.20345	280.20195	5.35	C15 H26 O2 N3	2.4	2636
	a	296.19718	296.19687	1.07	C15 H26 O3 N3	3.35	3666.9
	n'	337.25987	337.2598	0.2	C18 H33 O2 N4	11.3	12385.1
	n	353.25547	353.25472	2.14	C18 H33 O3 N4	4.64	5087
	M+H-H2O	455.26569	455.26528	0.89	C25 H35 O4 N4	1.82	1995.2
	M+H	473.27649	473.27585	1.37	C25 H37 O5 N4	14.78	16204.7
DR385	int	72.08017	72.08078	-8.47	C4 H10 N	0.92	5589.3
	int.	112.11142	112.11208	-5.84	C7 H14 N	0.64	3884.9
	m	121.02794	121.02841	-3.81	C7 H5 O2	11.69	71290.4
	int.	129.13828	129.13863	-2.71	C7 H17 N2	0.88	5385
	c-H2O	177.1021	177.10224	-0.81	C10 H13 O N2	0.7	4253
	d	178.08584	178.08626	-2.34	C10 H12 O2 N	100	609787.3
	d'	192.10159	192.10191	-1.64	C11 H14 O2 N	11.06	67415.6
	c	195.11224	195.1128	-2.87	C10 H15 O2 N2	1.09	6667.2
	c'	209.12826	209.12845	-0.91	C11 H17 O2 N2	0.49	2985.4
	a-H2O	248.17497	248.17574	-3.09	C14 H22 O N3	0.71	4349.8
	b	249.15956	249.15975	-0.77	C14 H21 O2 N2	5.21	31790.9
	a	266.18621	266.1863	-0.37	C14 H24 O2 N3	15.88	96856.3
	M+H-H2O	368.19719	368.19687	0.87	C21 H26 O3 N3	1.95	11897.4
	M+H-NH3	369.18014	369.18088	-2.01	C21 H25 O4 N2	1.34	8180.2
	M+H	386.20756	386.20743	0.32	C21 H28 O4 N3	26.29	160324.1

	ion type	*m/z measured*	*m/z theor.*	*rel. error (ppm)*	*Composition*	*rel. Int.*	*Int.*
DR399	int.	86.09586	86.09643	-6.63	C5 H12 N	1.03	14890.9
	m	121.02784	121.02841	-4.71	C7 H5 O2	11.46	165834.8
	int.	126.12712	126.12773	-4.79	C8 H16 N	0.82	11926.6
	int.	143.15371	143.15428	-3.94	C8 H19 N2	0.69	10027.2
	c-H2O	177.10308	177.10224	4.73	C10 H13 O N2	0.24	3492.7
	d	178.08571	178.08626	-3.05	C10 H12 O2 N	100	1446848.5
	c	195.11167	195.1128	-5.81	C10 H15 O2 N2	0.26	3692.7
	d'	206.11716	206.11756	-1.91	C12 H16 O2 N	1.39	20082
	c'	223.14364	223.1441	-2.08	C12 H19 O2 N2	0.88	12774.1
	a-H2O	262.19097	262.19139	-1.59	C15 H24 O N3	1.75	25271.1
	b	263.17518	263.1754	-0.86	C15 H23 O2 N2	3.79	54771.3
	a	280.20151	280.20195	-1.58	C15 H26 O2 N3	20.06	290199.7
	M+H-H2O	382.21183	382.21252	-1.81	C22 H28 O3 N3	1.9	27548.1
	M+H-NH3	383.1944	383.19653	-5.56	C22 H27 O4 N2	1.91	27569.8
	M+H	400.22259	400.22308	-1.24	C22 H30 O4 N3	22.28	322418.2
DR222	g	86.09565	86.09643	-9.02	C5 H12 N	11.85	358252.4
	o	103.12229	103.12298	-6.6	C5 H15 N2	1	30333.3
	m	121.0278	121.02841	-5.02	C7 H5 O2	9.4	284168.9
	M+H-NH3	206.11747	206.11756	-0.42	C12 H16 O2 N	100	3023950.3
	M+H	223.14539	223.1441	5.75	C12 H19 O2 N2	1.26	38041.9
DR238	g	86.09575	86.09643	-7.88	C5 H12 N	28.26	46818.3
	o	103.12234	103.12298	-6.14	C5 H15 N2	10.83	17944.7
	m	137.02262	137.02332	-5.08	C7 H5 O3	4.07	6749.9
	M+H-NH3	222.11229	222.11247	-0.83	C12 H16 O3 N	100	165677.9

ACKNOWLEDGMENTS

On this part, I would like to express my thanks to all people who contributed for the realization of this work. These are:

Prof. Dr. Stefan Bienz, head of the famous Bienz group, for the friendly acceptance in his research group, his guidance and supervision of my PhD-thesis and the interesting scientific and non-scientific discussions in the coffee-corner;

Prof. Dr. Jay Siegel for acting as co-referent and for his delightful manner how he leads the Institute;

Dr. Laurent Bigler for the introduction in the fascinating world of mass spectrometry and for supporting and encouraging me finding answers for the numerous analytical problems that occurred during my thesis. And, of course, for the nice time we had together, in and outside the lab.

Dr. Bertran Gerrits from the Functional Genomics Center Zurich (FGCZ) for the assistance during the nanoLC and high-resolution MS measurements. I really appreciate the confidence he gave to me to let me measure independently my venom samples with a 1 Million francs mass spectrometer and the patience he had for discussing my numerous analytical and technical questions. Without him, this work would not look like it looks now. Dankje well!

Urs Stalder for his spontaneous help when technical problems occured during my thesis, like PC-based problems or the abrupt appearance of “ghost peaks”.

Doc_2O Manuel Tzouros for the assistance in the beginning of my PhD work, for introducing me into my research topic, “spider venomics”, and also for the amusing moments we had outside the lab.

Michaël Merét from Paris for the synthetic products he provided for me, the plentiful funny moments we shared together and the free French courses I got during the last four years (Merci gros!!!).

Sergiy Chesnov from the FGCZ for the amino acid analyses he provided for me; Dr. Volker Niedan from LONZA AG for giving me the opportunity to measure my venom samples in the mass spec facilities in Visp; Armin Guggisberg for the assistance of the hydrolysis experiments and his advices concerning basic chemistry problems and Cornelia Moor, Marie Thérèse Bohley, and Sarah Amman for the assistance of administrative work.

All other actual and former members of the Bienz group, Pascal Bisegger, Fabienne Furrer, Denise Pauli, Maurizio Campagna, Daniel Marti, Nadine Bohni, Jean-Christophe Prost as well as Joëlle Räber, Anaëlle Dumas and Markus Seitz from the institute for the nice time we had, not only in but also outside the Irchel-Campus during the numerous group excursions, ski weekends, sport activities and, and, and….

The *Swiss National Science Foundation* and *Kanton Zürich* for the generous financial support.

At this point, I would also like to thanks people that were not directly involved into the realization of this work but also supported me during my chemistry study in the last nine "exil" years in Zurich, in particular, to:

All my colleagues behind the "Lötschberg" for their friendship and giving me the opportunity to refuel my energy at the weekends during climbing, running, supporting FC Sion or simply relaxing;

My parents and my brother for everything they did during this time. Without their financial support, and their love, I would never be where I am now. Vergälts Gott!!

And, of course, Vanessa, for the gorgeous time I could spent with her, and for always being here in good and difficult times.

CURRICULUM VITAE

Personal Data

Name:	Silvan Eichenberger
Date and Place of birth:	16th May 1979 in Visp (VS)
Origin	Gränichen (AG)

Education

1994 – 1999	Kollegium Spiritus Sanctus Brig, 1999, Federal matriculation type C
1999 – 2004	Swiss Federal Institute of Technology (ETH) Zurich, Departement of Chemistry and Applied Biosciences, 2004, Diploma in Chemistry (Dipl. Natw. ETH)
	Diploma thesis in Analytical Chemistry under the supervision of Prof. Dr. Ernö Pretsch "Reduktion von Ionenflüssen durch Polymer-Membranelektroden mit Hilfe von Doppelmembranen mit immobilisierten Ionentauscher"
Since 2004	Ph. D. student at the University of Zurich, Institute of Organic Chemistry under the supervision of Prof. Dr. Stefan Bienz and Dr. Laurent Bigler

Experiences

1994	LONZA AG, Visp, Abteilung Analytik F&E, 3 month practical training in Analytical Chemistry
Since 2005	Research assistant position in the Mass Spectrometry Laboratory

LIST OF PUBLICATIONS AND SCIENTIFIC PRESENTATIONS

Silvan Eichenberger, Laurent Bigler, and Stefan Bienz. Structure Elucidation of Polyamine Toxins in the Venom of the Spider Larinioides folium, *Chimia*, **2007**, 61, 161-164.

Silvan Eichenberger, Laurent Bigler, and Stefan Bienz. Polyamine Toxins in the Venom of the Spider Larinioides folium, Swiss Chemical Society, Fall Meeting **2006**, poster presentation. SCS Poster Price for the best poster in the Section Analytical Chemistry.

Silvan Eichenberger, Stefan Bienz, and Laurent Bigler. Does a Mass Spectrum Really Mirror the Sample Composition? — Gas–Phase Reduction in the API Source as the Origin of Artifacts, Swiss Group for Mass Spectrometry, 25th Anniversary Meeting, **2007**, Beatenberg, oral presentation.